USTC-PNP-Nuclear Physics Mini Workshop Series

ALICE 实验进展综述

周代翠

华中师范大学

2024年9月29，合肥，中国科学技术大学

相对论重离子碰撞物理

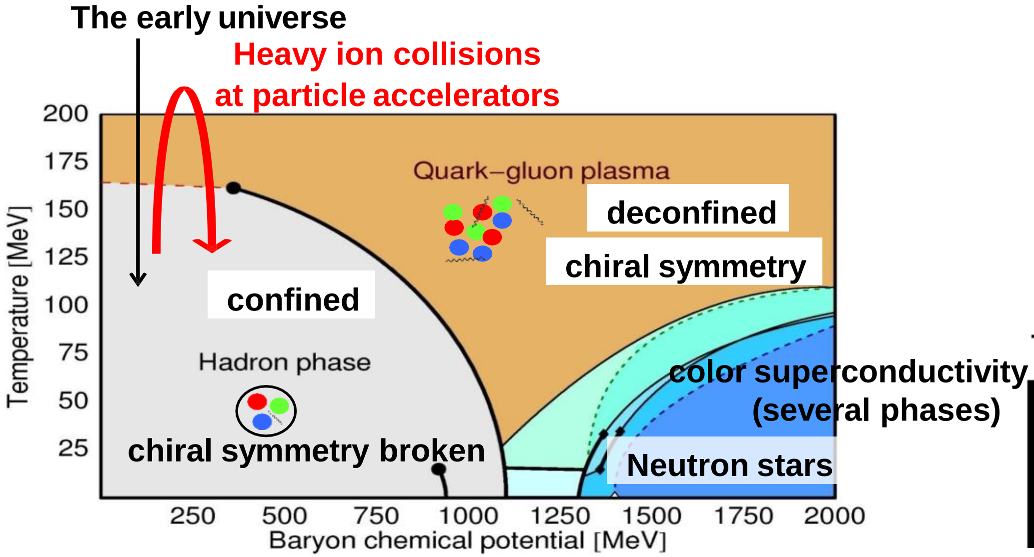

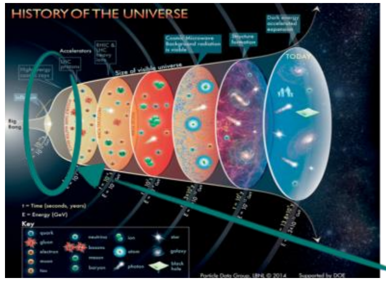

重大基础前沿科学问题

- 早期宇宙形态（夸克–胶子等离子体，简称夸克物质）及其演化规律
- 强相互作用核力在极端高温、高密条件下的行为和特性

大爆炸后的早期宇宙（10^{-6}秒）：夸克-胶子等离子体

TeV能区极端相对论重离子碰撞

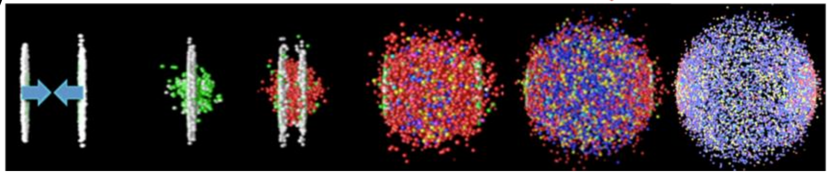

“极端高温、高密下的新物质形态” 被美国国家基础科学委员会列为本世纪十一大科学问题之一

运行十年综述文章

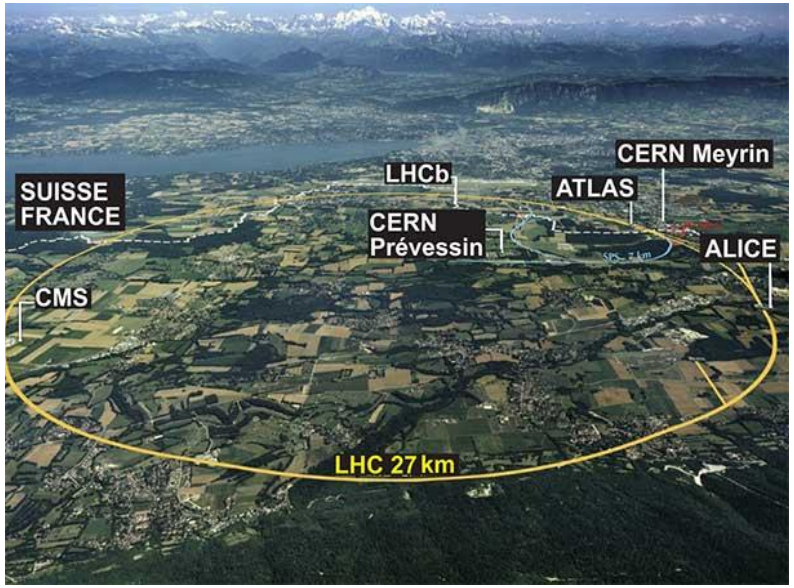

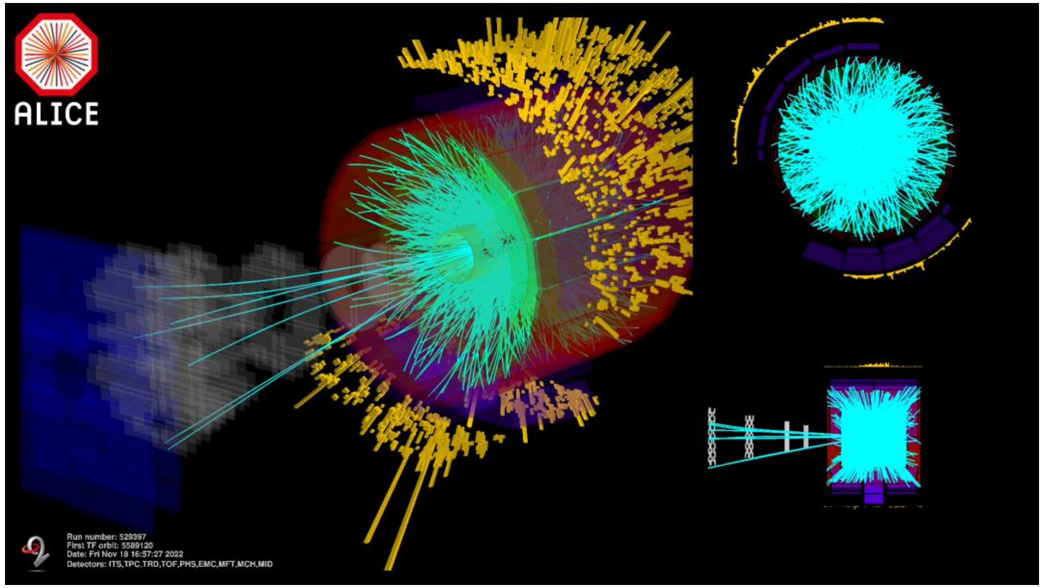

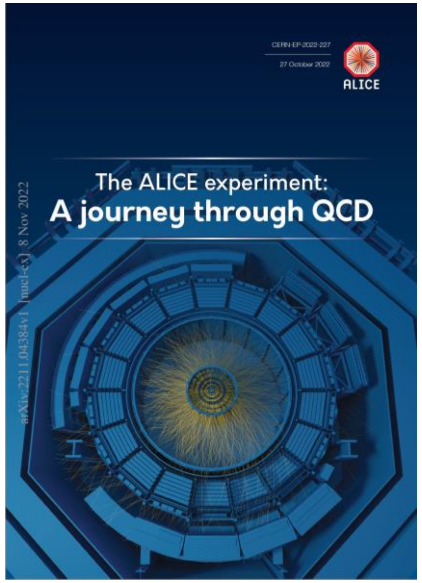

相对论重离子碰撞及其演化

Initial state	Hard scatterings	QGP formation	Hydrodynamic expansion	Hadronization and freeze-out	Detection
	τ=0	τ=0.2-1 fm	τ=5 fm	τ=10−15 fm	

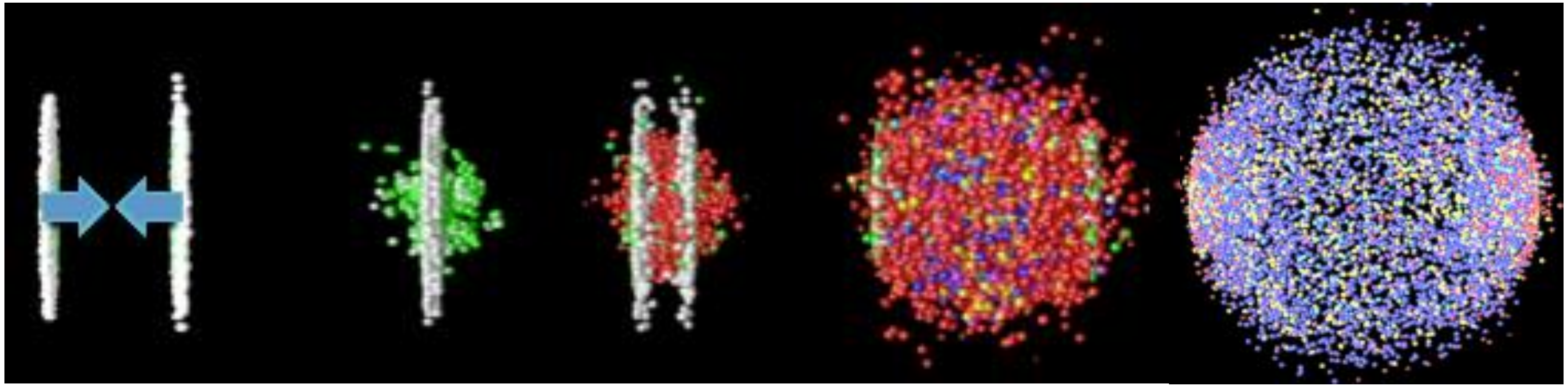

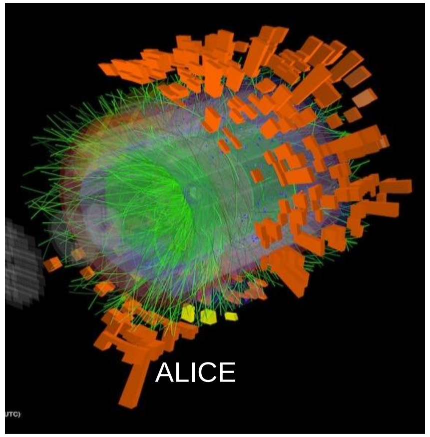

1 fm/c = 3x10^{-24} s, 1 MeV ~ 10^{10} K

Time

Temperature

$T_{c,\,lQCD}$ ~ 156-159 MeV [1-4]

[1] F. Gardim et al. Nature Phys. 16 (2020) 6, 615-619
[2] A. Bazavov et al., Phys. Lett. B 795 (2019)
[3] Borsaniy et al. PRL 125 (2020) 5, 052001
[4] A. Andronic et al., Nature 561 (2018) 7723, 321-330

- **QGP 温度高达～4万亿摄氏度，比太阳中心温度（1500万度）高～20万倍以上**
- **Characteristics: extremely high temperature O(1012 K)，high energy density, vanishing baryon chemical potential**

QGP probes

- High-p_T partons (jets)
- Heavy flavors (charm and beauty quarks)
  - produced in early hard processes
  - interaction with QGP constituents
  - Perturbative QCD

➢ In-medium interaction (energy loss) and transport properties

➢ In-medium modification of the strong force and of fragmentation

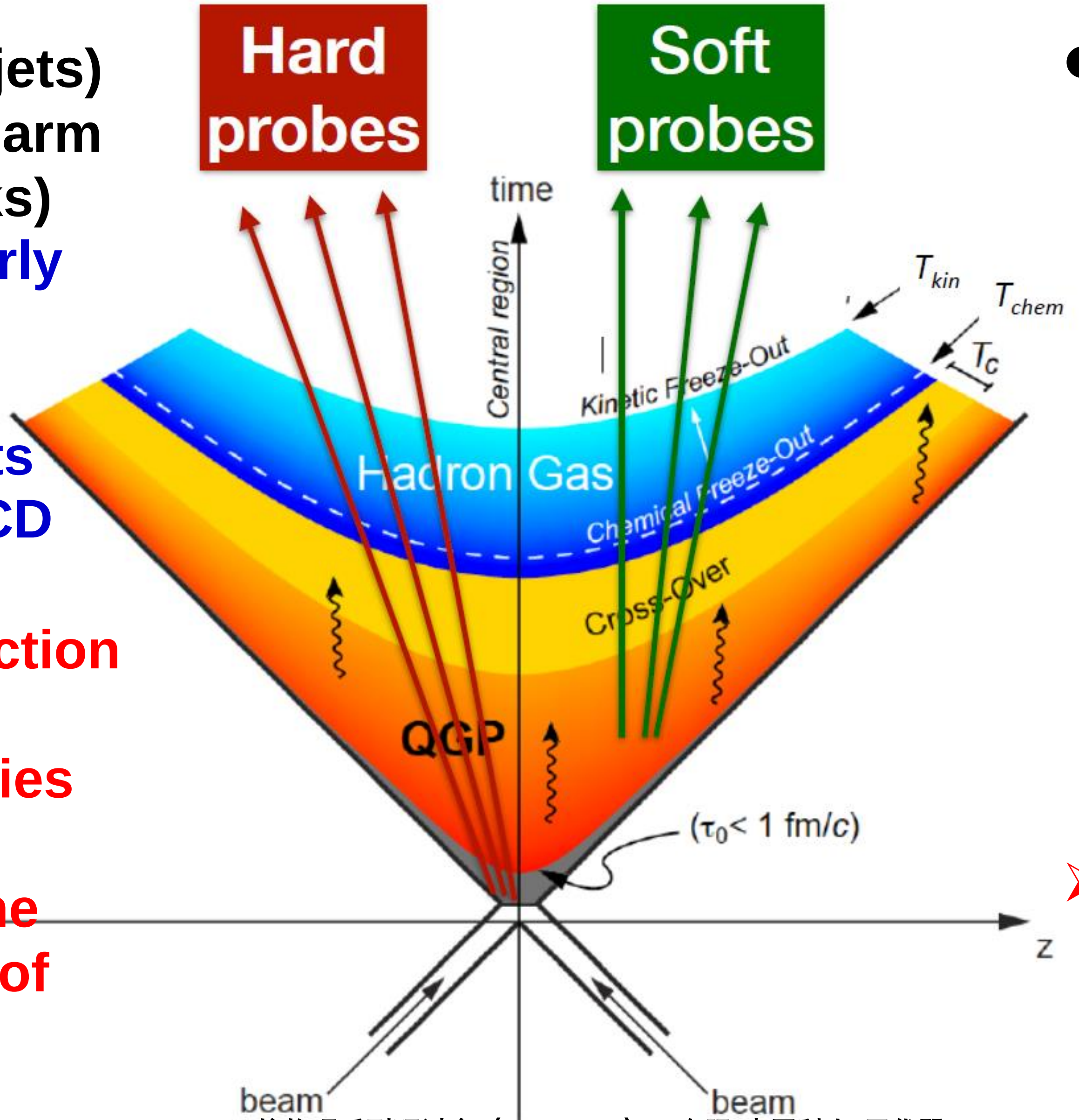

- Low-p_T particles:
  - light flavour hadrons (u,d,s, + exotic states) produced from hadronization of the strongly-interacting, thermalized QGP constitutes
  - non-perturbative QCD regime

➢ thermodynamical and transport properties

Probing QGP with jets

Vacuum fragmentation (pp collisions)

Collimated sprays of hadrons resulting from fragmentation and subsequent hadronization of "high-energy" partons (quarks&gluons)

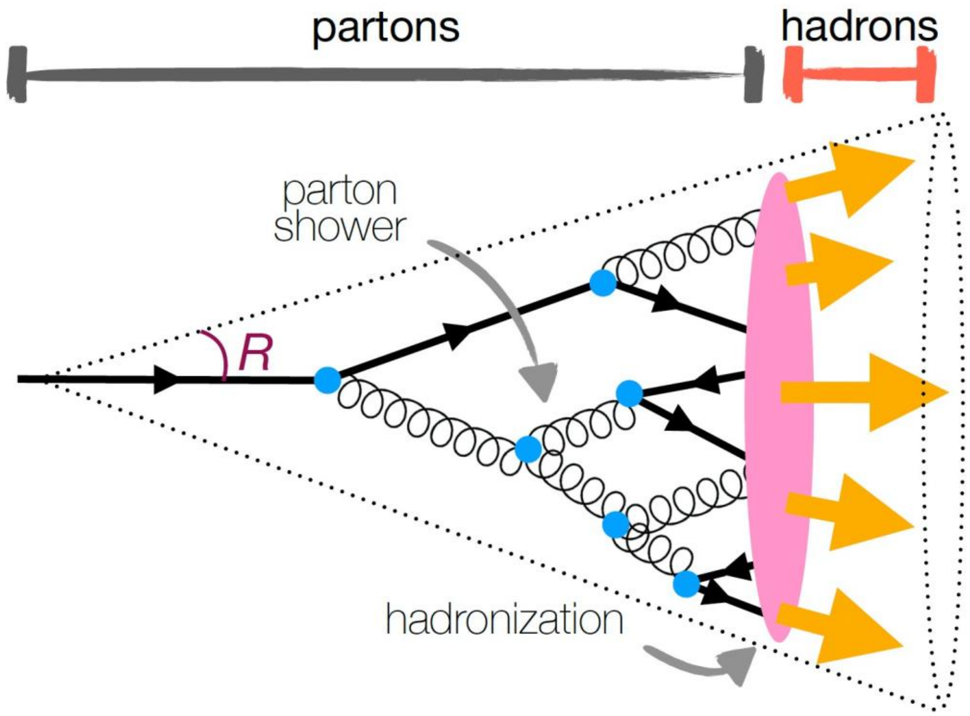

pp

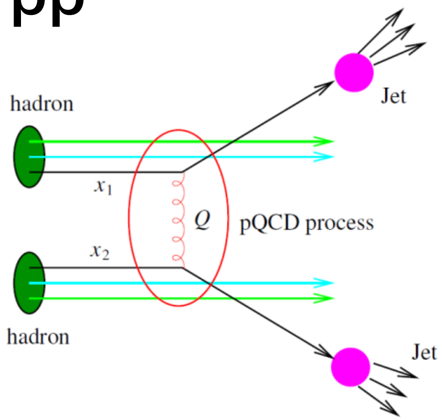

In-medium fragmentation (Pb-Pb collisions)

Quenching→parton lose energy through medium-induced gluon radiations and collisions with medium constituents

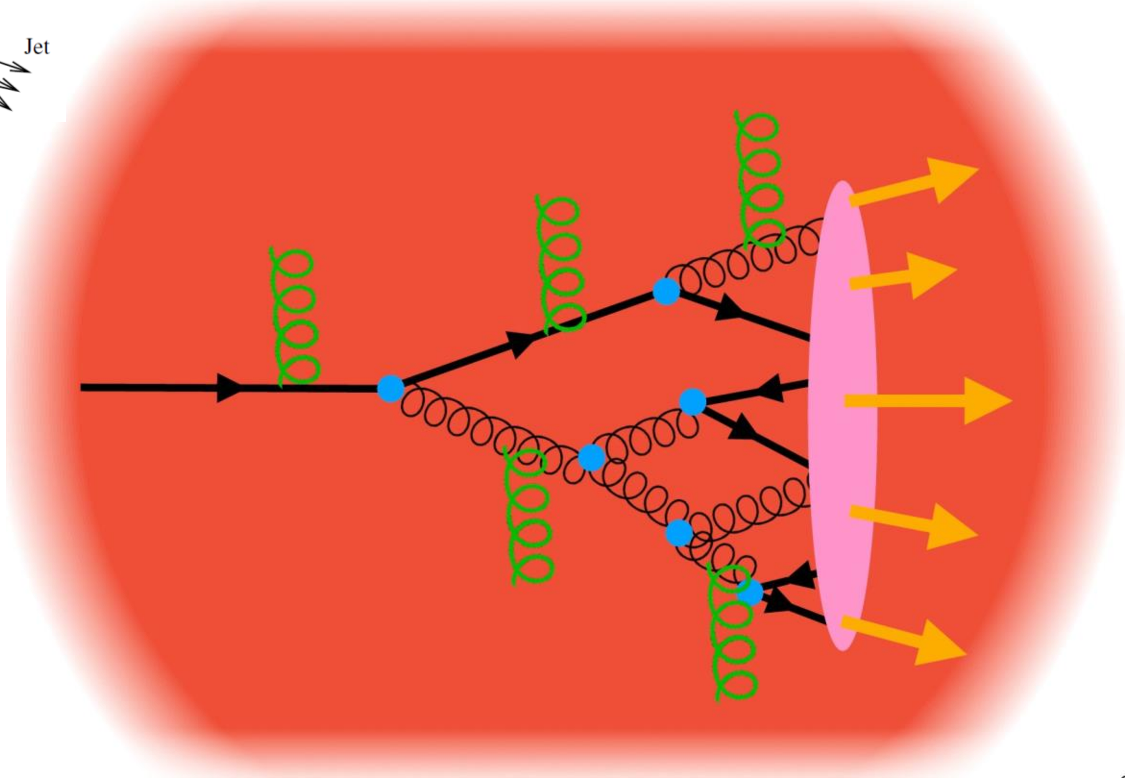

Nuclear modification factor: R_{AA}

$$R_{AA} = \frac{1}{\langle N_{coll} \rangle} \frac{dN_{AA}/dp_T}{dN_{pp}/dp_T}$$

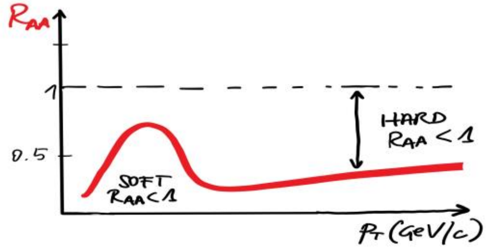

Parton energy loss in QGP

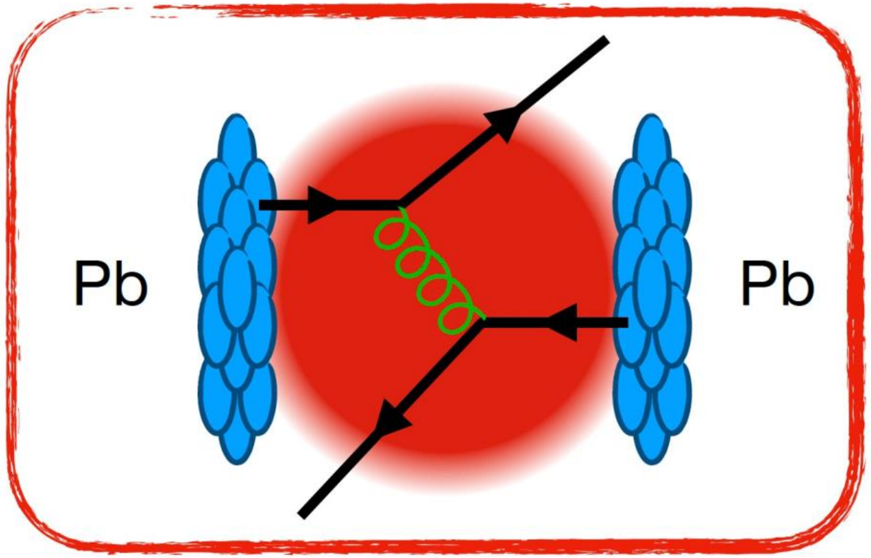

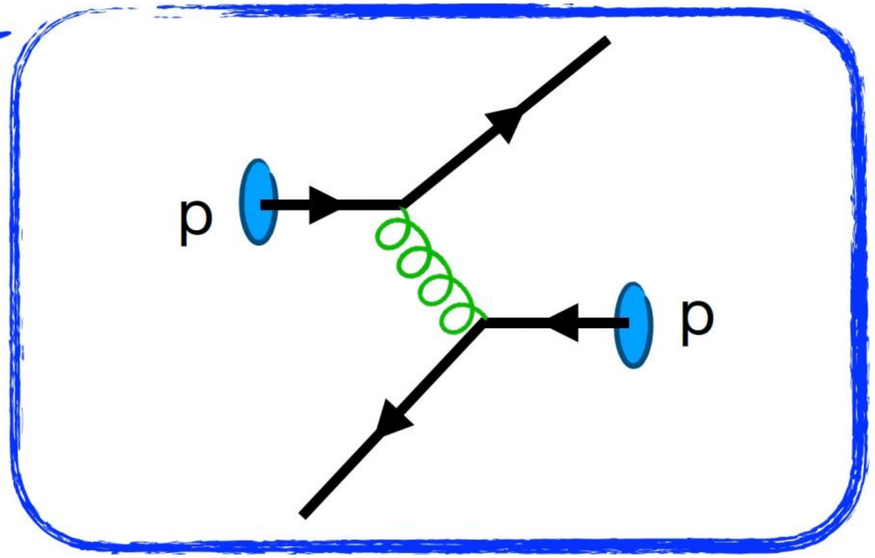

$R_{AA} > 1 \rightarrow$ enhancement

$R_{AA} = 1 \rightarrow$ no medium modification

$R_{AA} < 1 \rightarrow$ supression

Anisotropic flow

- Initial geometrical anisotropy ("almond" shape) in non-central HI collisions → eccentricity

$$\varepsilon = \frac{y^2 - x^2}{y^2 + x^2}$$

Coordinate space

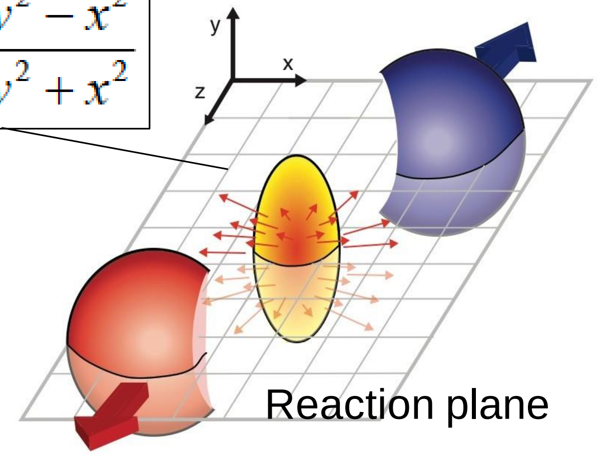

- **Pressure gradients** develop → more and faster particles along the reaction plane than out-of-plane

Scatterings among produced particles convert **anisotropy** in coordinate space into an observable momentum anisotropy

→ **anisotropic flow**

→ quantified by a Fourier expansion in azimuthal angle !

Momentum space

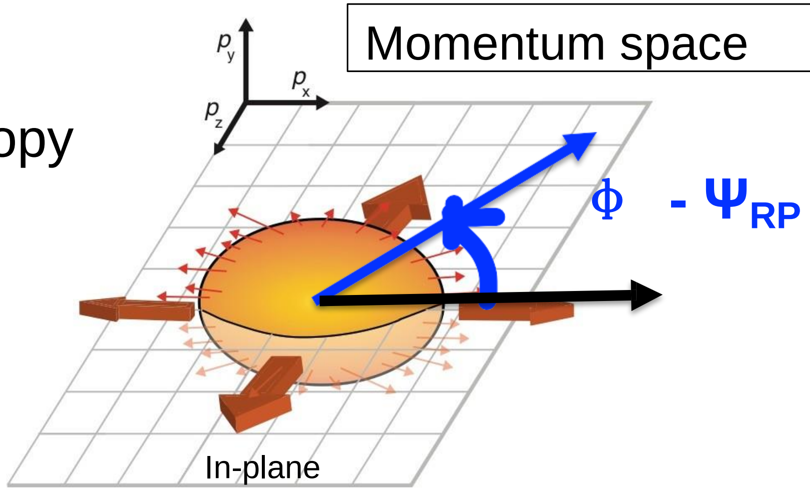

v_n = **harmonics**

$$E\frac{d^3N}{dp^3} = \frac{1}{2\pi}\frac{d^2N}{p_T dp_T dy}\left(1 + 2\sum_{n=1}^{\infty} v_n \cos[n(\varphi - \Psi_n)]\right),$$

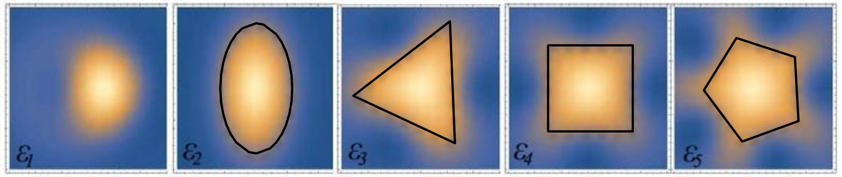

Fig. 2. (color online) Characteristic shapes of the deformed initial state density profile, corresponding to anisotropies of $\mathcal{E}_1$, $\mathcal{E}_2$, $\mathcal{E}_3$, $\mathcal{E}_4$ and $\mathcal{E}_5$ (from left to right).

ALICE detector

Detector:
Length: **26** meters
Height: **16** meters
Weight: **10,000** tons

Solenoid: magnetic field B = 0.5 T

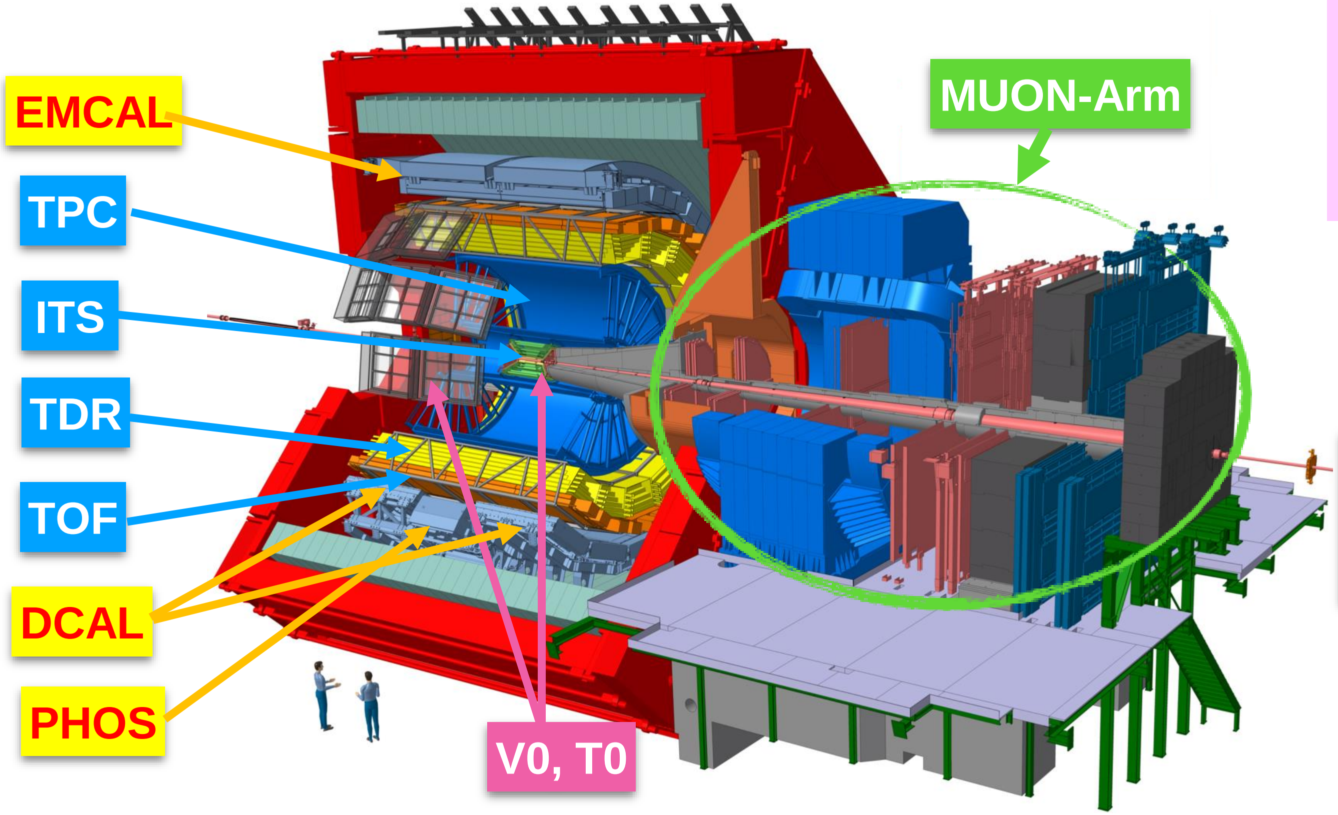

Dedicated to measure hadrons, electrons, muons and photons to cope with very high multiplicities

Muon-Arm ($-4<\eta<-2.5$):
Muon trigger, tracking, PID;
Heavy-floavor hadrons and W/Z^0

Central Barrel ($|\eta|<0.9$)

- **ITS, TPC**: vertexing + 2π tracking and PID down to very low pT~0.1 GeV/c
- **EMCal/Dcal, PHOS:** high-p_T electron trigger, PID, photon, high pT pi0 and electrons

TOF, TRD, HMPID, etc.:
Particle identification detectors

Forward rapidity detector (**V0, T0, ZDC, SPD):**
Trigger, centrality selection, event plane rec.

ALICE detector

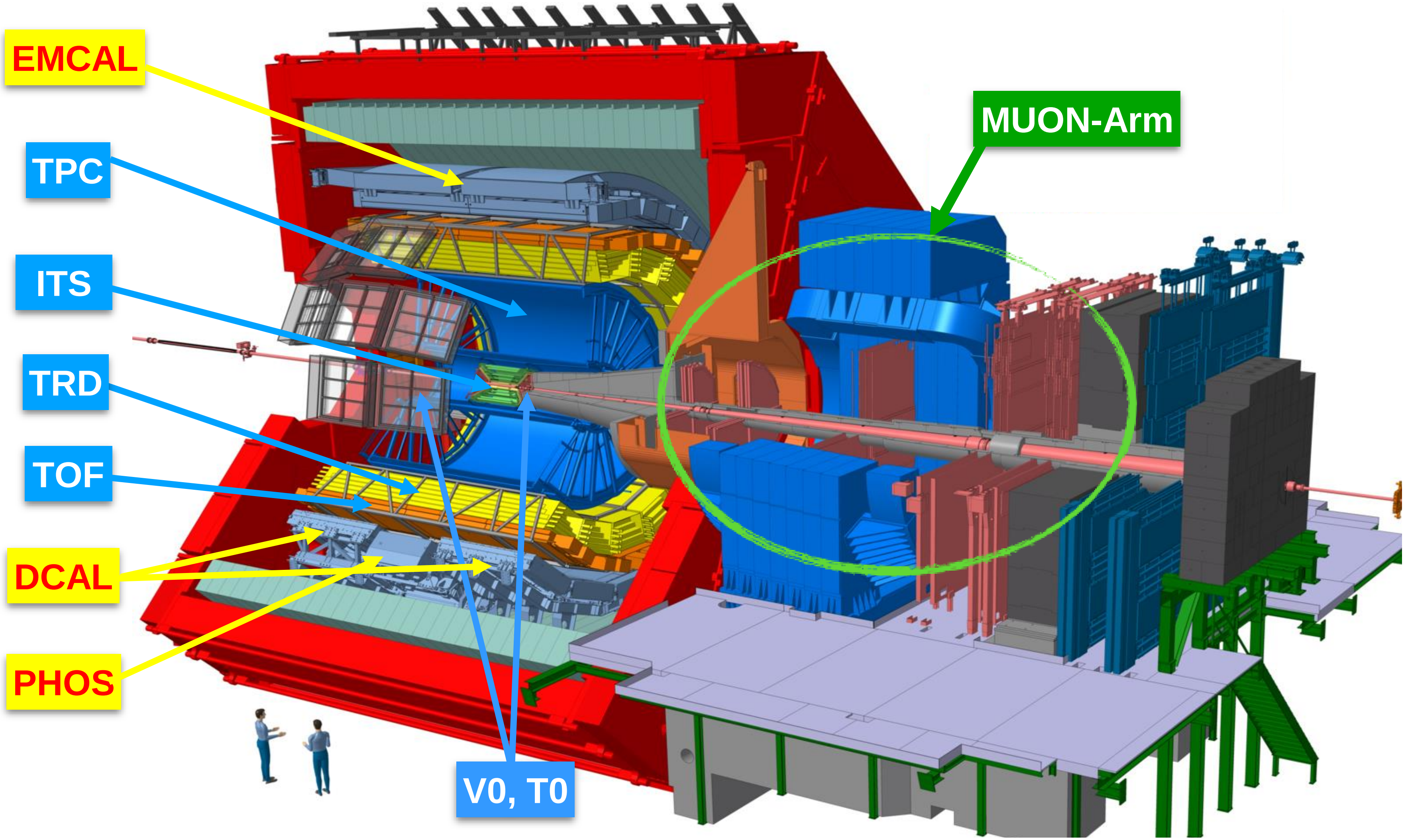

ALICE 国际合作组

- 40个国家
- 169个研究机构
- 2000名合作者

中国组（七个单位）

华中师范大学
中国原子能科学研究院
复旦大学
中国科学技术大学
中国地质大学
华中科技大学
湖北工业大学

中国组的贡献： 光子谱仪(PHOS)，取样电磁量能器（DCAL/EMCAL），硅像素内层径迹探测器（ITS2），前向缪子径迹探测器（MFT），正在研制中的前向强子量能器（FOCAL）和 内层探测器升级（ITS3）

LHC上运行的粒子束流

Comprehensive study of Pb-Pb, p-Pb, pp as well as the collision of lighter ions: Xe (done), O (planned for 2024)

pp

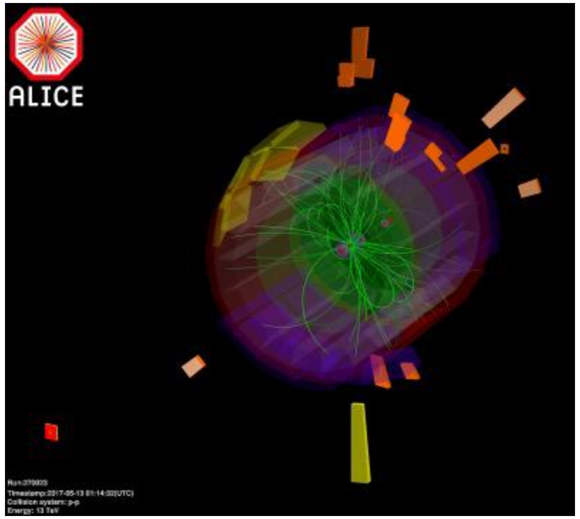

$^{(*)}\sqrt{s_{\mathrm{NN}}} = 0.9, 2.76, 5.02, 7, 8, 13\ TeV$

p-Pb

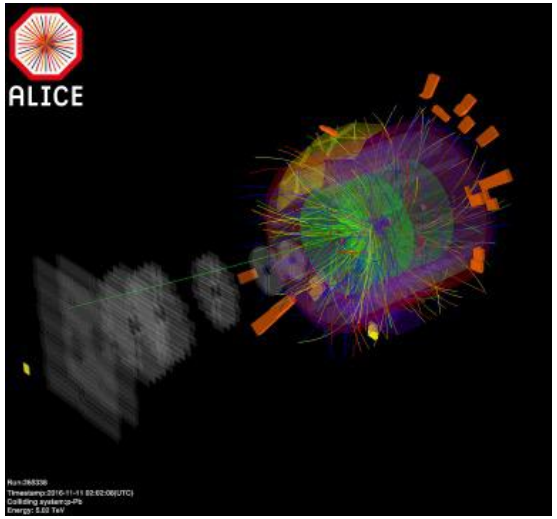

$^{(*)}\sqrt{s_{\mathrm{NN}}} = 5.02, 8.16\ TeV$

Xe-Xe

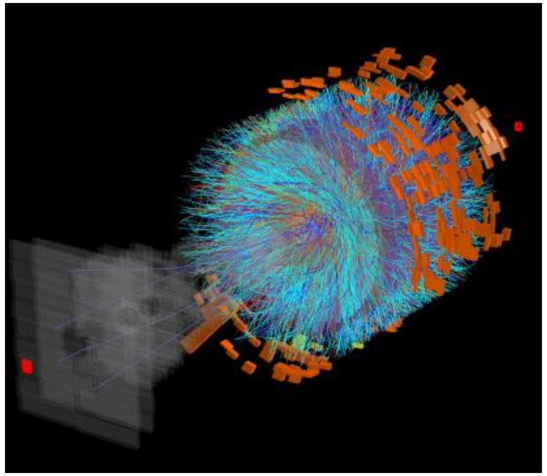

$^{(*)}\sqrt{s_{\mathrm{NN}}} = 5.44\ TeV$

Pb-Pb

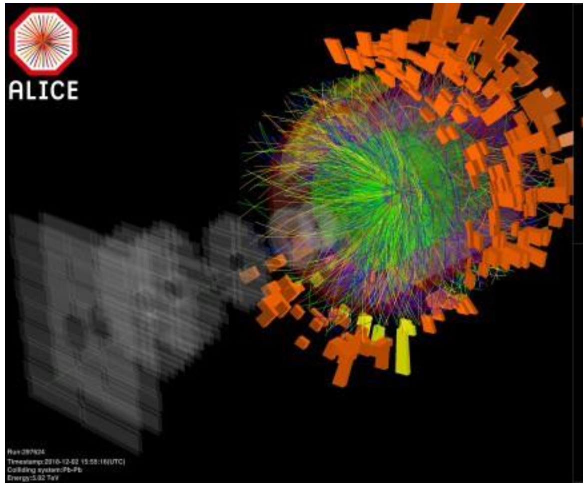

$^{(*)}\sqrt{s_{\mathrm{NN}}} = 2.76, 5.02\ TeV$

(*) collisions energy in Run 1 and 2

QGP物质基本性质观测：能量密度-温度-寿命

According to LQCD, the QGP is formed when

$$\varepsilon_c = (0.42 \pm 0.06)\ GeV/fm^3$$ critical energy

$$T_c = (156.5 \pm 1.5)\ MeV$$ critical temperature

For comparison
T=156 MeV ≙ $1.8 \cdot 10^{12}$ K
Sun core: $1.5 \cdot 10^{7}$ K
Sun surface: 5778 K

能量密度

Phys. Rev. D **27**, 140

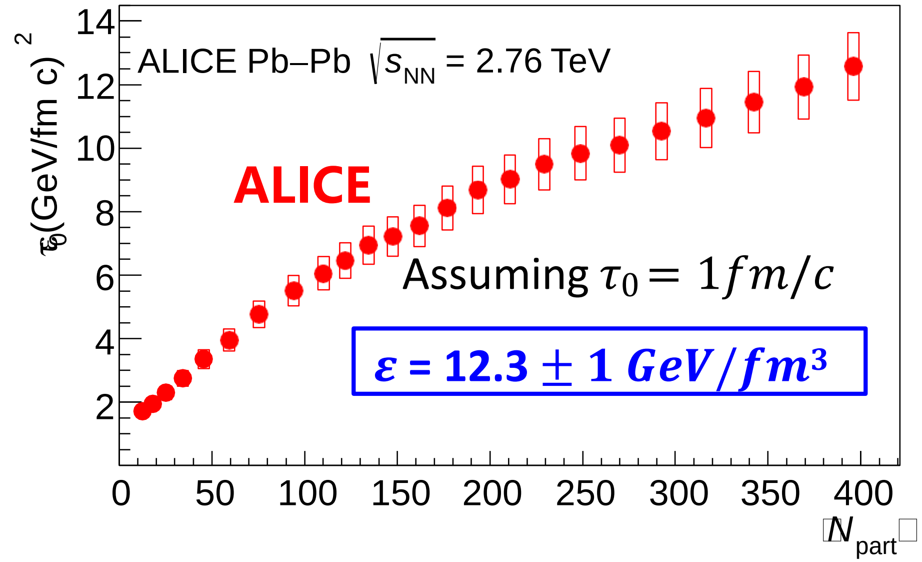

温度

PLB 754 (2016) 235

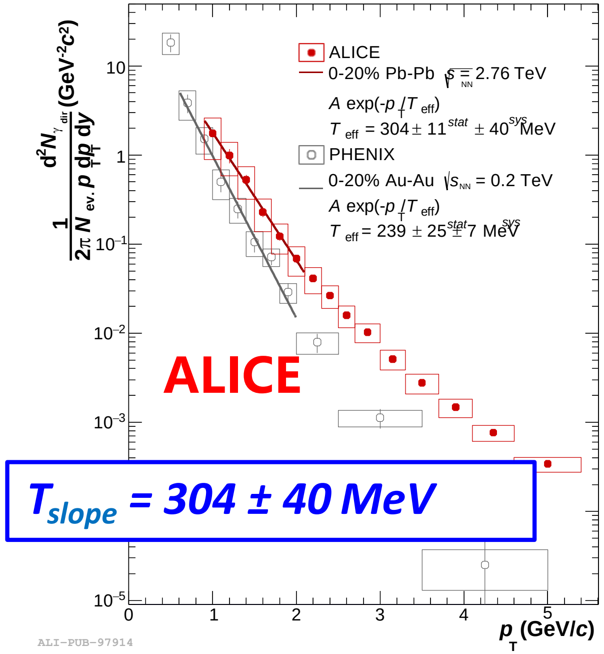

寿命和体积

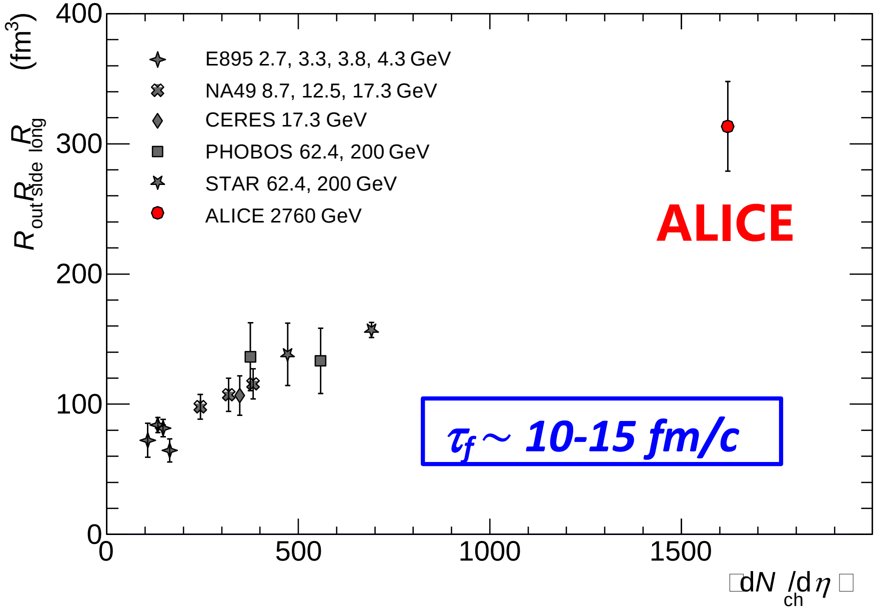

Charged particle R_{AA}

ALICE, *PLB* 720 (2013) 52

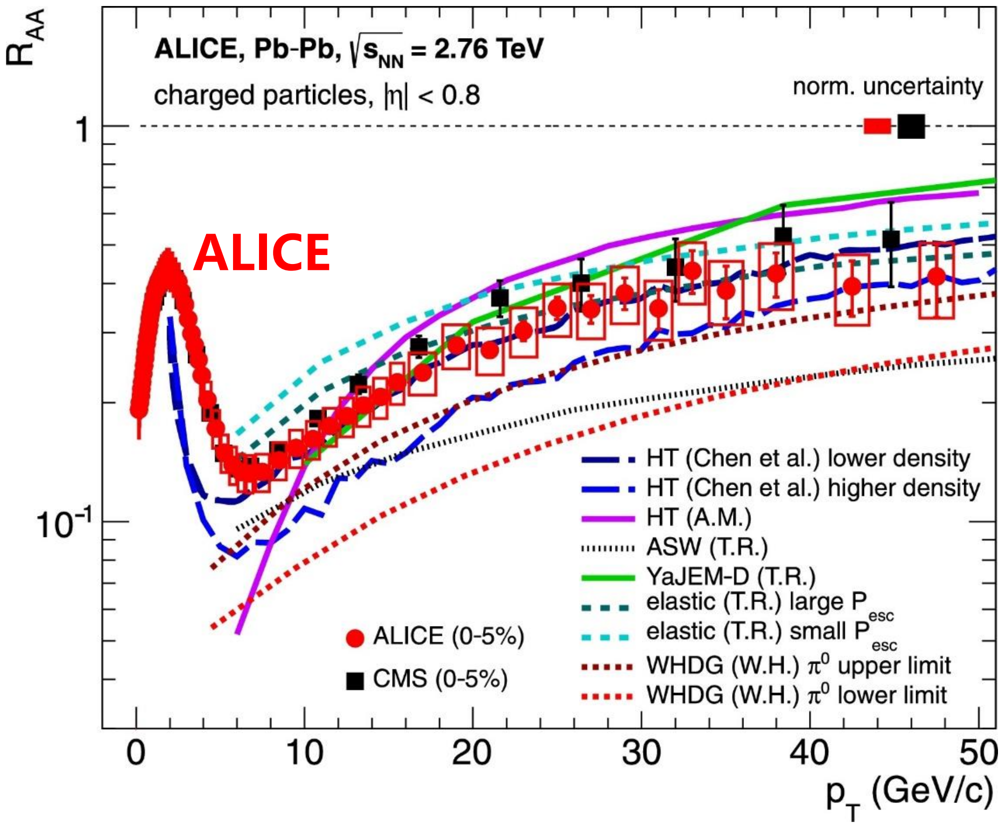

PHENIX: PRC69, 034910(04) STAR: PRL91, 172302(03)

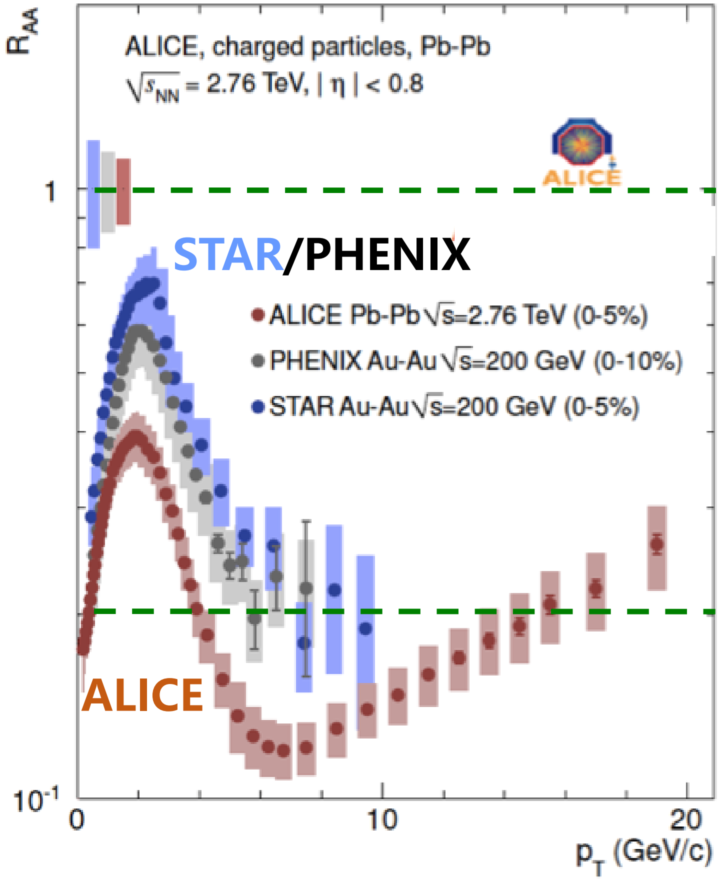

1) At LHC(2.76TeV), the energy loss is stronger than that from RHIC (0.2TeV)
➔ hotter/denser medium created at higher collision energy

T = 304 ± 40 MeV

2) pQCD predictions consistent at larger p_T region: > 10 GeV/c

$\varepsilon = 12.3 \pm 1\ GeV/fm^3$

Charm particle R_{AA}

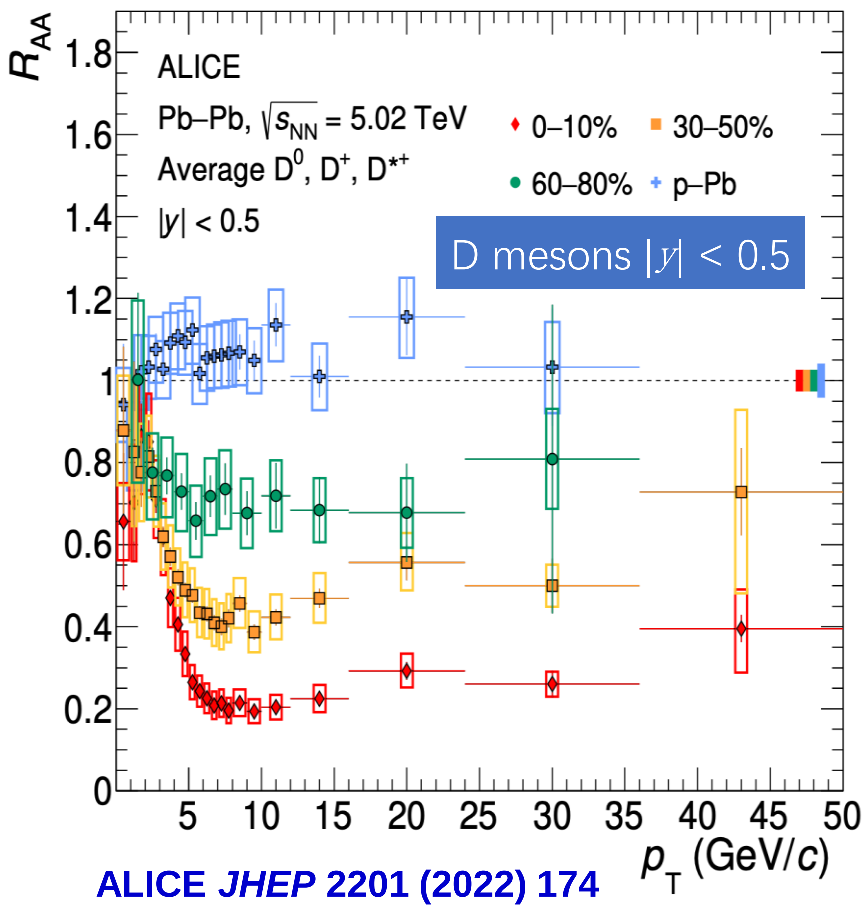

ALICE *JHEP* 2201 (2022) 174

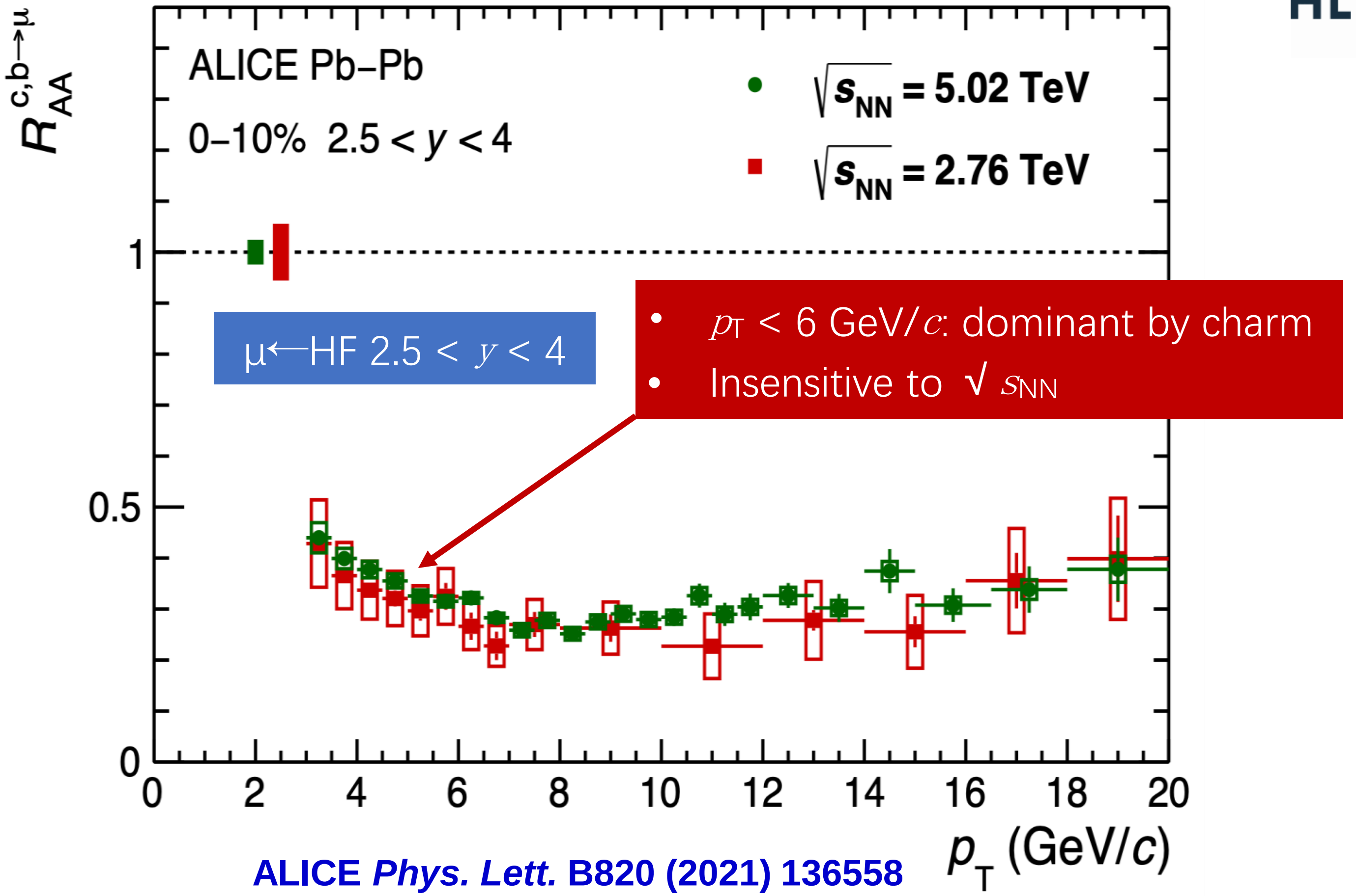

ALICE *Phys. Lett.* B820 (2021) 136558

- Suppression increases from peripheral to central collisions
- Similar suppression in the most central collisions between mid- and forward-rapidity

→ Charm quarks undergo strong energy loss in a wide rapidity range

Mass dependence of energy loss

JHEP 12 (2022) 126
JHEP 05 (2021) 220

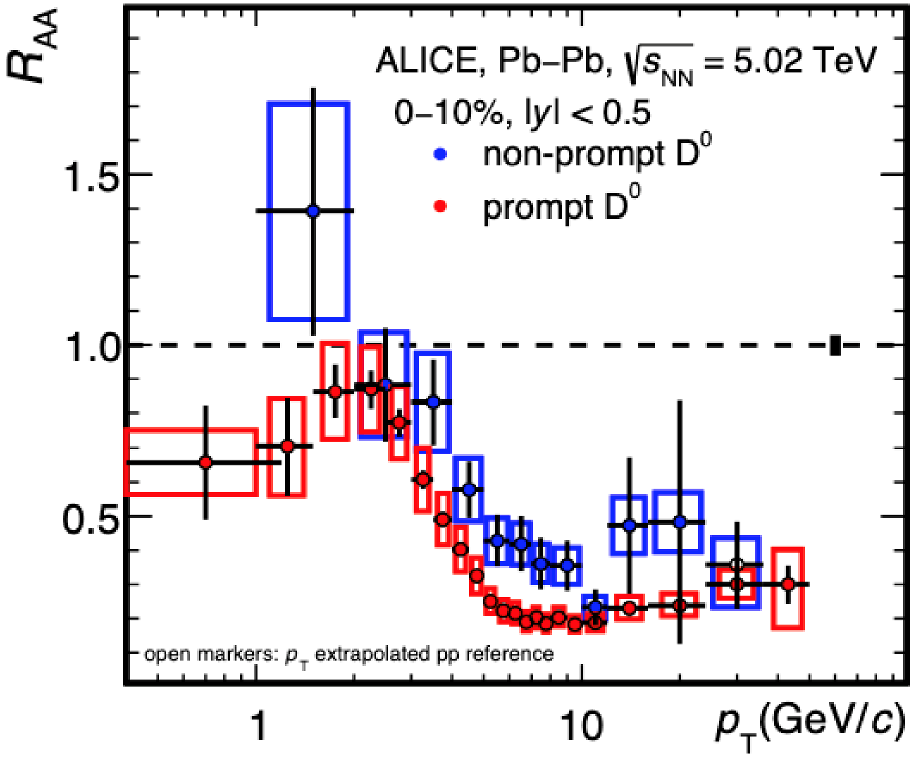

JHEP 01(2022)174

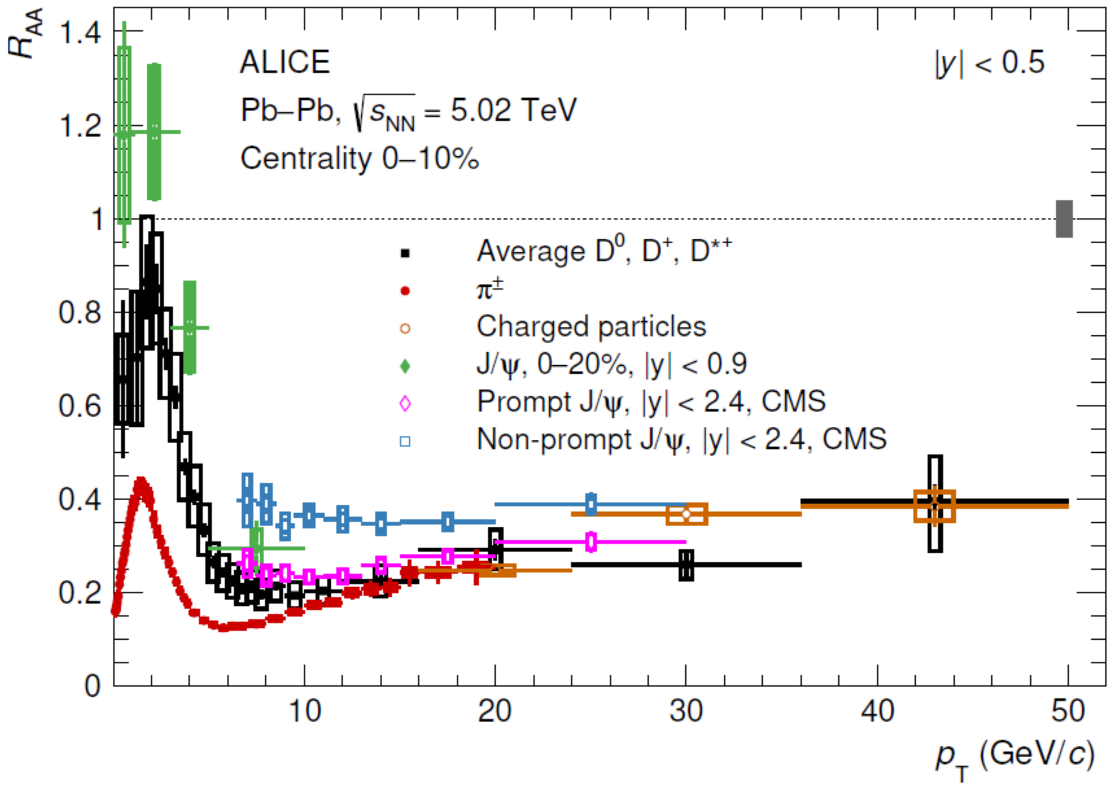

- Less suppression observed in the R_{AA} of non-prompt D0 mesons than the prompt D0
- Stronger suppression observed in the R_{AA} of charged particles than the heavy quarks

➢ **$\Delta E\pi$** > ΔE_c > ΔE_b

Charm quark energy loss: comparison with models

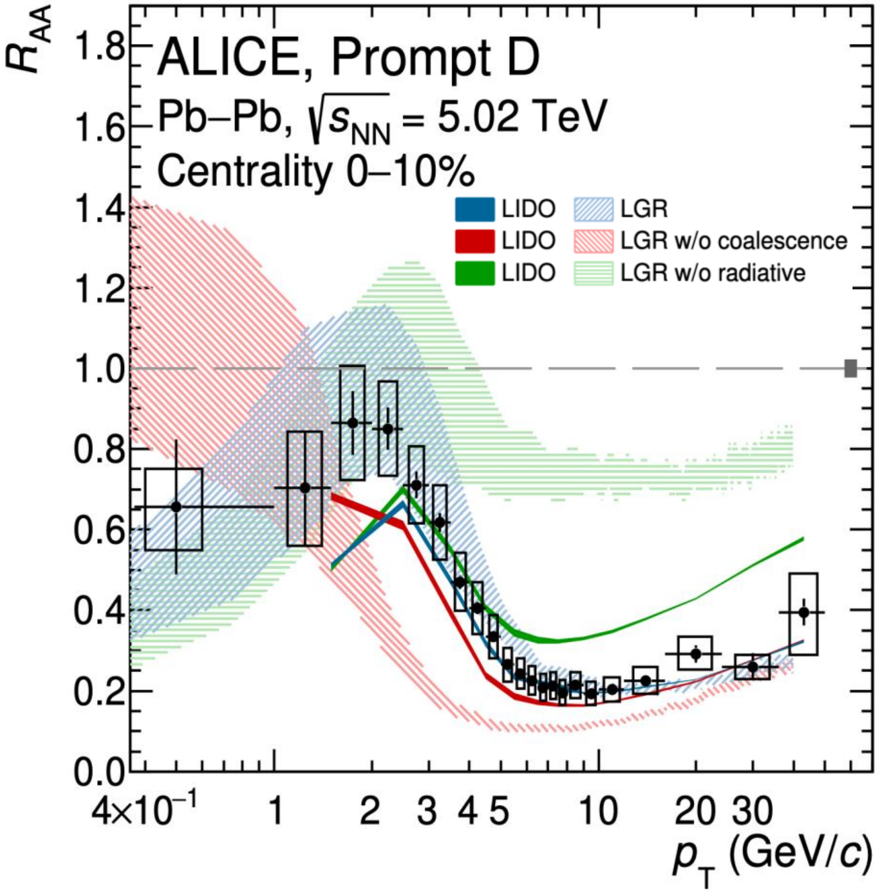

***JHEP* 2201 (2022) 174**

- **W/o coalescence**: large deviation from data
  - ➞ Hadronization via coalescence is important to interpret data
- **W/o radiative energy loss**: reasonably describe data in p_T < 5 GeV/c, but largely overestimate data at high p_T
  - ➞ Radiative energy loss is dominant at high p_T, while collisional energy loss is predominant at low and intermediate p_T

J/ψ suppression & regeneration

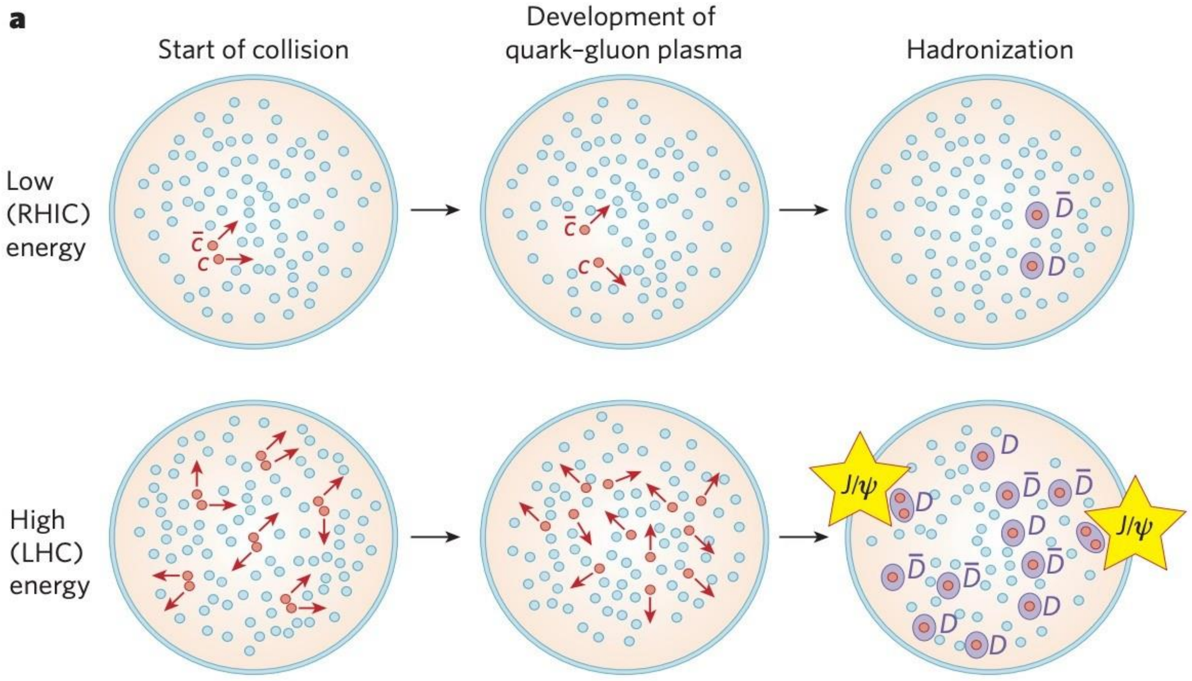

P. Braun-Munzinger, J. Stachel., Nature 448, 302–309 (2007)

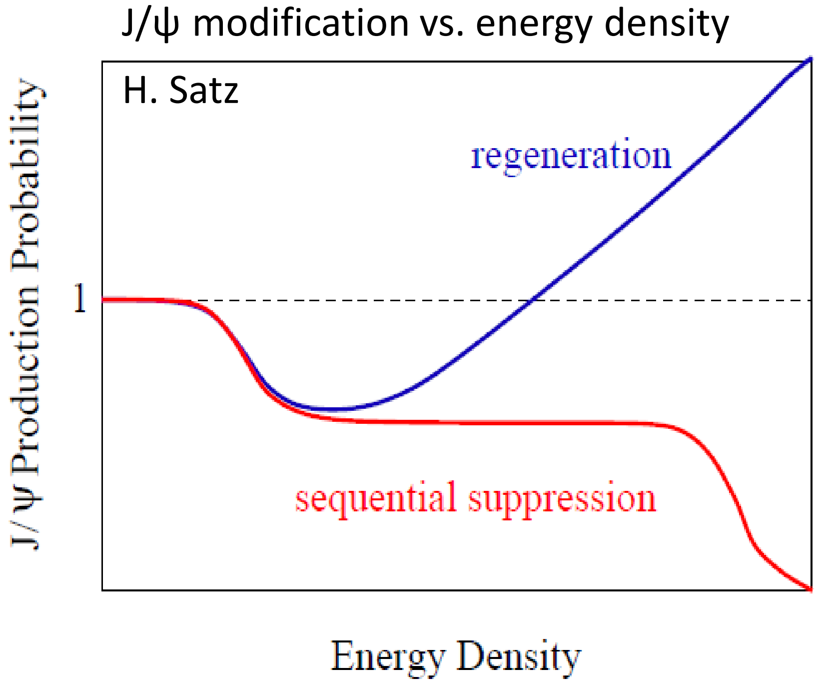

Regeneration of charmonium and charmed hadron production take place at the phase boundary or in QGP.

Dissociation and regeneration take place in opposite directions vs energy density.

J/ψ suppression & regeneration

PLB 849 (2024) 138451; *JHEP* 02 (2024) 066

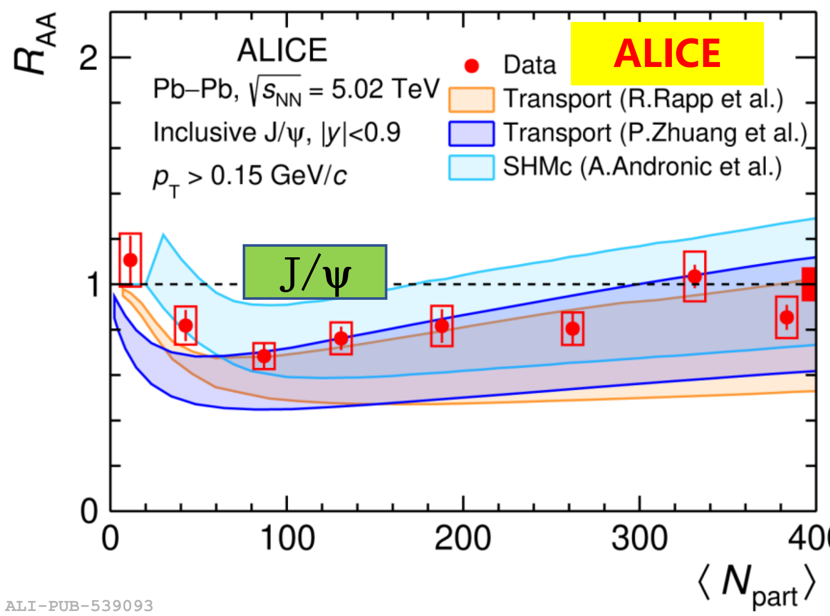

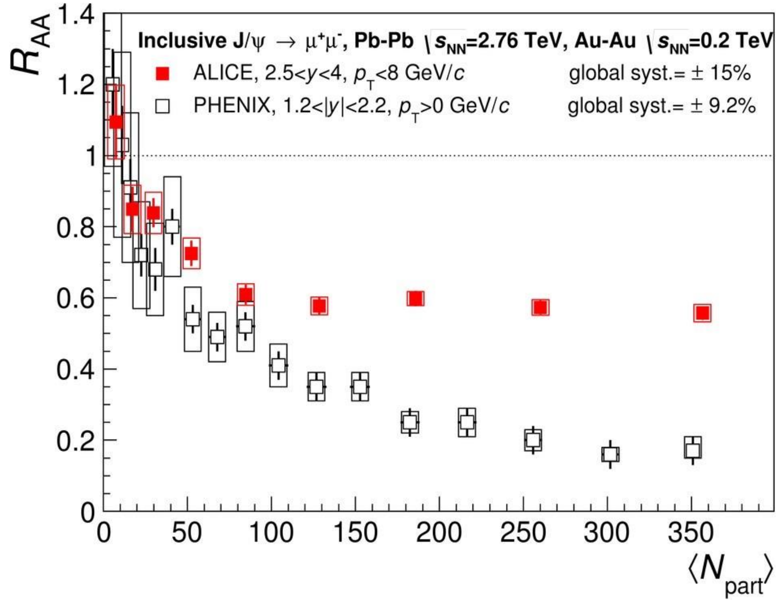

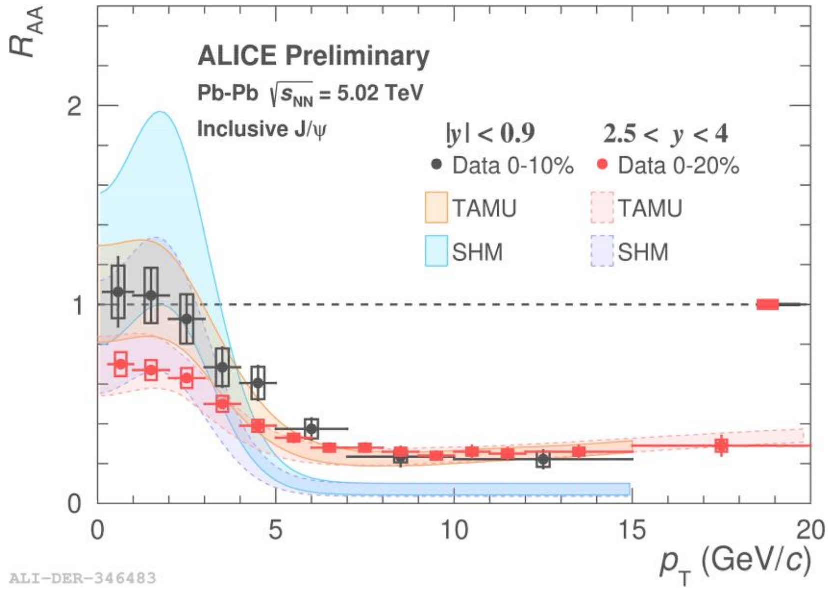

- ALICE data from 5.02 TeV Pb-Pb collisions confirm the J/ψ recombination picture:
  - ➢ R_{AA} increase with centrality
  - ➢ R_{AA}(LHC) > R_{AA}(RHIC)
  - ➢ R_{AA} midrapidity > R_{AA} forward rapidity,
- Evidence for the deconfinement and (re)generation

2.5.1 Study of the charmonium ground state: evidence for the (re)generation and demonstration of deconfinement at LHC energies

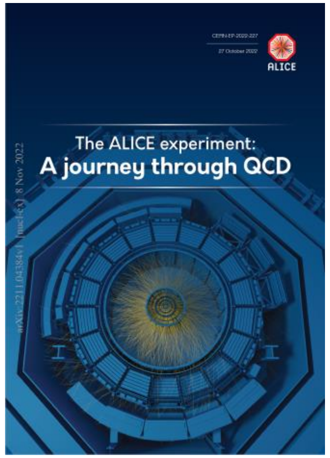

Medium response and recoil jet broadening

R=0.4, 0−10%

$10 < p_{T,jet} < 20 GeV/c$

ALICE: ***PRL* 133, 022301 (2024) & *PRC* 110, 014906 (2024)**

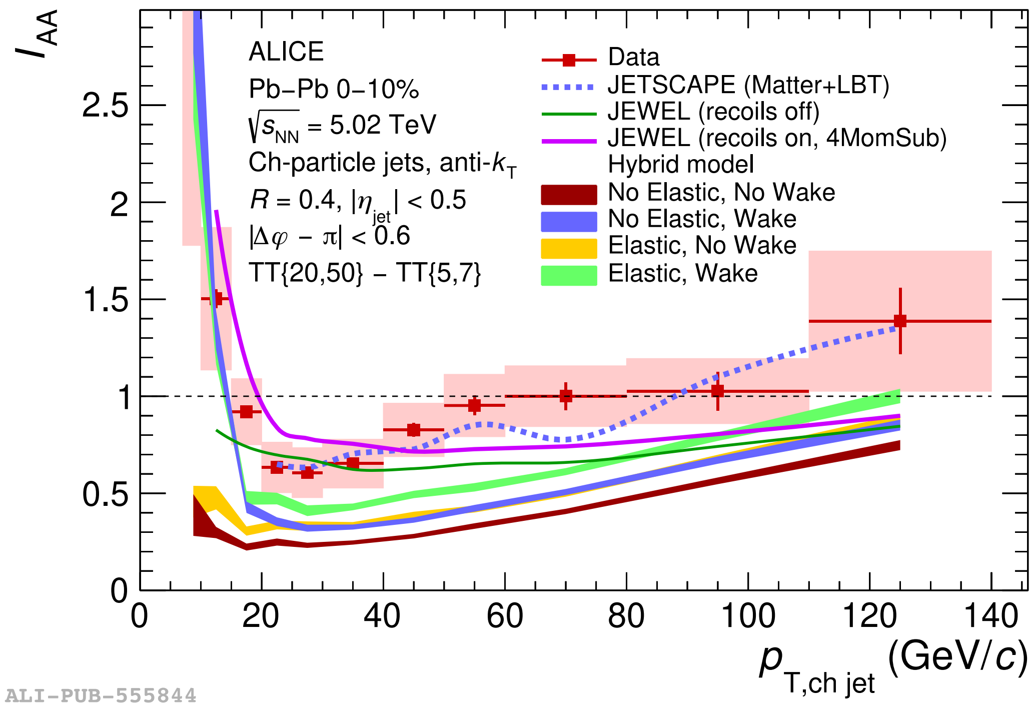

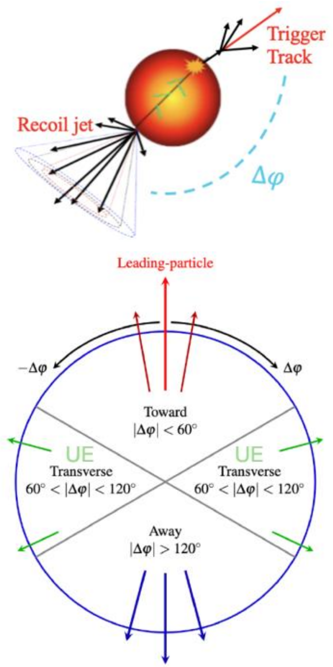

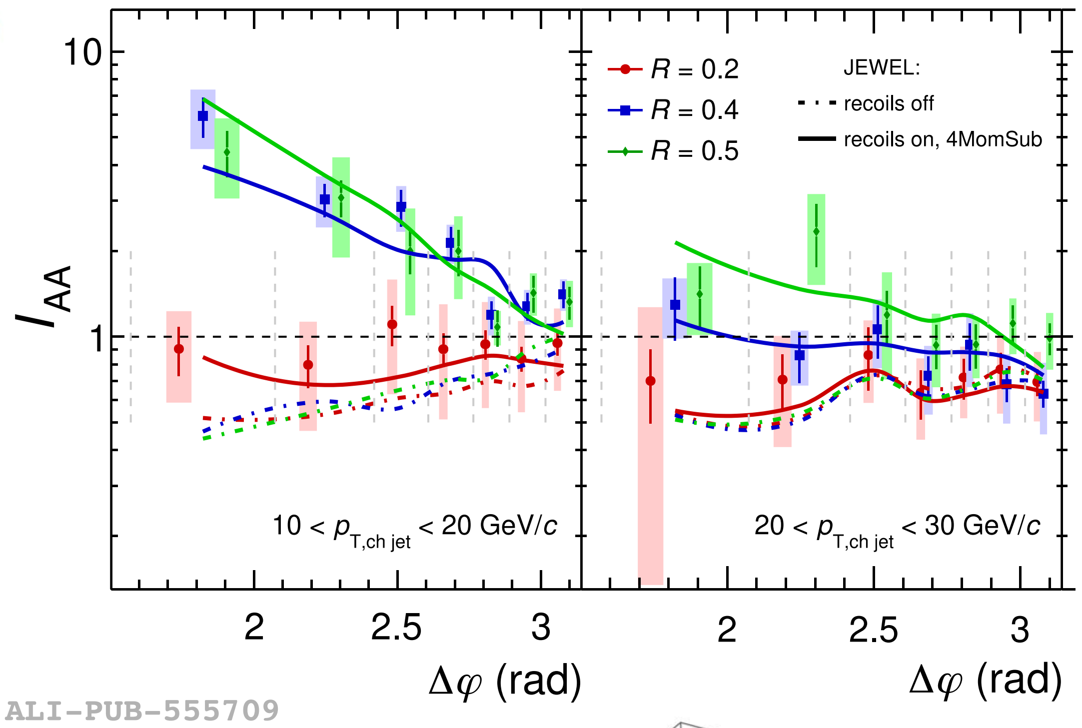

- First observation of recoil jet yield enhancement and medium-induced acoplanarity broadening at low-p_T with ALICE

➢ Medium response is favored

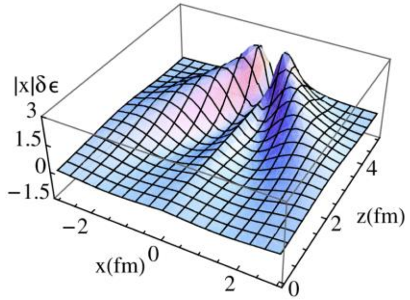

G-Y. Qin et. al, PRL103, 152303 (2009)

Elliptic flow

ALICE: ***Phys. Rev. Lett.*** **105, 252302 (2010)**

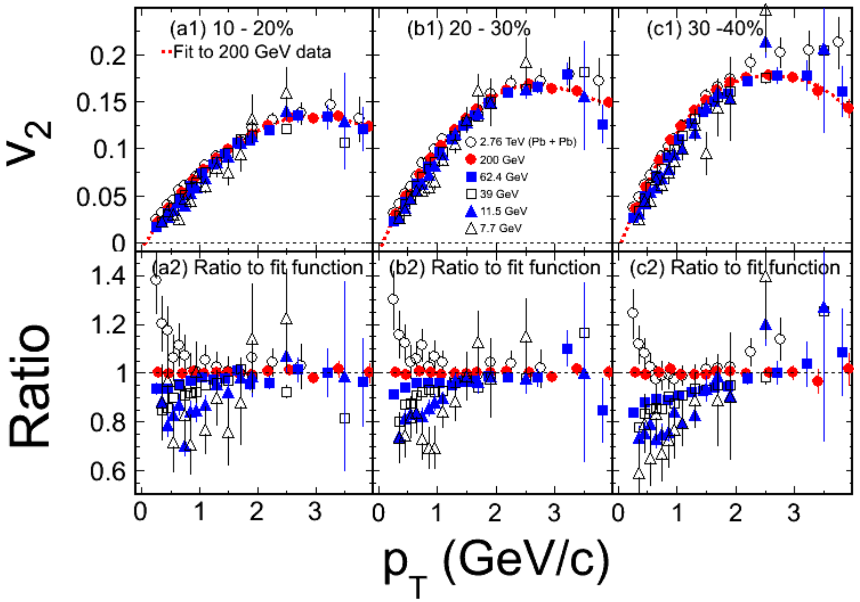

JHEP **06 (2015) 190**

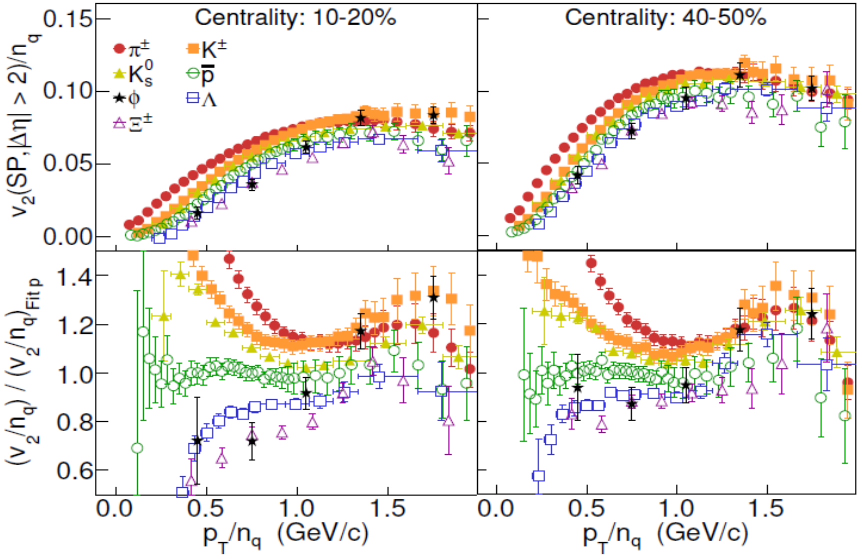

EPJC **83(2023)1123**

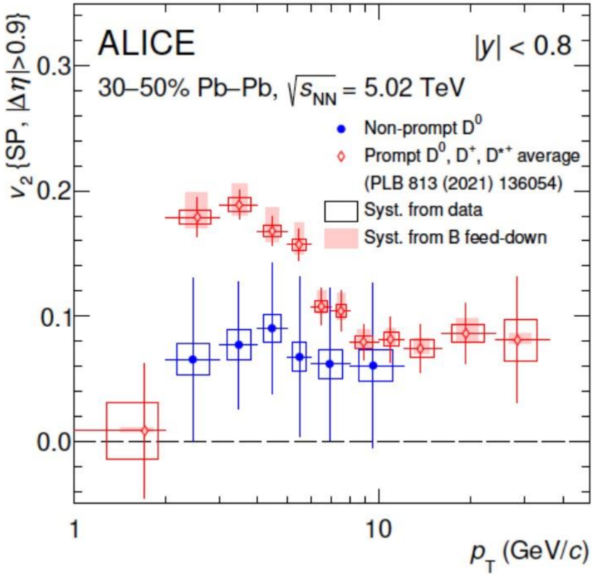

- Stronger elliptic collective flow observed in charged particle at the LHC energies
- Non-zerzo elliptic flow observed in prompt and nor-prompt D0 from bottom hadron decays and lower than that of prompt D0 for pT <~ 6 GeV/c
- Deviations from NCQ scaling at the level of ±20% indicated

Elliptic flow from large to small systems

Elliptic flow from two(multi)-particle correlations:

$v_2\{2\} > 0$

- subtract jets and other physical 2-particle correlations due to non-flow
- measure with rapidity gap

In AA collisions, collectivity originates from the presence of a strongly-interacting QGP

OPEN QUESTION: what is the origin of the emerging collectivity in pp, p-Pb collisions?

Elliptic flow from multi-particle correlations in all systems

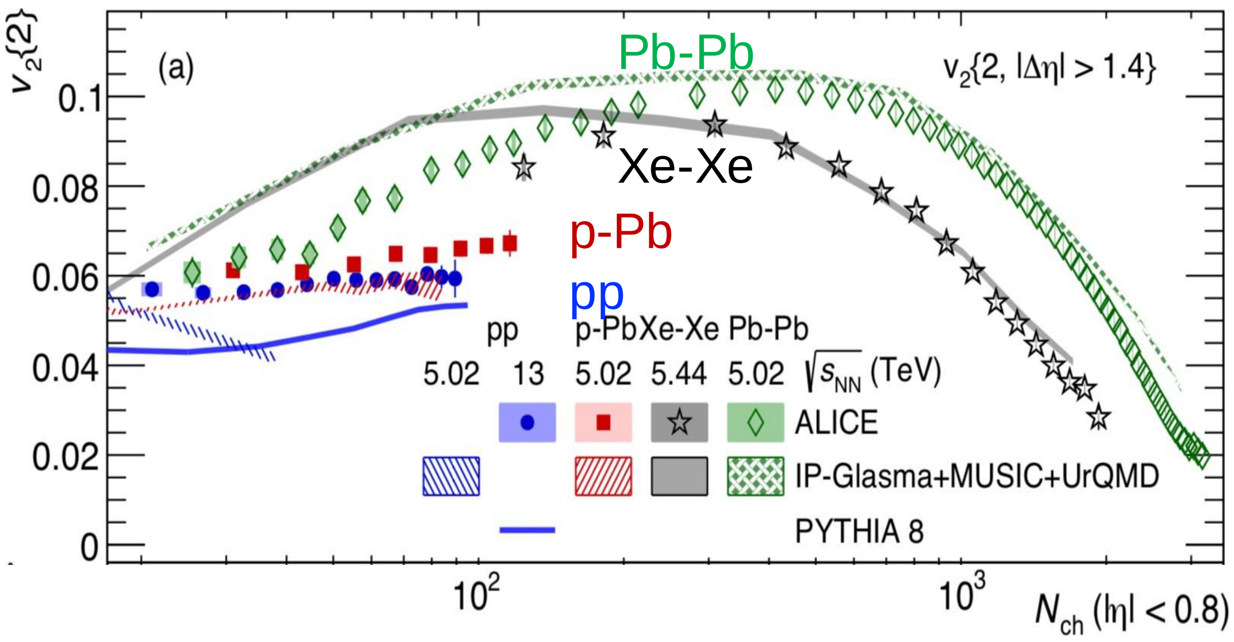

***PRL* 123 (2019)142301**

- 初始几何
- 流体力学演化
- 夸克"聚并"强子化

小系统碰撞中的奇异增强

ALICE：*Nature Phys.* 13 (2017) 535-539

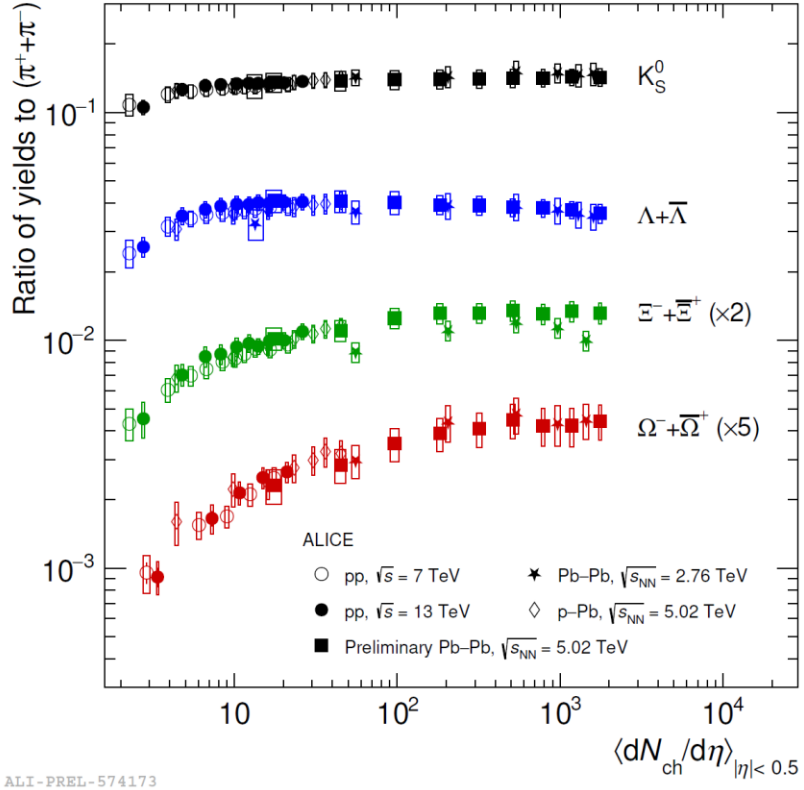

nature physics LETTERS
PUBLISHED ONLINE: 24 APRIL 2017 | DOI: 10.1038/NPHYS4111
OPEN

Enhanced production of multi-strange hadrons in high-multiplicity proton–proton collisions

ALICE Collaboration†

At sufficiently high temperature and energy density, nuclear matter undergoes a transition to a phase in which quarks and gluons are not confined: the quark–gluon plasma (QGP)[1]. Such an exotic state of strongly interacting quantum chromodynamics matter is produced in the laboratory in heavy nuclei high-energy collisions, where an enhanced production of strange hadrons is observed[2–6]. Strangeness enhancement, originally proposed as a signature of QGP formation in nuclear collisions[7], is more pronounced for multi-strange baryons. Several effects typical of heavy-ion phenomenology have been observed in high-multiplicity proton–proton (pp) collisions[8,9], but the enhanced production of multi-strange particles has not been reported so far. Here we present the first observation of

equilibrium and can be described using a grand-canonical statistical model[12,13]. In peripheral collisions, where the overlap of the colliding nuclei becomes very small, the relative yields of strange particles to pions decrease and tend toward those observed in pp collisions, for which a statistical-mechanics approach can also be applied[14,15]. Extensions of a pure grand-canonical description of particle production, such as statistical models implementing strangeness canonical suppression[16] and core–corona superposition[17,18] models, can effectively produce a suppression of strangeness production in small systems. However, the microscopic origin of enhanced strangeness production is not known, and the measurements presented in this Letter may contribute to its understanding. Several effects, such as azimuthal correlations and mass-dependent hardening of p_T distri- ... typically attributed to the

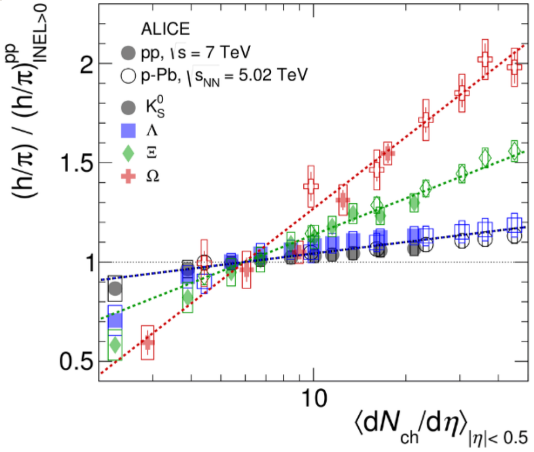

- 首次在小系统pp和p-Pb碰撞中观测到奇异粒子产额随多重数增强的现象，并与核-核碰撞光滑链接；
- 没有碰撞能量依赖性; 高奇异数粒子增强更强
- 物理模型难于解释（粒子产生的微观机制）
  - ➢ 奇异产额增强否是QGP物质生成的信号 (thermalization, equilibration?)
  - ➢ 对碎裂函数的普适性和因子化的一种挑战 (string overlap, color reconnection? Hadron scattering)

Strange baryon-to-meson enhancement in p-Pb coll.

- Understanding hadronization & non-perturbative effects of the underlying event
- Baryon-to-meson enhancement observed in A+A: flowing medium + quark coalescence

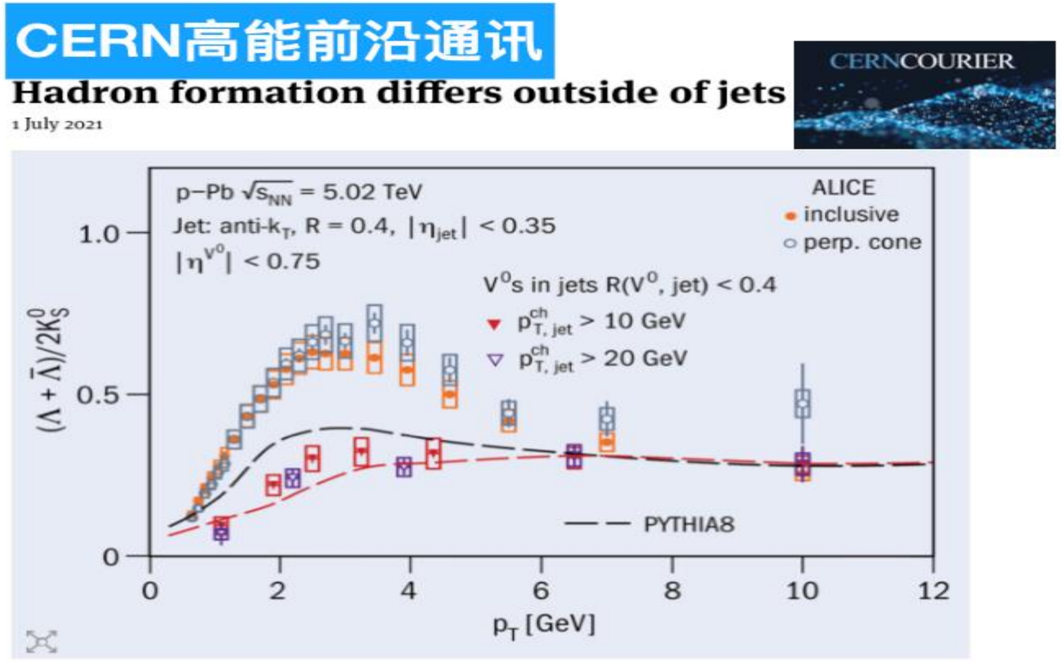

PLB 827 (2022) 136984; JHEP 07 (2023) 136

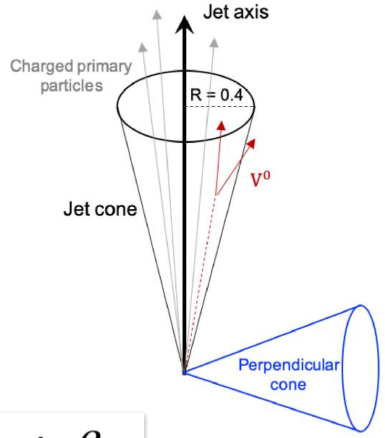

$p = p_0 + \beta m$

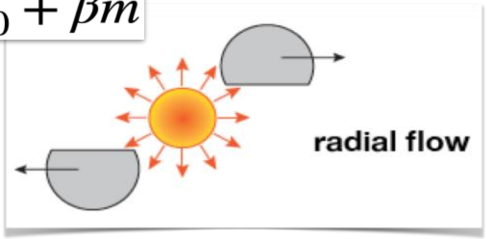

- Ratio in jets does not show a maximum at intermediate p_{T}, ratio with UE selection is systematically higher than the inclusive in 2 < p_{T} < 5 GeV/c
- PYTHIA 8 hard QCD is consistent with ratio in jets but does not reproduce the inclusive ratio at low and intermediate p_{T}
- No baryon-to-meson enhancement observed in jets , only soft contribution from bulk –> property of soft UE
- input to modelling (hadronization / coalescence)

Charm hadronization

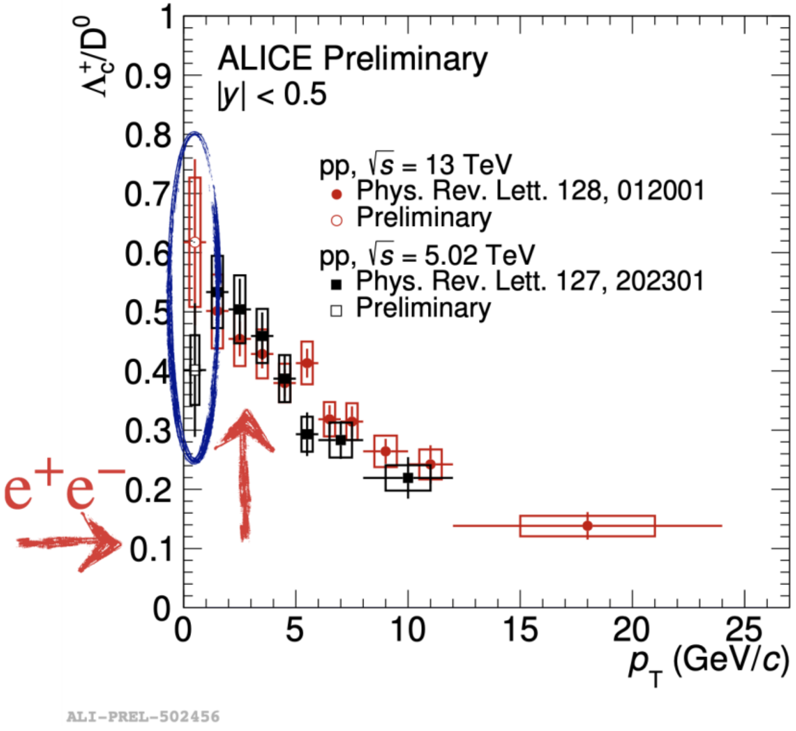

PRL 128 (2022) 012001
PRC 107 (2023) 064901

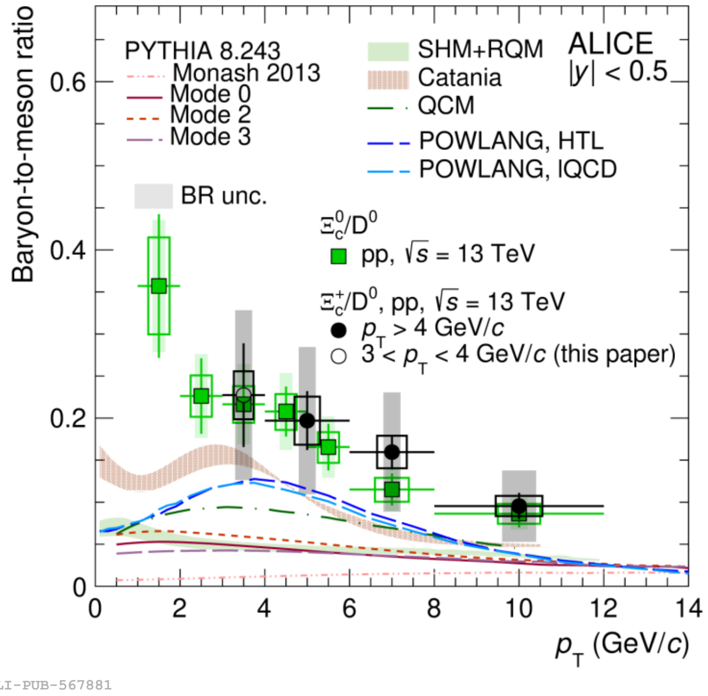

PRL 127 (2021) 272001
JHEP 12 (2023) 086
JHEP 10 (2021) 159

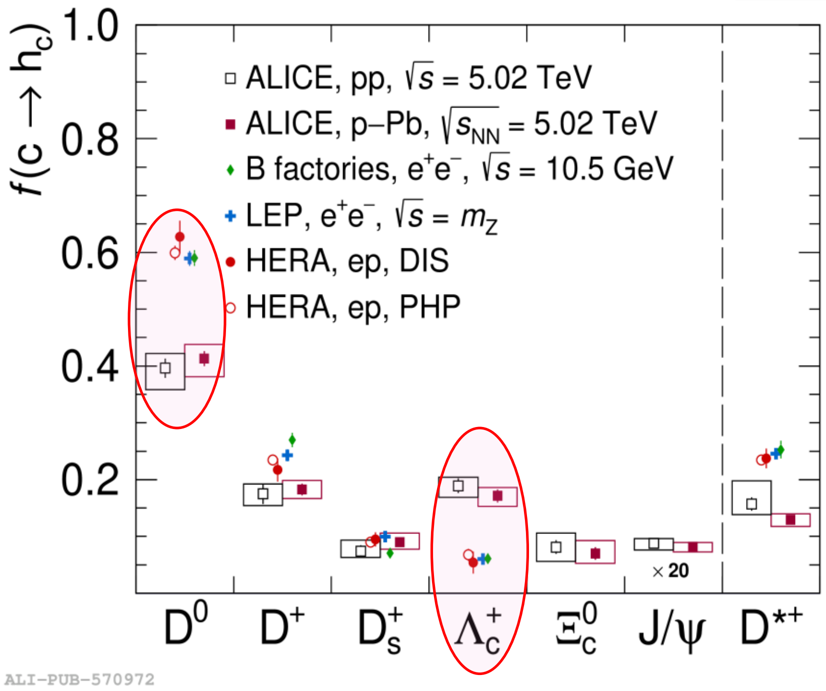

PRD 105 (2022) L011103
JHEP 12 (2023) 086
PLB 846 (2023) 137625
arXiv:2405.14571 (Submitted to *EPJC*)

- 首次观测到Λ_c^+/D^0、$\Xi_c^{0,+}/D^0$ 和 Ω_c^0/D^0 比值的显著增强现象 ($\Sigma_c^{0,++}$对Λ_c^+/D^0比值增强贡献~40%)
- 强子化理论模型明显低估奇异粲重子$\Xi_c^{0,+}/D^0$与Ω_c^0/D^0的增强效应
- 首次观测到粲夸克碎裂份额在强子碰撞与e^+e^-碰撞有明显差异，表现出粲夸克强子化修正

QCD死角效应的直接观测

Dokshitzer, Khoze, Troian,J. Phys. G 17 (1991) 1602

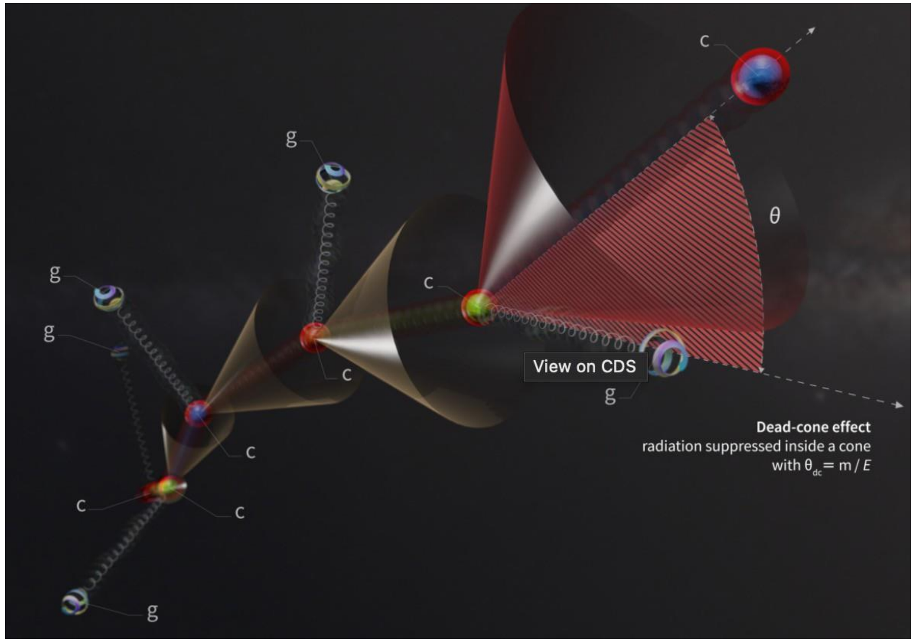

D. Dominguez / CERN

A fundamental QCD feature : Gluon emission suppressed in a cone with

$\theta_{dc} = m_Q / E_{radiator}$

$$R(\theta) = \frac{dn/d\ln 1/\theta|_{D0\ jets}}{dn/d\ln 1/\theta|_{incl.,jets}}$$

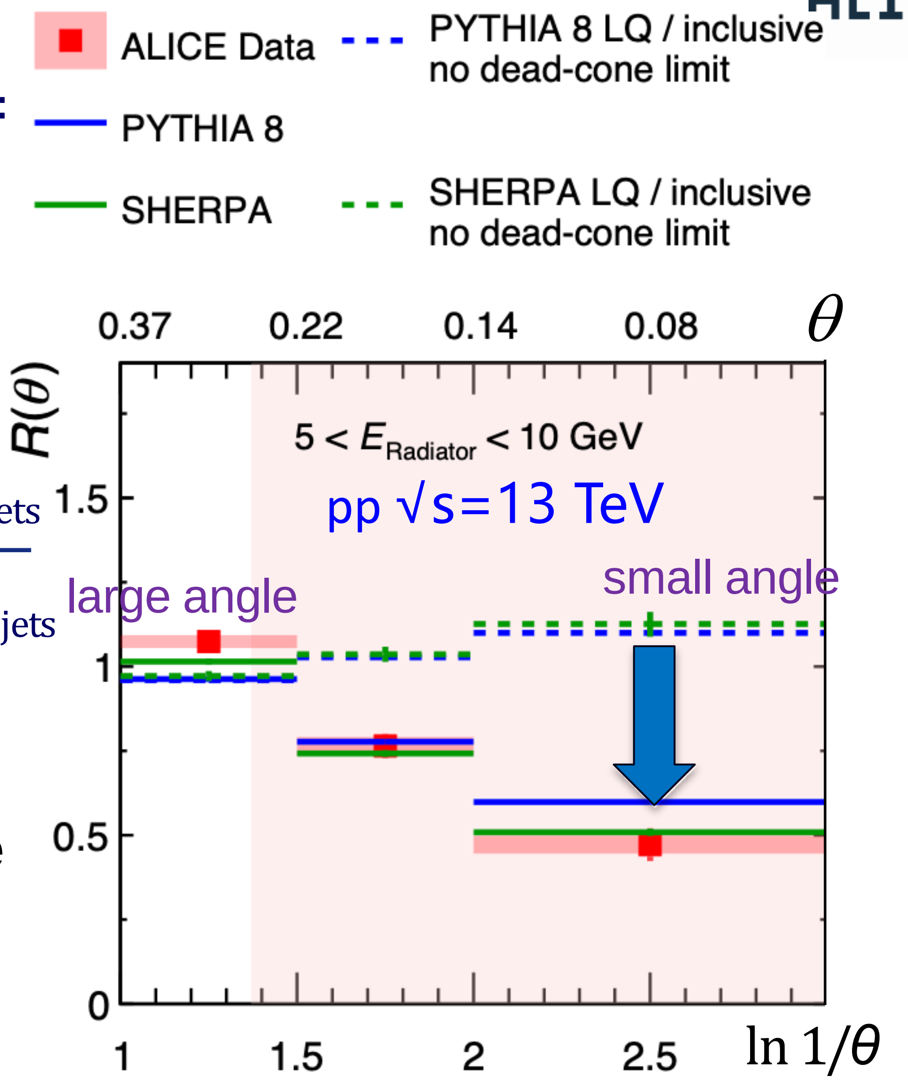

ALICE：*Nature* 605 (2022) 7910, 440

- First direct observation for charm quarks in pp — QCD vacuum by using jet iterative declustering and **Lund plane** analysis of jets that contain a soft D^0 meson
  - ➢ Reduction of gluon radiation from heavy quarks at small angles

Whether is it still validated in QCD medium?

手征反常效应：手征磁波测量

手征反常效应：检验强相互作用下CP对称性、理解非微扰QCD新颖拓扑结构；

超高能原子核碰撞可以产生自然界最强电磁场：

B ~10^{14-16} 特斯拉，量子电动力学+量子色动力学

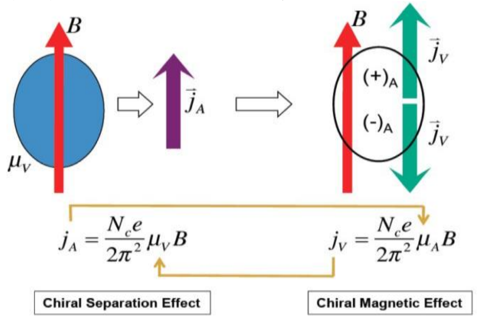

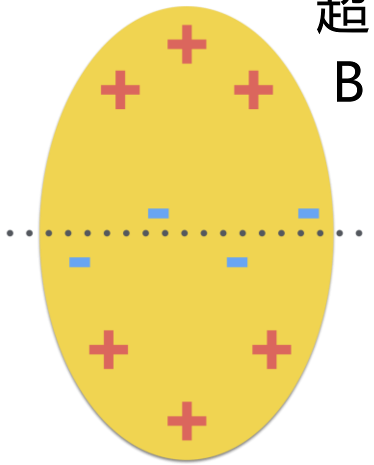

CMW

Possible effect: Out-of-plane quadrupole dipole moment

Observables: Charge asymmetry dependent v_2

$$\Delta v_2 = v_2^- - v_2^+ \sim rA_{ch}$$

with $A_{ch} = (N^+ - N^-) / (N^+ + N^-)$

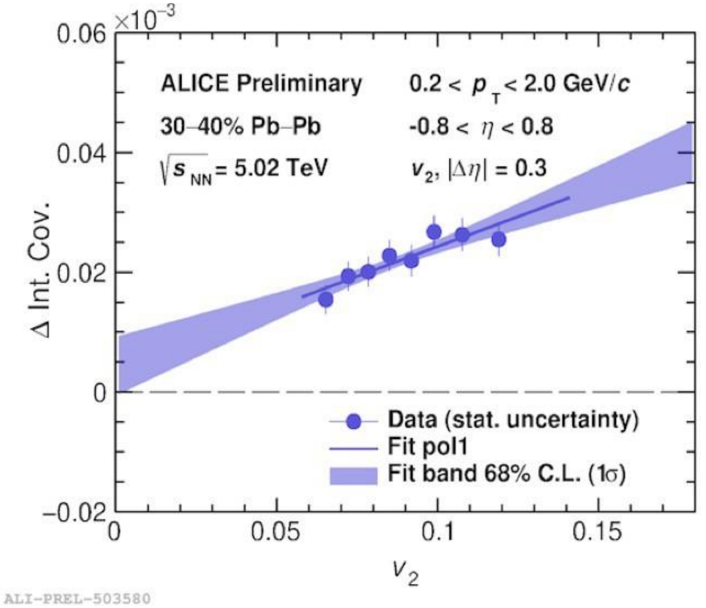

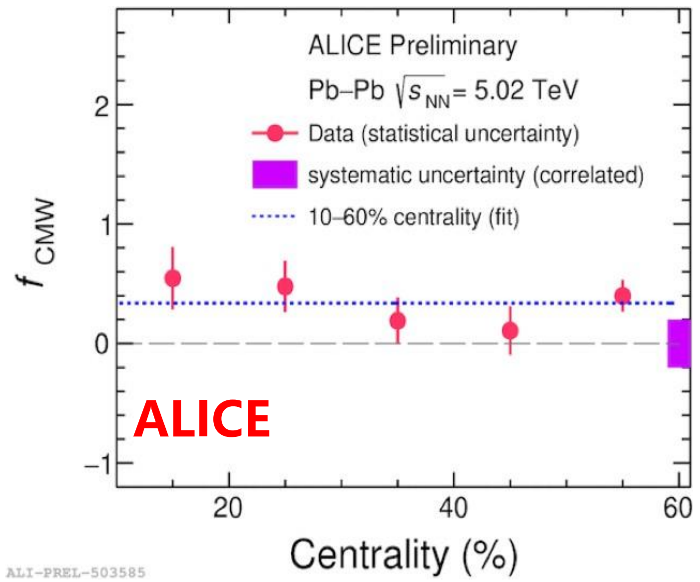

- 提出采用事件形状选择（ESE）方法分离手征磁波测量中的局域电荷守恒背景
- 首次提取出手征磁波信号强度

质子-超子间强相互作用

- 如何从第一原理出发理解原子核中夸克含量不同的强子之间的有效相互作用，在核物理中是一个挑战

ALICE： *Nature* 558 223-238(2020)

- Proton-hyperon (p-Y) strong interaction poorly known
  - Traditional scattering measurements mostly limited to proton-proton
  - Relevant to neutron star modeling in the case of Λ and Σ
- Momentum-correlation of p-Y pairs produced by a source of well-measured size in pp and p-Pb → big jump in precision
- Latest result: attractive strong interaction precisely measured for **p-Ξ⁻** and **p-Ω⁻**

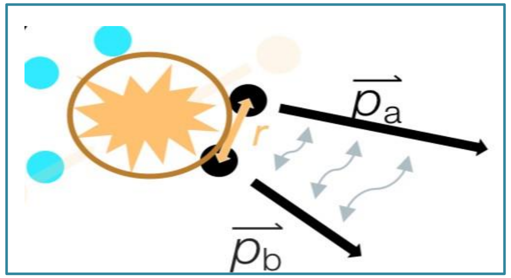

Correlation peak at small momentum difference $k^* = |\boldsymbol{p}_a - \boldsymbol{p}_b|/2$ induced by interaction

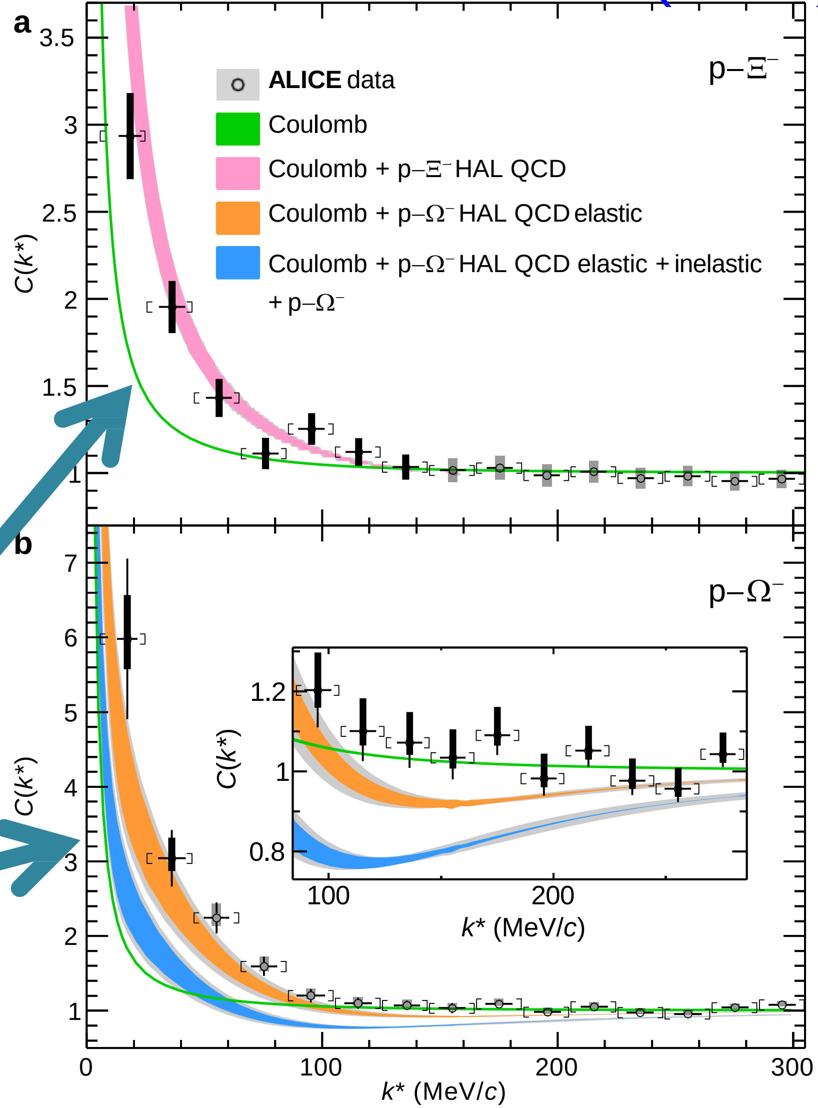

ALICE in Run 3 (Ongoing)

Materias mainly from
Xiaozhi's talk at HP2024

Major upgrades installed in 2019-

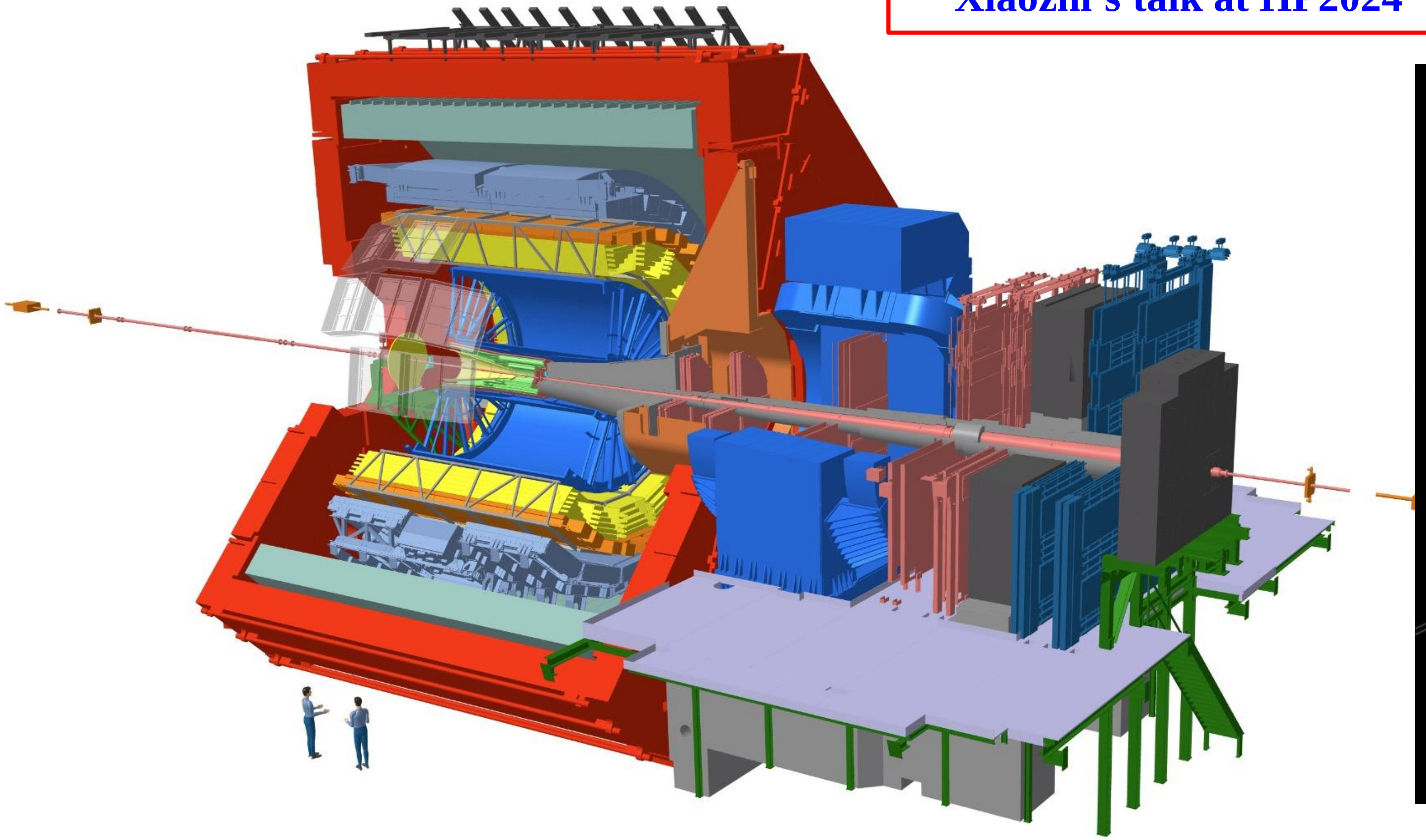

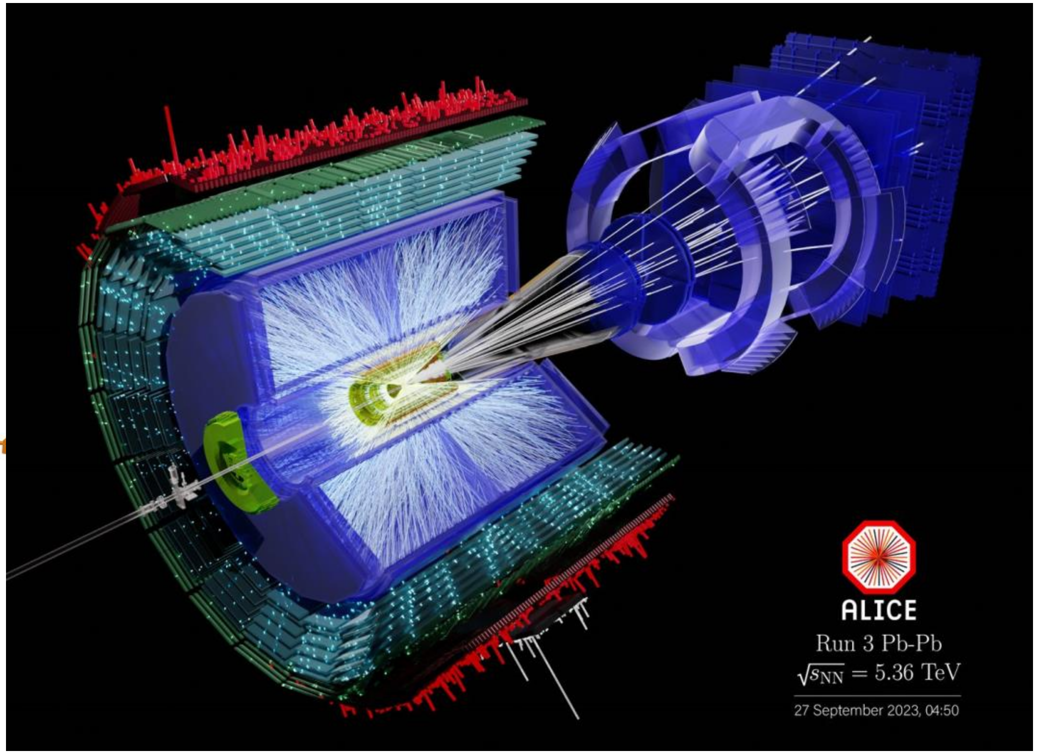

LHC LS2	LHC RUN 3	LHC LS3	LHC RUN 4	LHC LS4	LHC RUN 5 and RUN 6
2019-2021					

ALICE in Run 3 (MFT and ITS2)

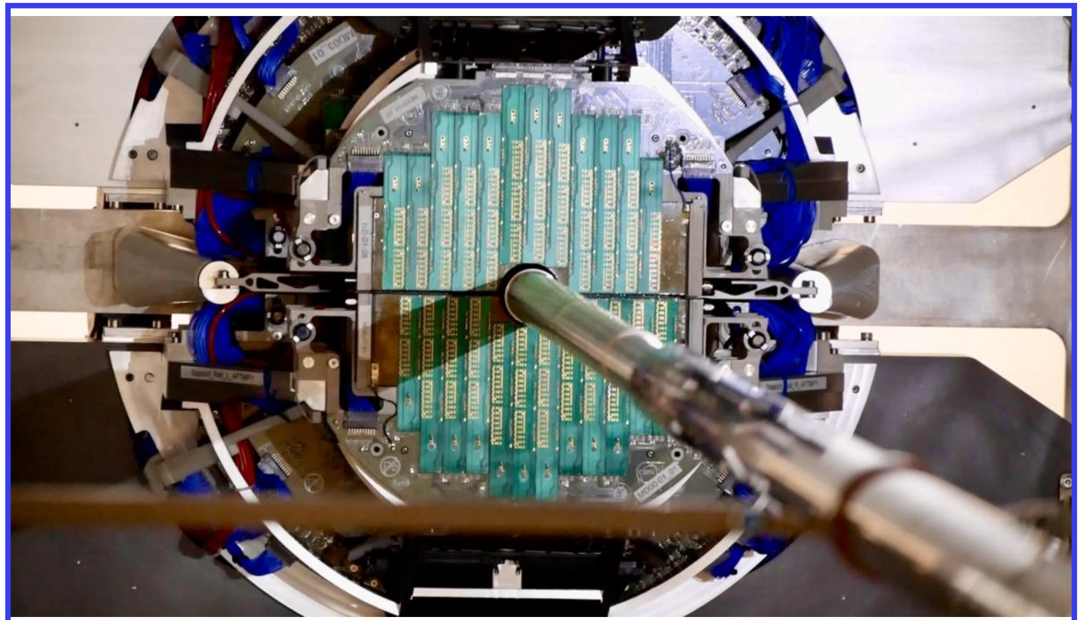

New Muon Forward Tracker

MFT CDS LINK

- Monolithic Active Pixel Sensor technology
- Spatial resolution: 5 μm
- Pixel size: 27 μm x 29 μm
- Integration time: 5 μs

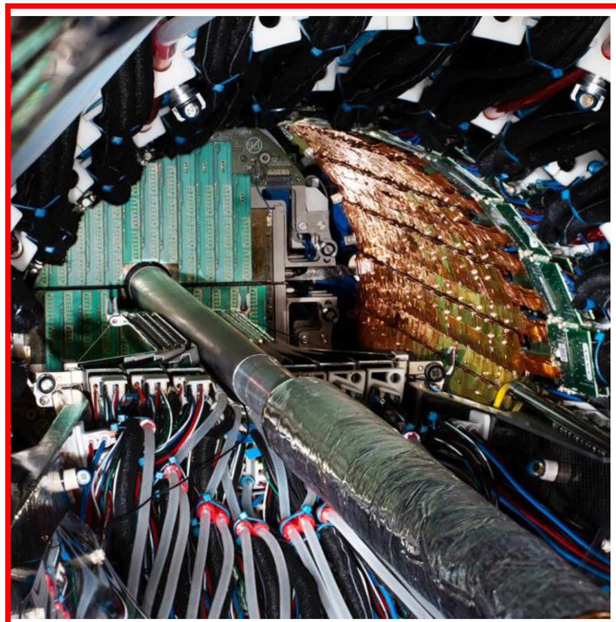

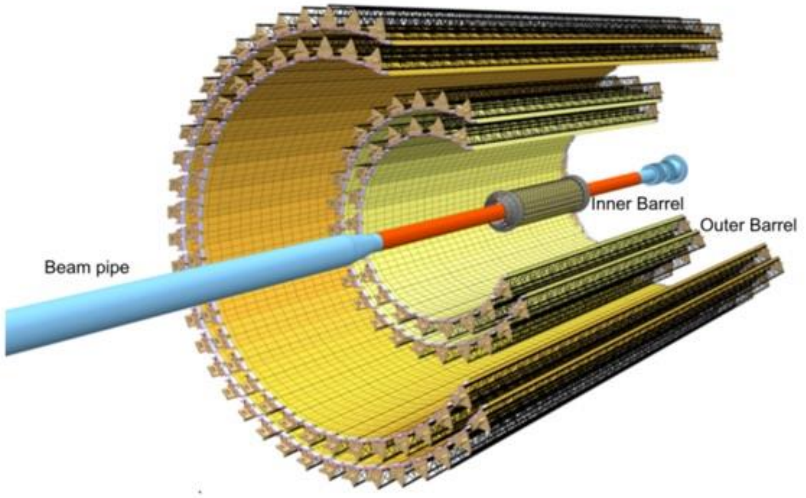

Upgraded Inner Tracking System

TDR ITS2 LINK

- 3 layers in inner barrel (IB), 4 in outer barrel (OB)
- Get closer to IP: from 39 mm to 23 mm
- Reduced material budget: from 1.14% X_0 to 0.36% X_0 per layer
- Reduced pixel size: from 50 x 425 μm^2 to 29 x 27 μm^2

Performance of the ITS2 and MFT in Run 3

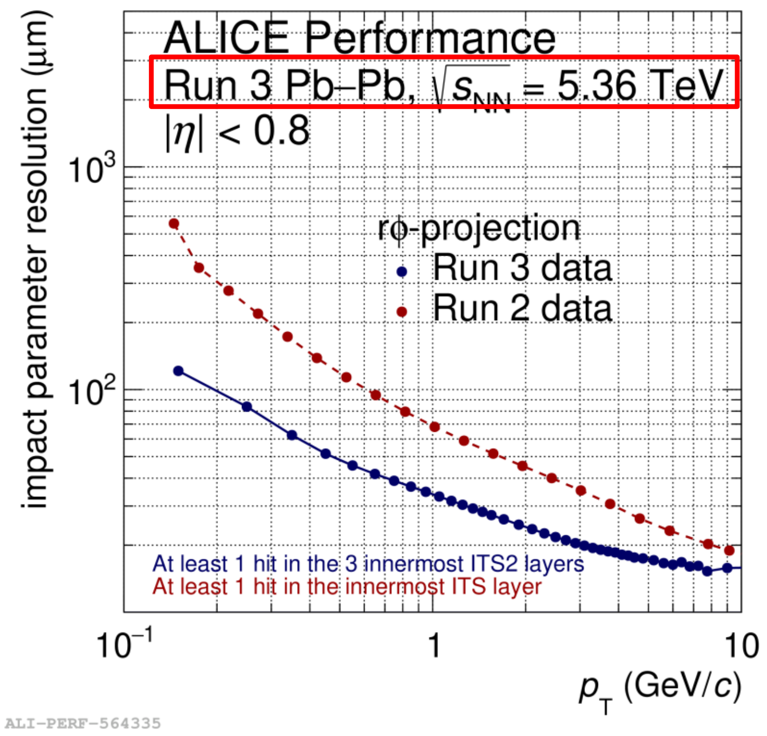

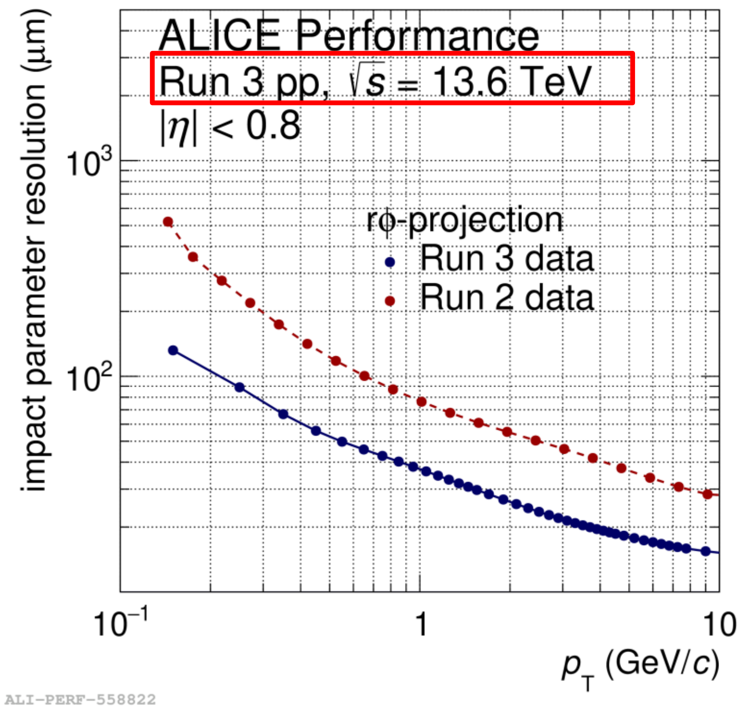

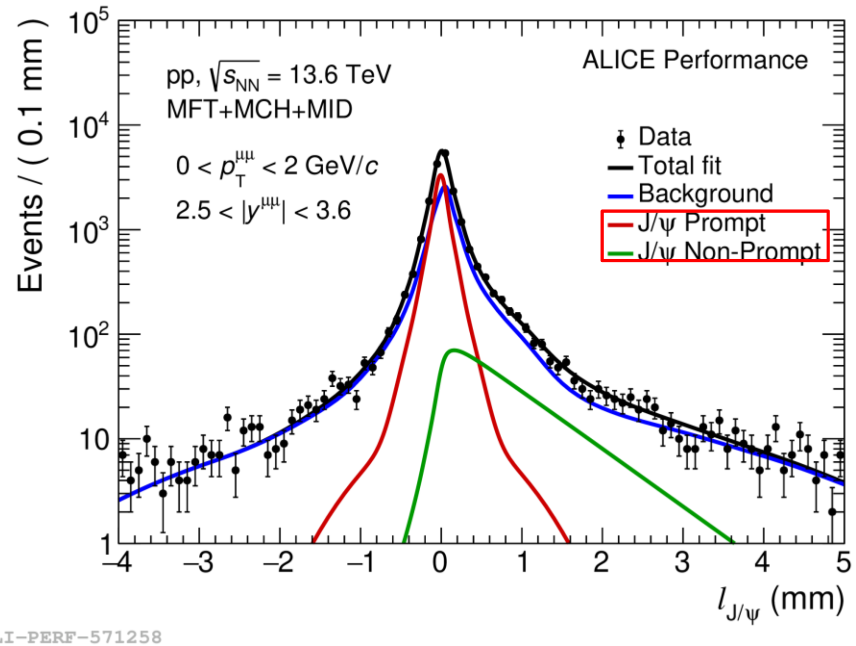

Improved pointing resolution at midrapidity

already now by factors of 2 and 6 in the transverse plane and beam-line direction, respectively

Secondary vertex reconstruction enabled at forward rapidity

separation of J/ψ contributions from beauty-hadron decays

ALICE in Run 3 (TPC)

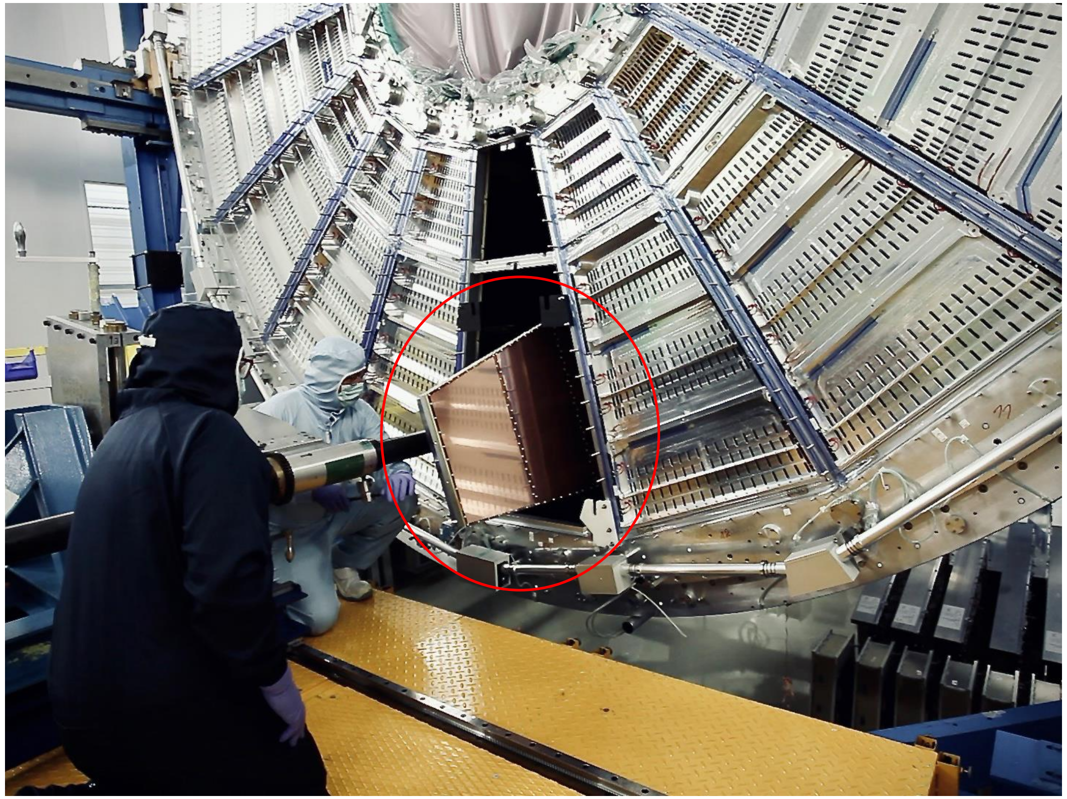

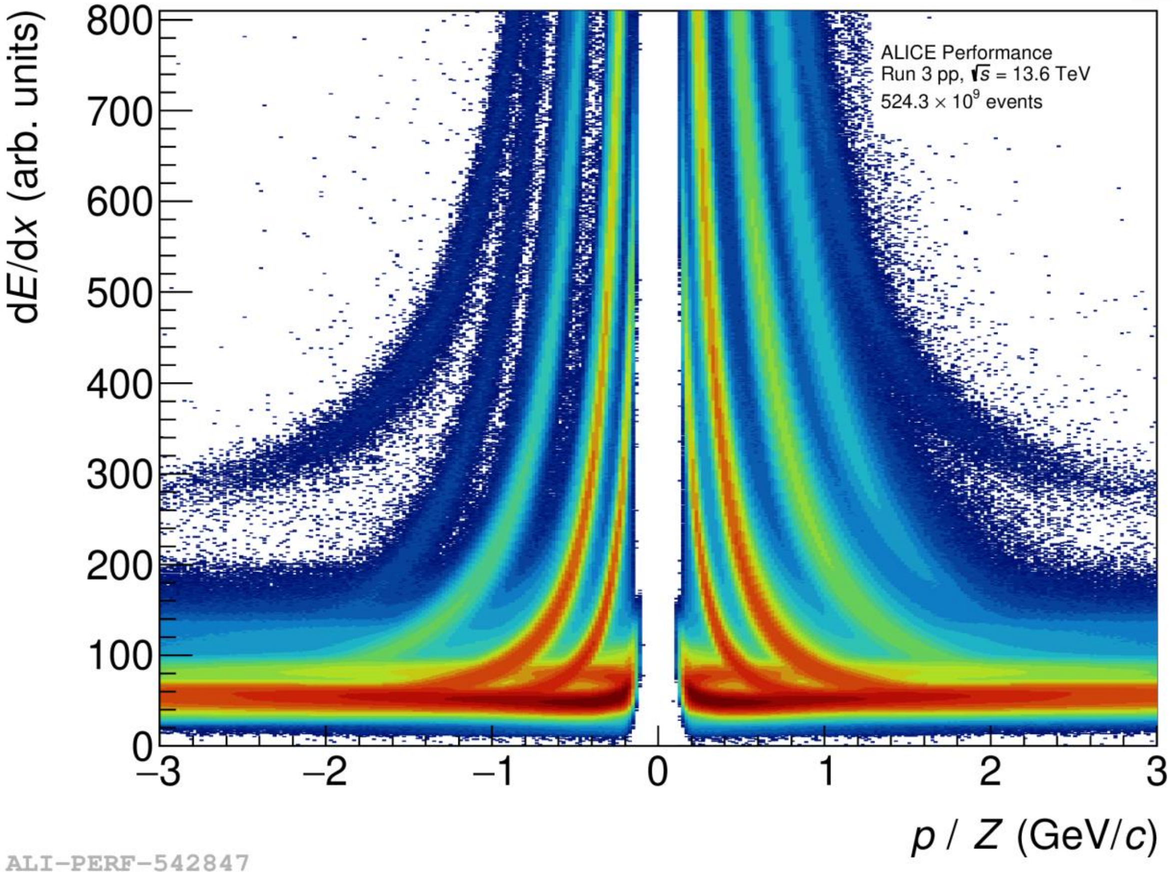

Upgraded Time Projection Chamber -> **GEM, continuous readout**

TPC UPGRADE CDS LINK

- pp data taking at 500 kHz
- Pb-Pb data taking at 50 kHz

Run 3 data taking

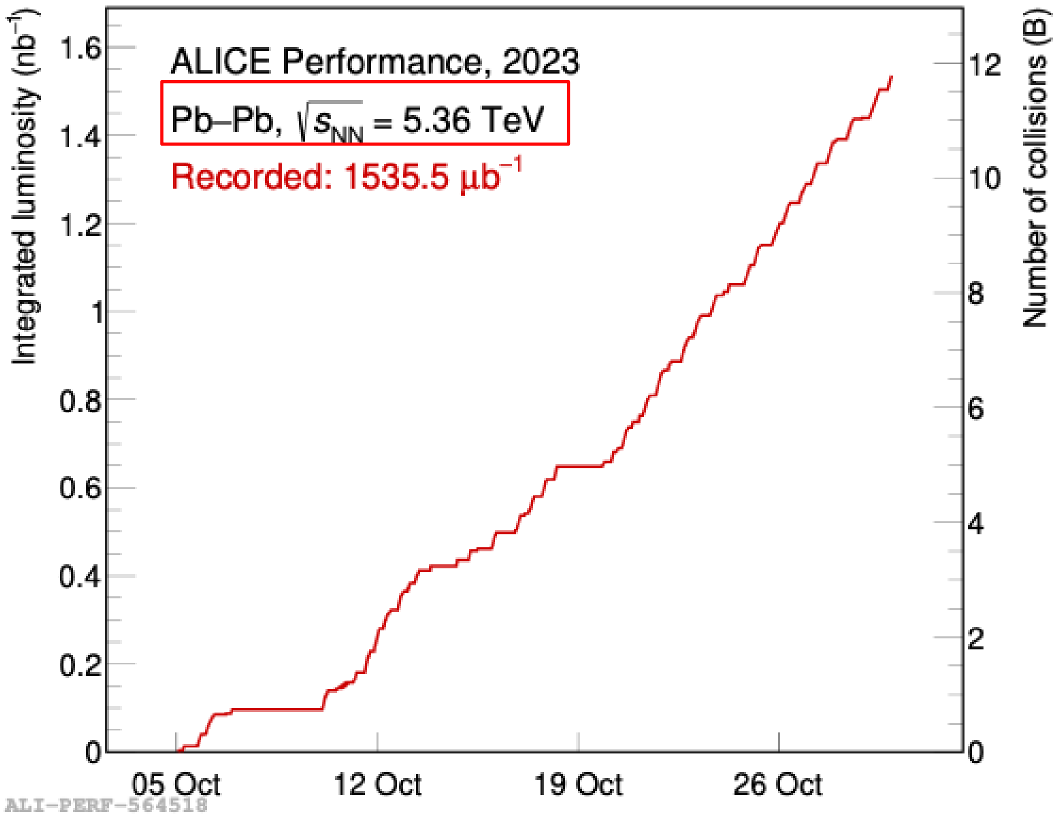

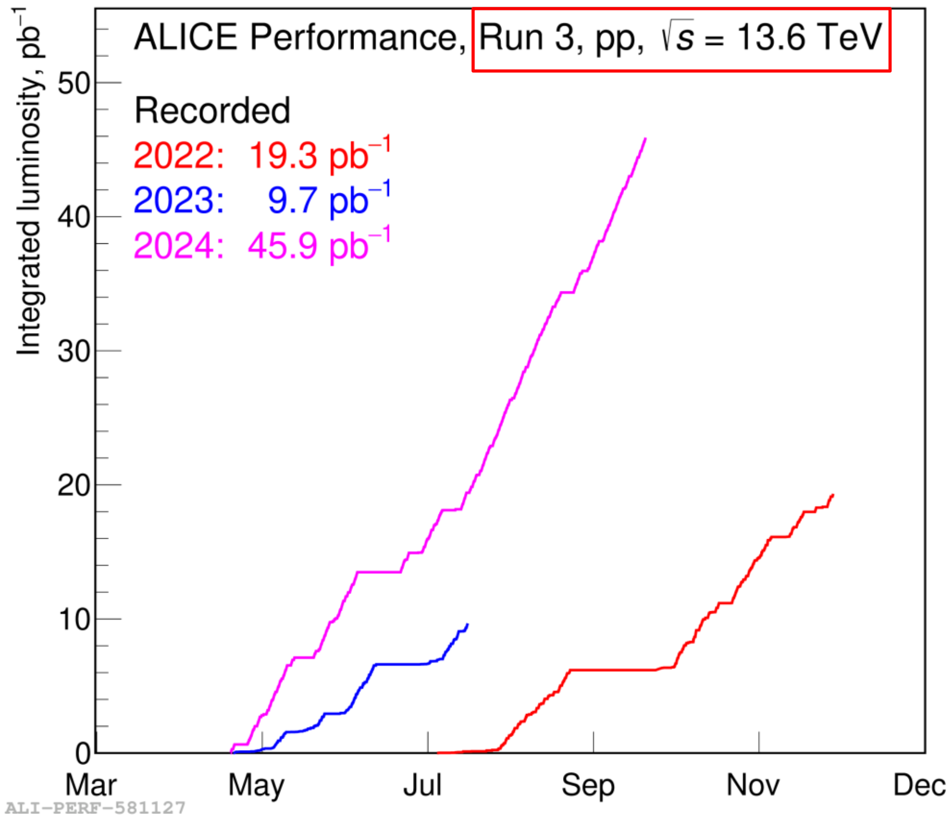

- Pb−Pb data taking at **50 kHz**
- Collected approx. 12 B minimum bias events
- pp data taking at **500 kHz**
- 75 pb^{-1} minimum bias events are currently recorded

Charmonia in pp collisions at √s = 13.6 TeV

Zhang yuan，Zhenjun Xiong，Xiaozhi Bai

Run 3 Preliminary

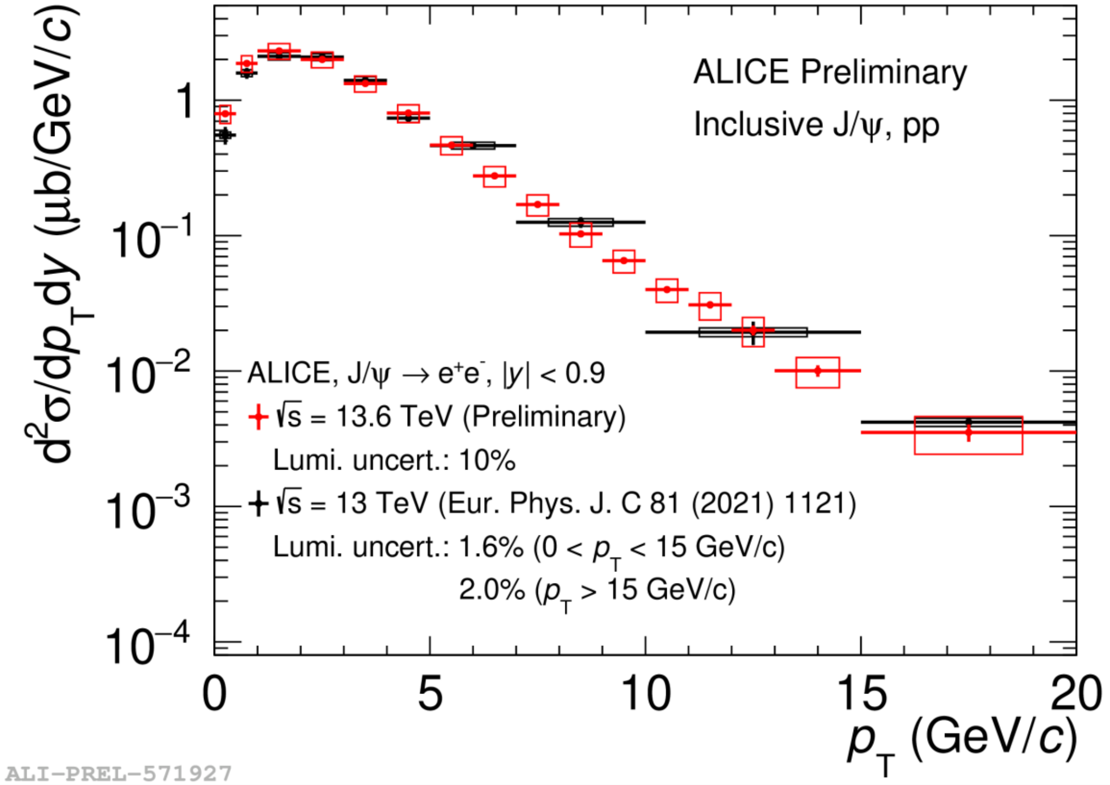

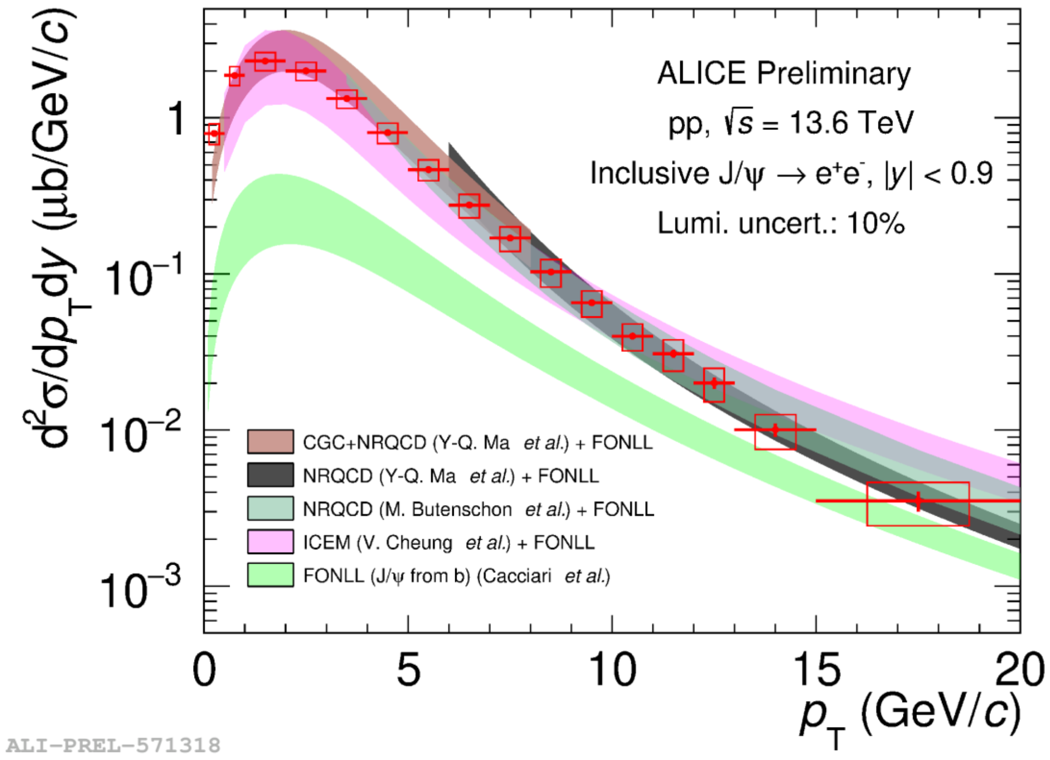

- The new J/ψ cross section is consistent with the Run 2 results
- The data are described by ICEM and NRQCD based models coupled with FONLL to account for the non-prompt J/ψ contribution

ψ(2S) in pp collisions at √s = 13.6 TeV

Zhang yuan，Zhenjun Xiong，Xiaozhi Bai

Run 3 Preliminary

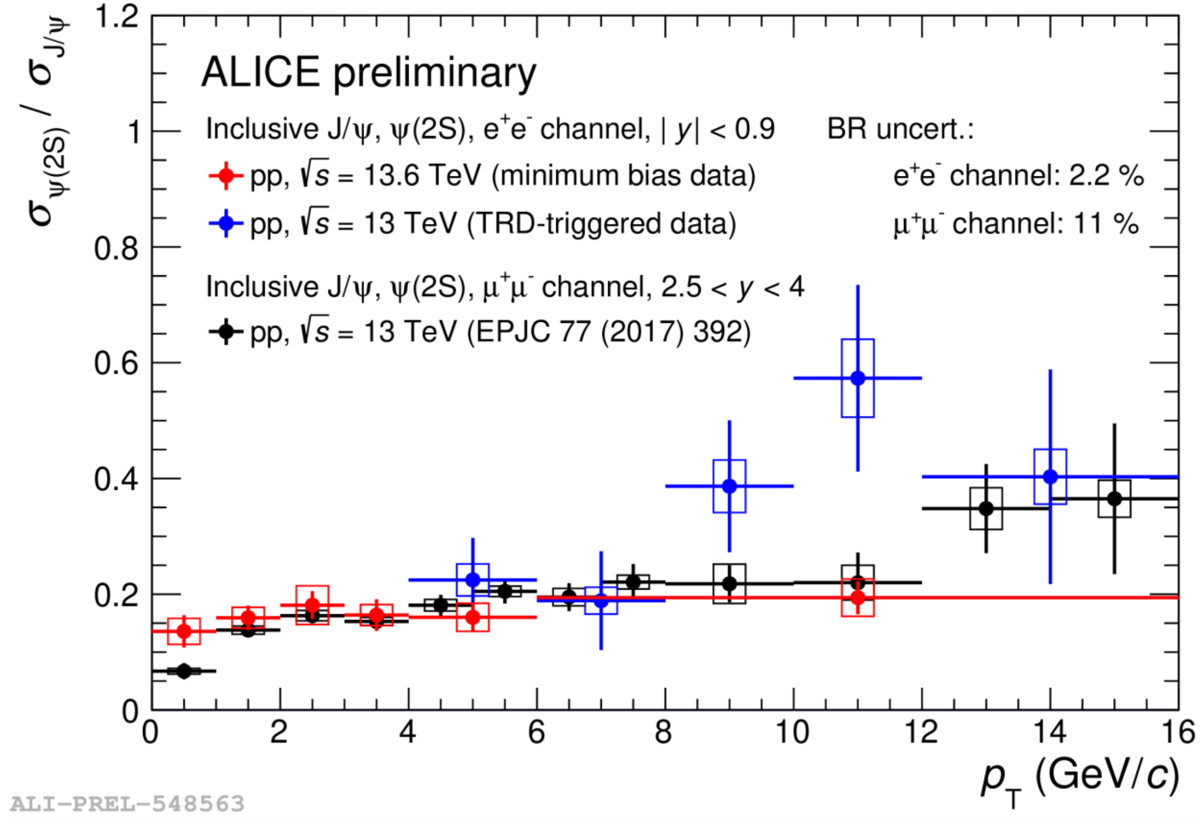

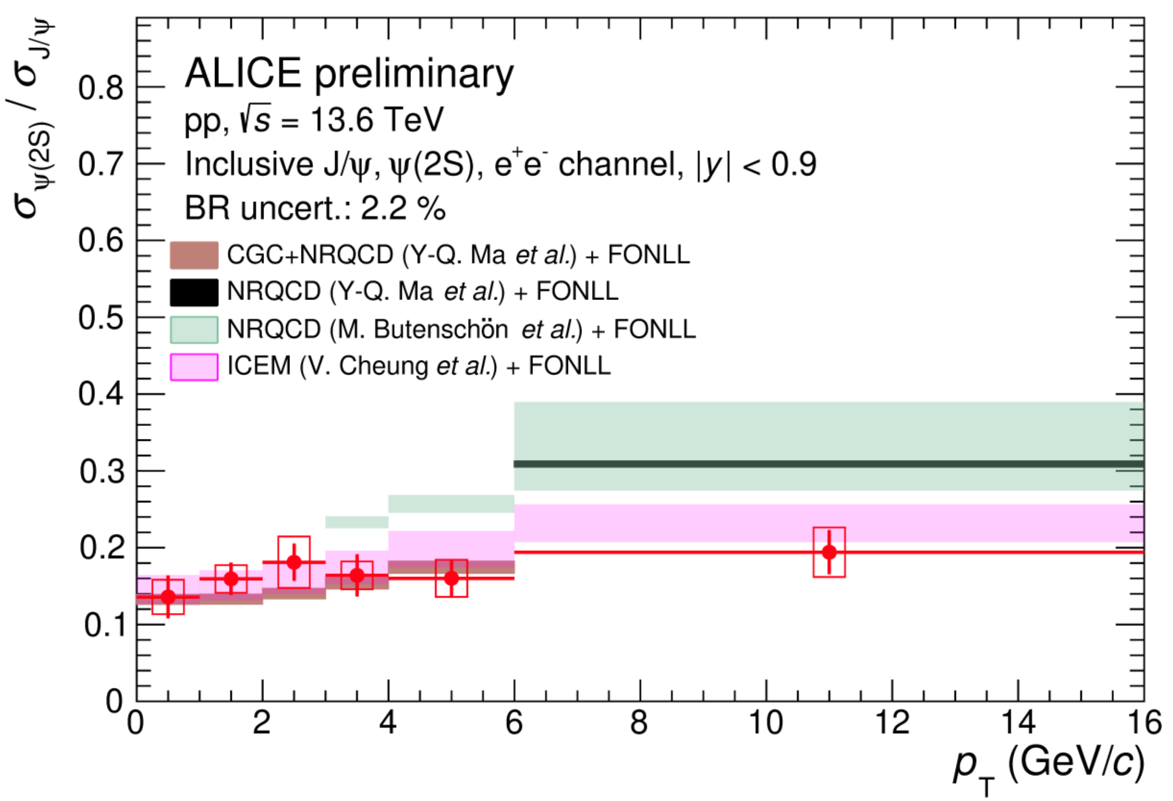

- Run 3 with the significantly increased statistics allow to reconstruct ψ(2S) via dielectron decays
- The CGC + NRQCD and ICEM can describe the data at low p_T

Yiping Wang 24/09 09:00

$\Sigma_c^{0,++}$ in pp collisions at $\sqrt{s}$ = 13.6 TeV

Run 3 Preliminary

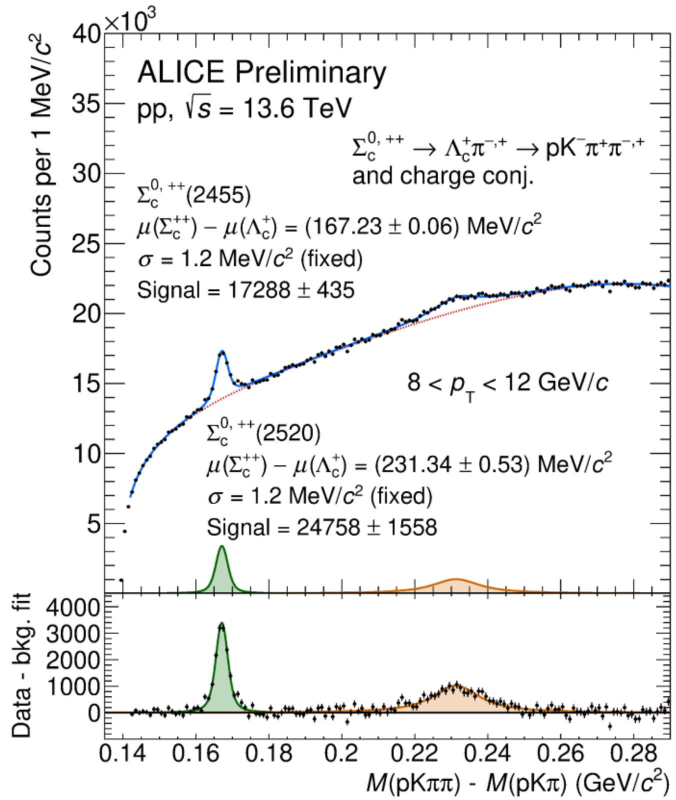

ALI-PREL-571534

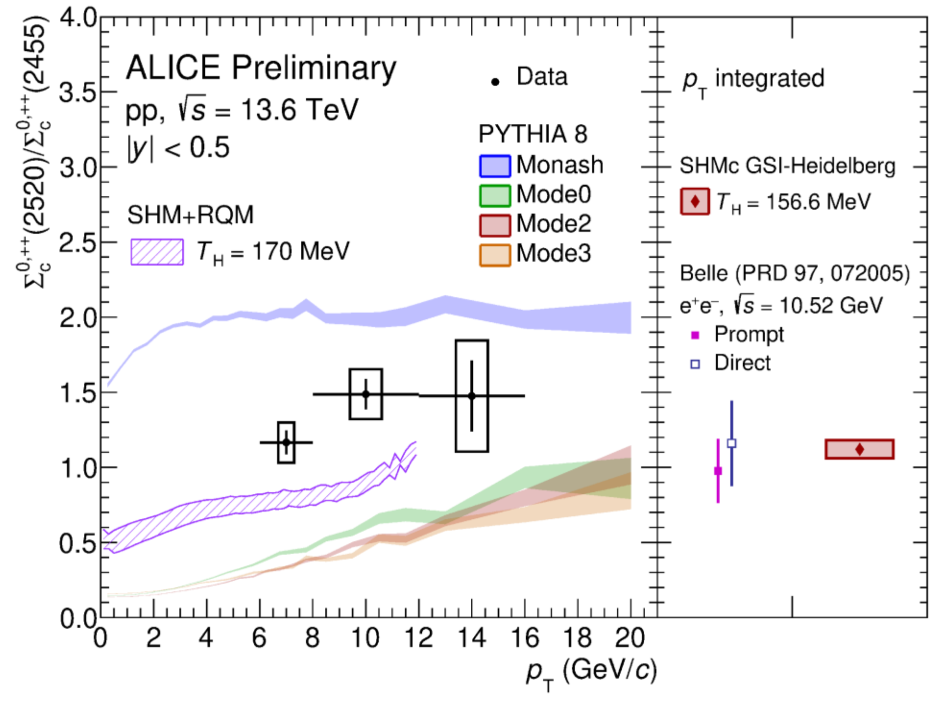

ALI-PREL-574270

- First measurement of the production of $\Sigma_c^{0,++}$(2520) relative to $\Sigma_c^{0,++}$(2455) in pp collisions at $\sqrt{s}$ = 13.6 TeV
- No evidence of difference w.r.t. e^+e^- collisions considering current uncertainties
- PYTHIA 8 Monash (default tune) overestimates the ratio, PYTHIA 8 with with additional color reconnection topologies underestimates the ratio

Probe the charm baron fragmentation function

Run 3 Preliminary

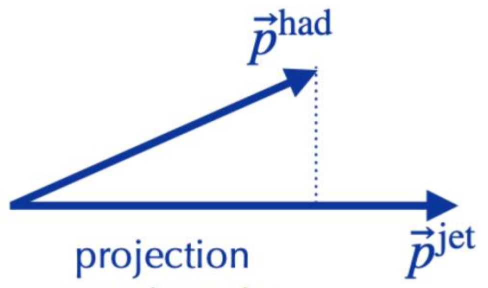

$$z_{\parallel} = \frac{\vec{p}_{\text{jet}} \cdot \vec{p}_{\text{had}}}{\vec{p}_{\text{jet}} \cdot \vec{p}_{\text{jet}}}$$

NEW

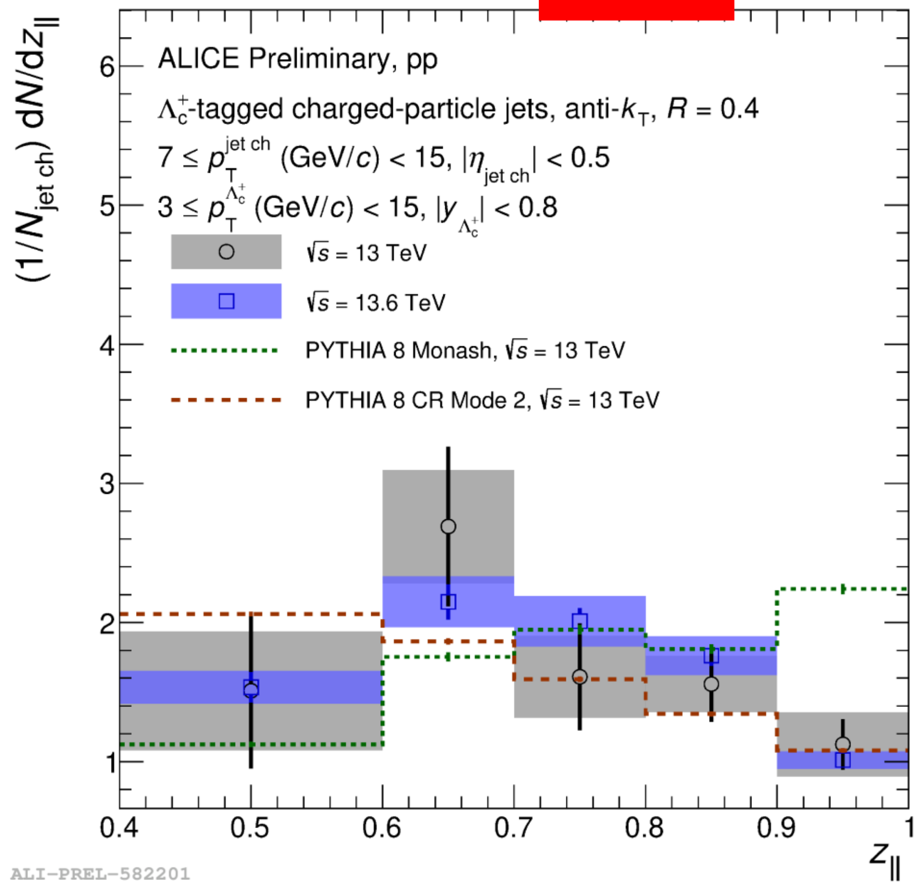

- ➢ Λ_C probing the non-universality of charm baryon hadronisation
- ➢ The precision of the new results from Run 3 improved significantly

Jochen Klein 25/09 12:10

Probing the charm splitting function

NEW

NEW

Run 3 Preliminary

$$z_g = \frac{p_{T,g}}{p_{T,c} + p_{T,g}}$$

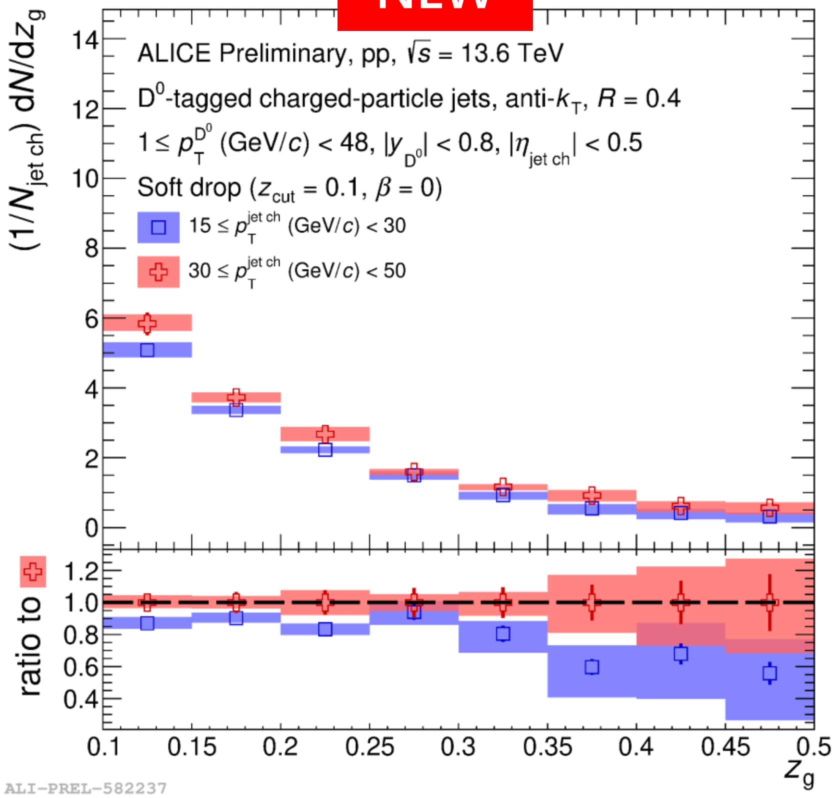

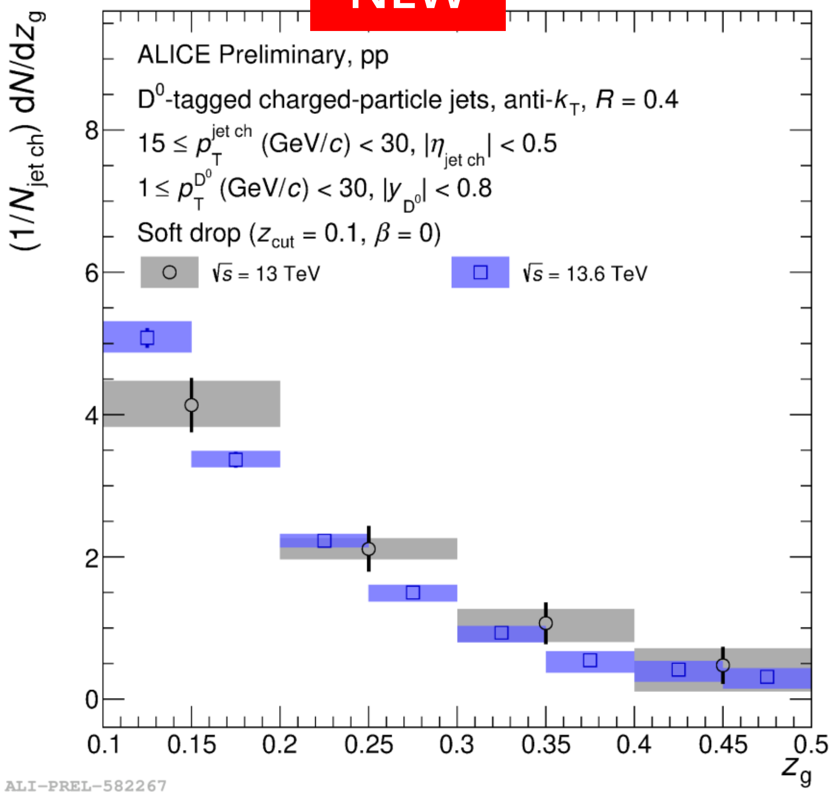

- ➢ The momentum fraction of the first splitting in groomed charm jets converges to the charm splitting function(c->cg).
- ➢ Run 3 allows us to make differential measurements in jet p_T
- ➢ In inclusive jets Zg has no dependence on jet p_T, but in heavy-flavour jets mass effect decreases with increasing p_T

Jochen Klein 25/09 12:10

Energy-energy correlators in jets in pp and p-Pb collisions

New publication

arXiv:2409.12687

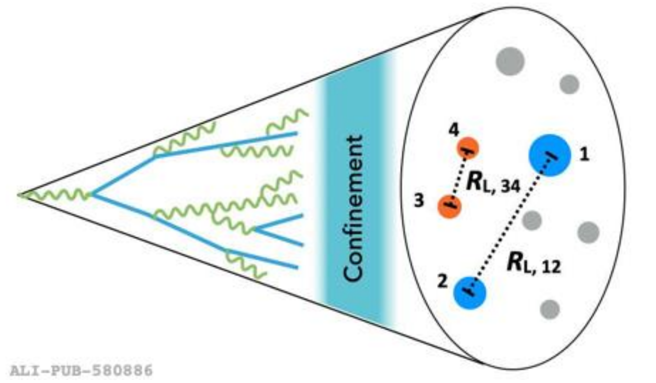

$$\frac{d\sigma_{EEC}}{dR_L} = \sum_{i,j}\int d\sigma(R'_L)\frac{p_{T,i}p_{T,j}}{p'_{T,jet}}\delta(R'_L - R_{L,ij})$$

$$R_L = \sqrt{\Delta\phi_{ij}^2 + \Delta\eta_{ij}^2}$$

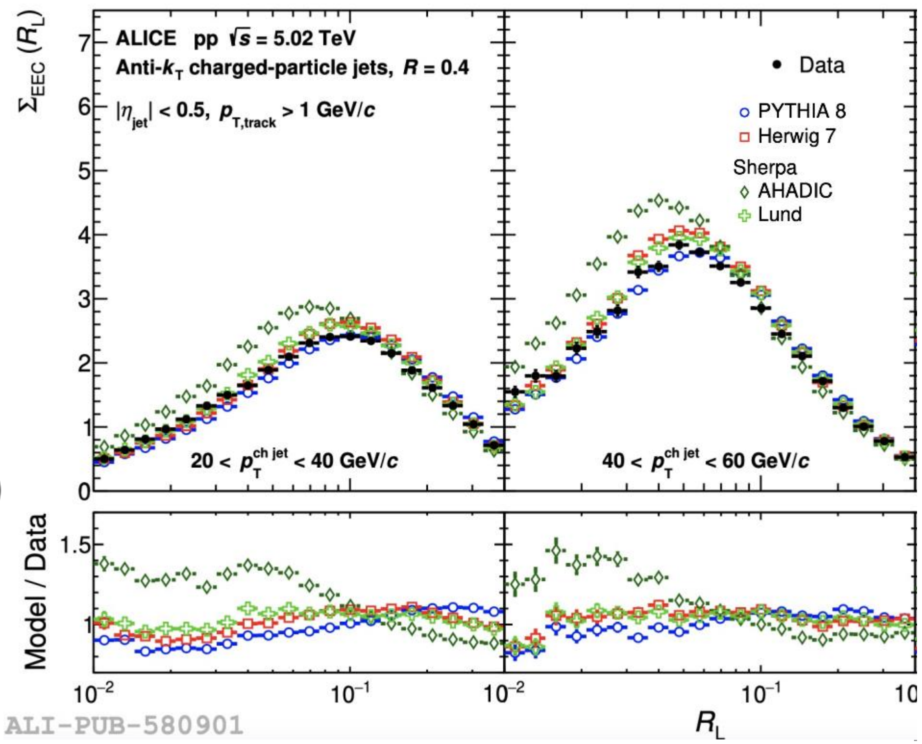

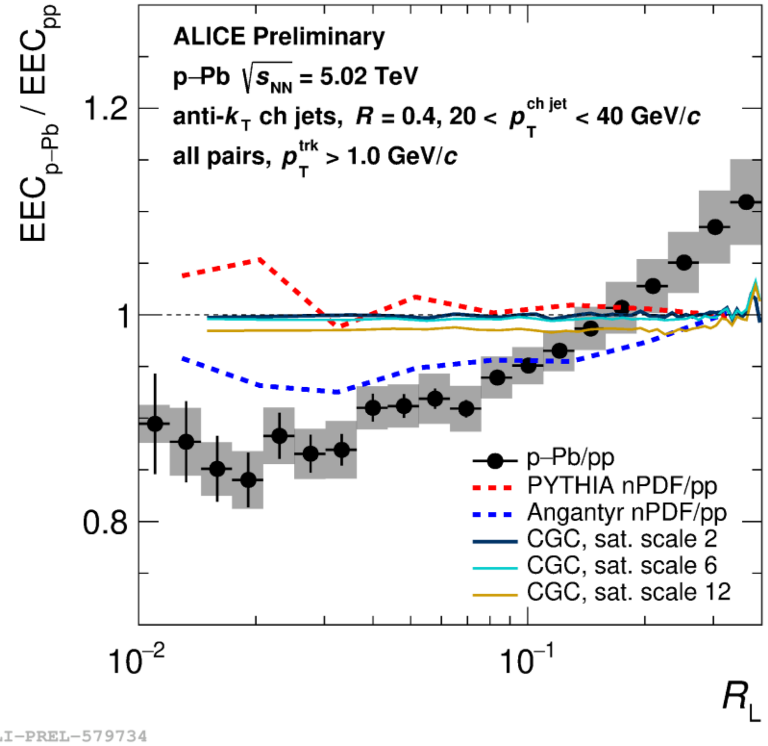

- A novel jet substructure observable describing the energy flow inside jets, can be calculated from first principles in QCD in the perturbative limit
- **Separation of the perturbative and non-perturbative** regimes
- Modification of the energy-energy correlator (EEC) seen in p-Pb collisions, but not explained by purely initial-state effects

Ananya Rai 24/09 12:10

Mass dependence of the energy-energy correlators

New Preliminary

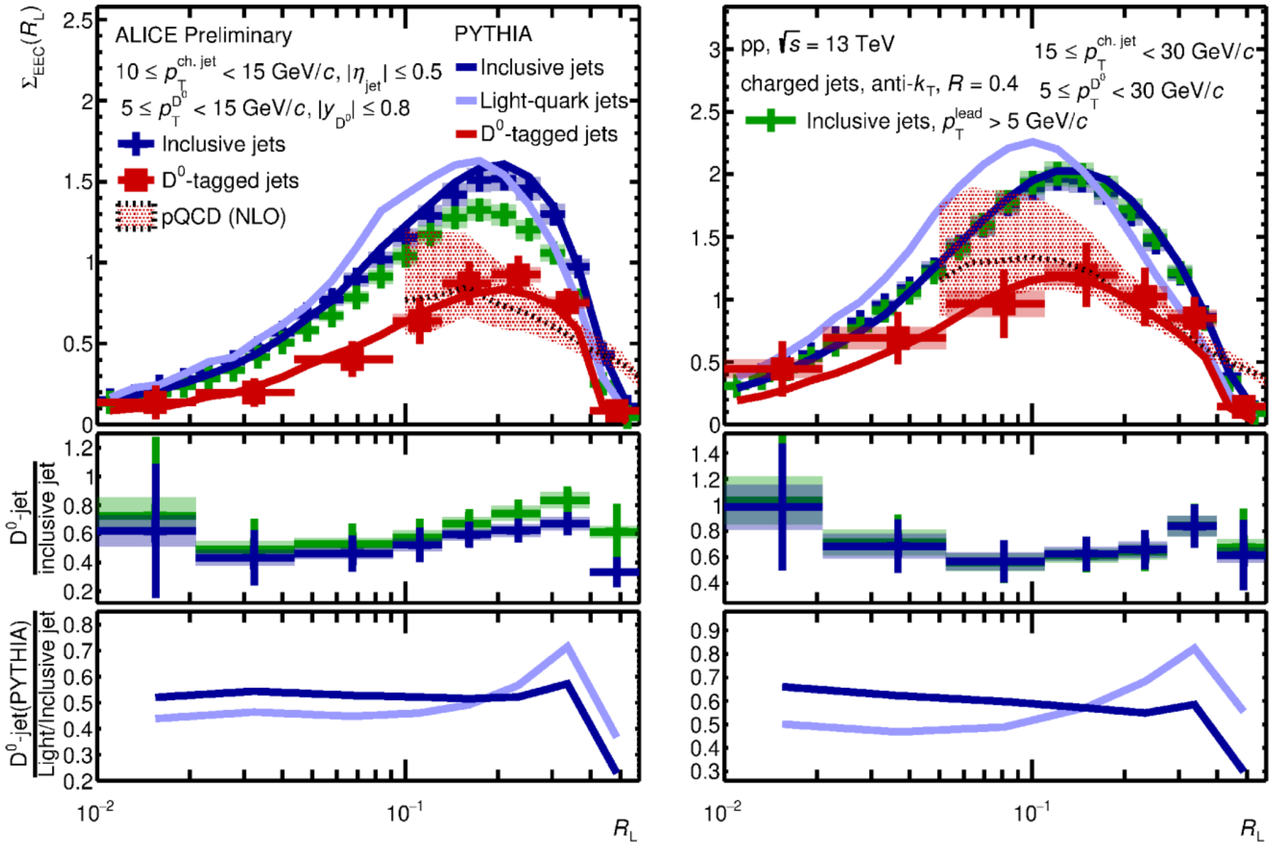

➢ First heavy flavor energy-energy correlator measurement

Anjali Nambrath 24/09 09:00

➢ Flavour effect is seen as a decrease in the EEC amplitude, peak position is not significantly shifted compared to inclusive jets

Open beauty production in Run 3

Run 3 Preliminary

NEW

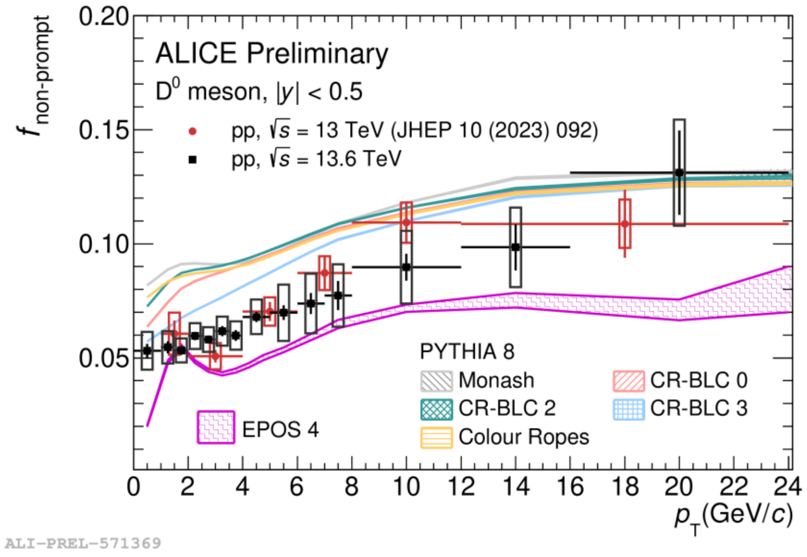

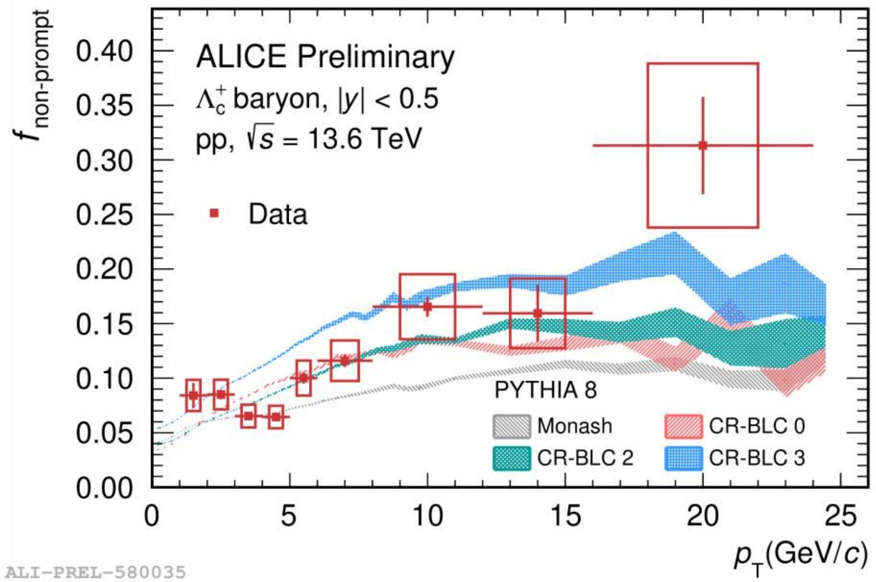

NEW

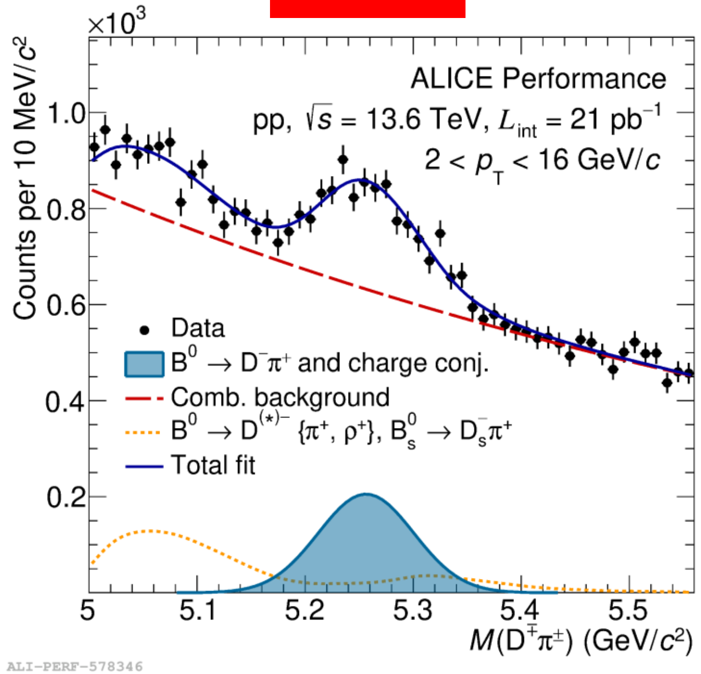

- ➢ Non-prompt D⁰ fraction measured in Run 3: improved precision compared to Run 2 results and extended down to $p_T = 0$
- ➢ Non-prompt Λ_c^+ measured p_T down to 1 GeV/c
- ➢ **First direct observation of B⁰ meson in ALICE**, measured down to $p_T = 2$ GeV/c
    - Better constraint of the open beauty production

Andrea Tavira Garcia 23/09 14:40

Isolated photon nuclear modification factor R_{AA}

New publication

arXiv:2409.12641

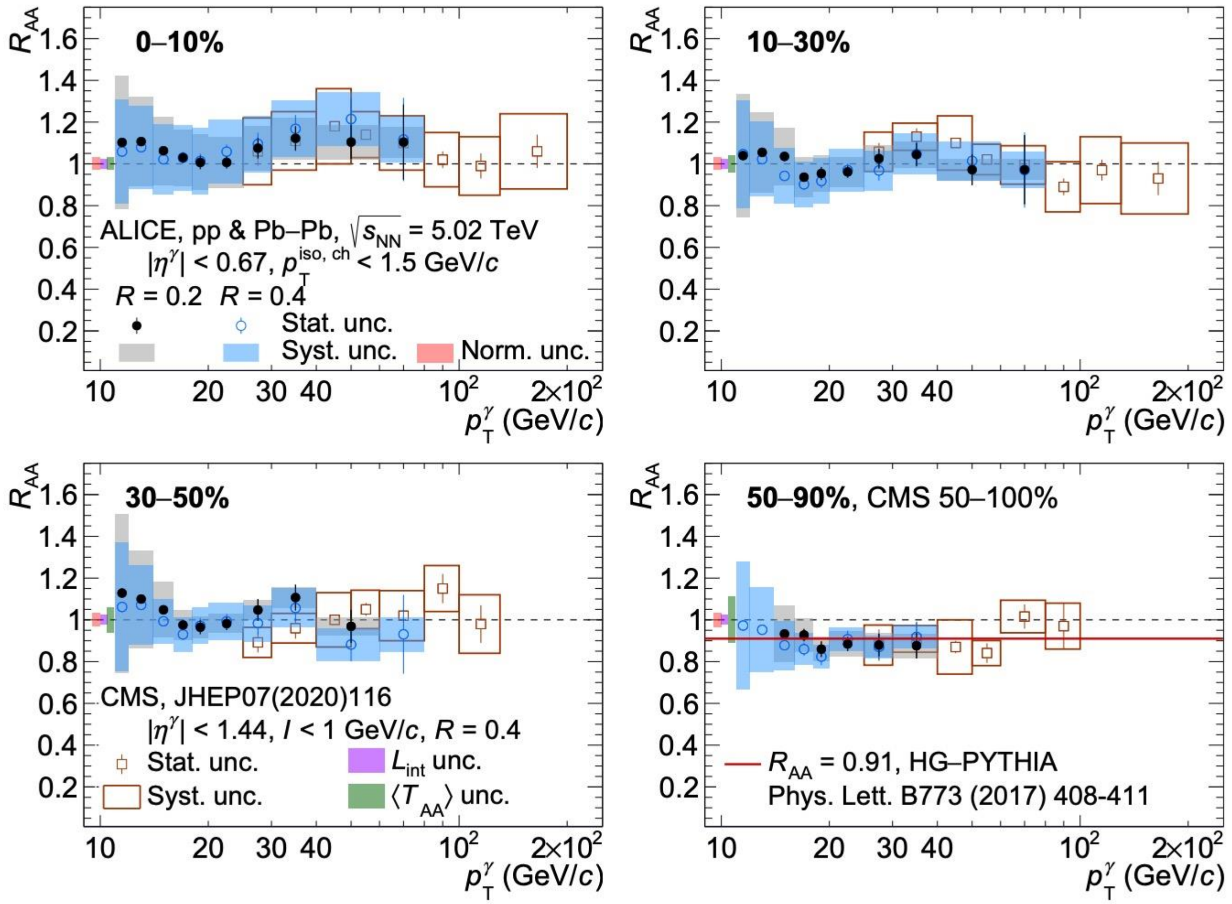

- **R_{AA} consistent with unity** within the uncertainties for both R= 0.2 and 0.4, **no radiation from QGP at these p_T**
- Peripheral collision in agreement with PYTHIA prediction including bias on centrality estimation

Charmonium Polarization

ALICE, PRL 131 (2023) 4, 042303

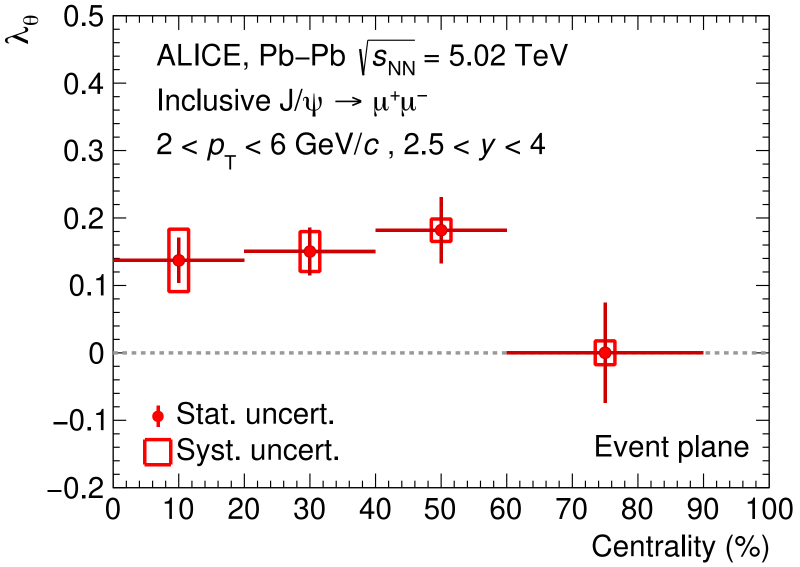

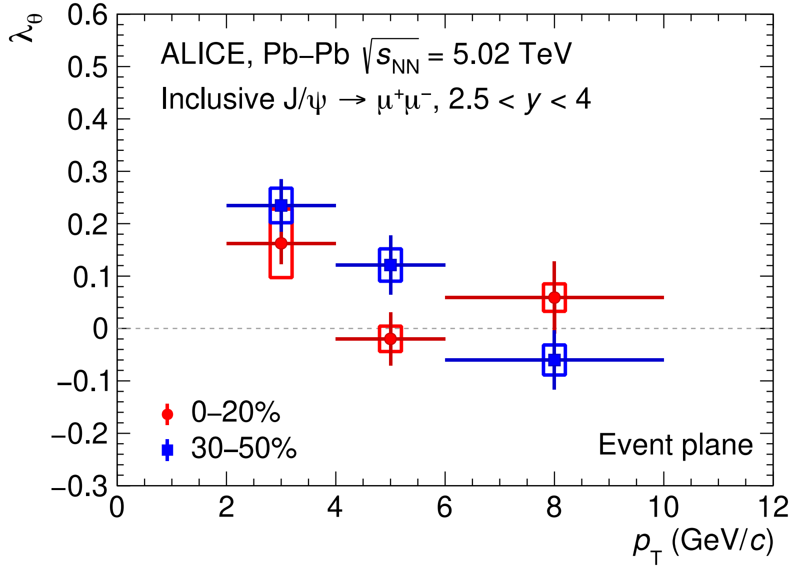

New performance

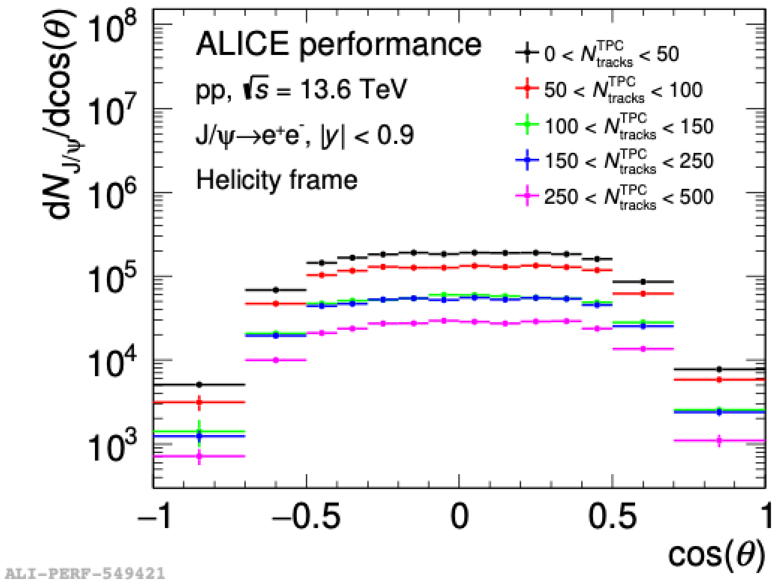

Zhenjun Xiong

- First measurement of quarkonium polarization **w.r.t the event plane**
- Significant polarization **(~3.9σ)** observed in semicentral collisions
- Polarization measurements are ongoing at midrapidity with Run 3 data

D^{*+} spin alignment in pp and Pb-Pb collision

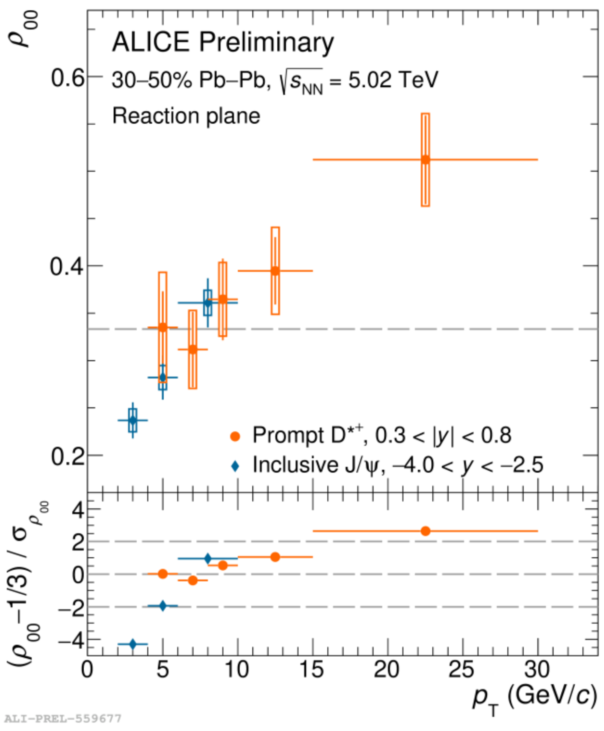

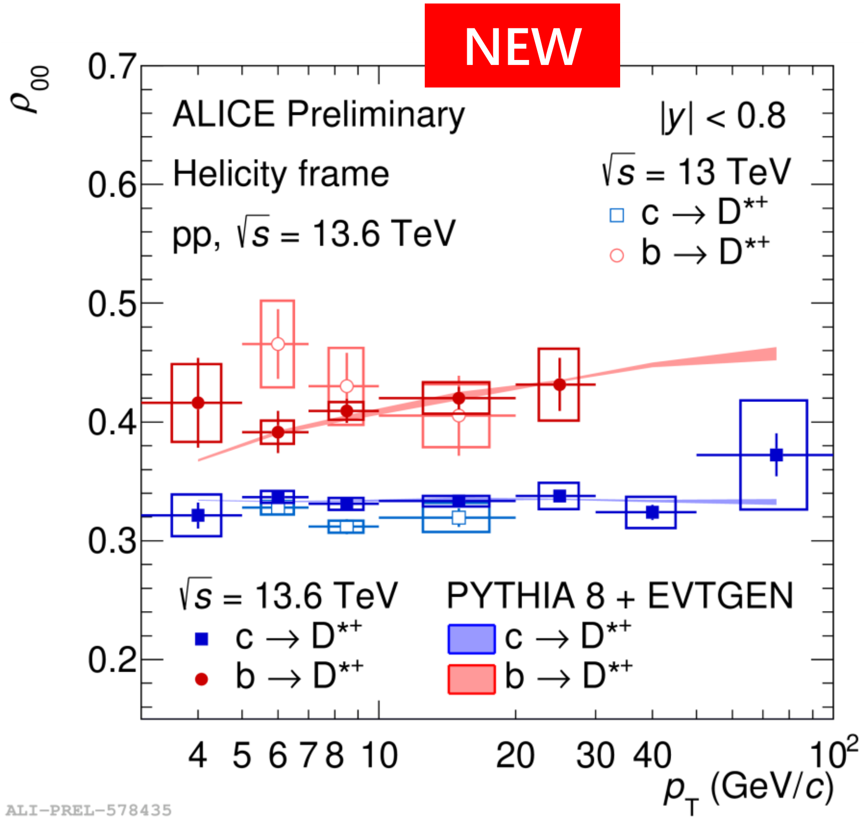

Run 3 Preliminary

Mingze Li

- In Pb-Pb collisions:
  - Spin density matrix $\rho_{00} > ⅓$ for D^{*+} at high p_T ⇒ quark fragmentation scenario
- In pp collisions:
  - ρ_{00} = ⅓ for prompt $\mathbf{D}^{*+}$, ρ_{00} larger than ⅓ for non-prompt $\mathbf{D}^{*+}$, due to the helicity conservation in weak decays
  - New measurement in pp collisions provides an important baseline for Pb-Pb collisions

Charmonium elliptic flow in Run 3

NEW **Run 3 Preliminary**

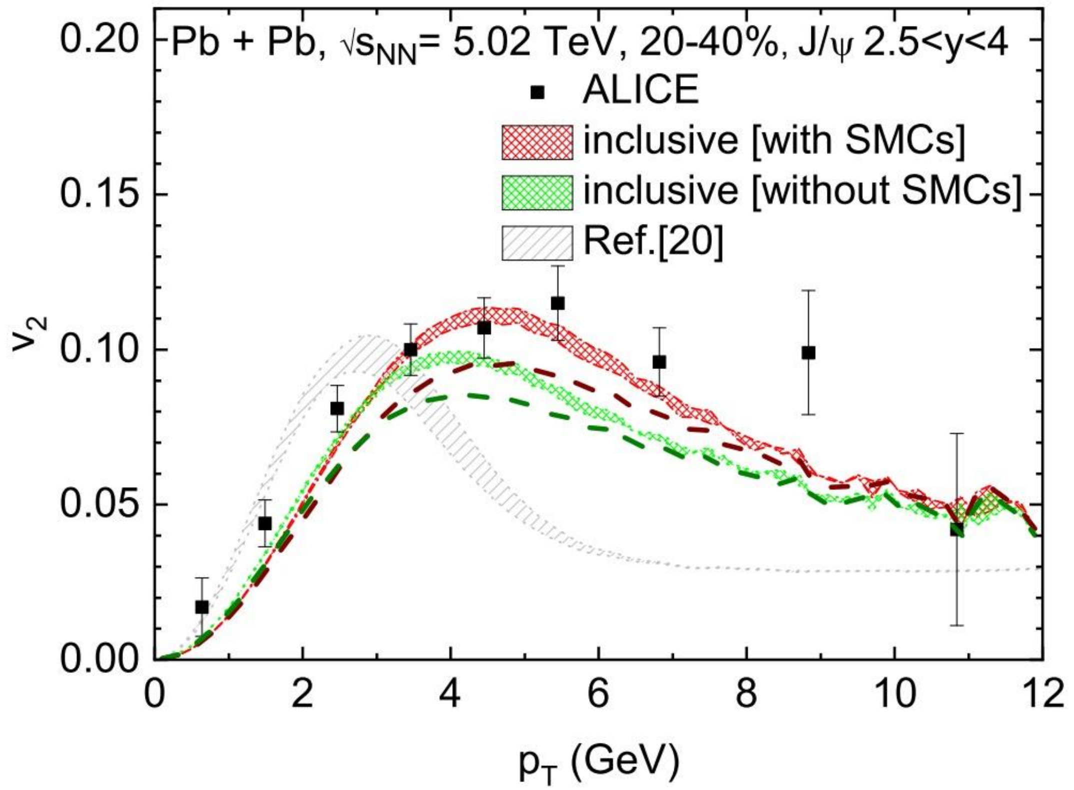

M. He, et al., PRL.128, 162301 (2022)

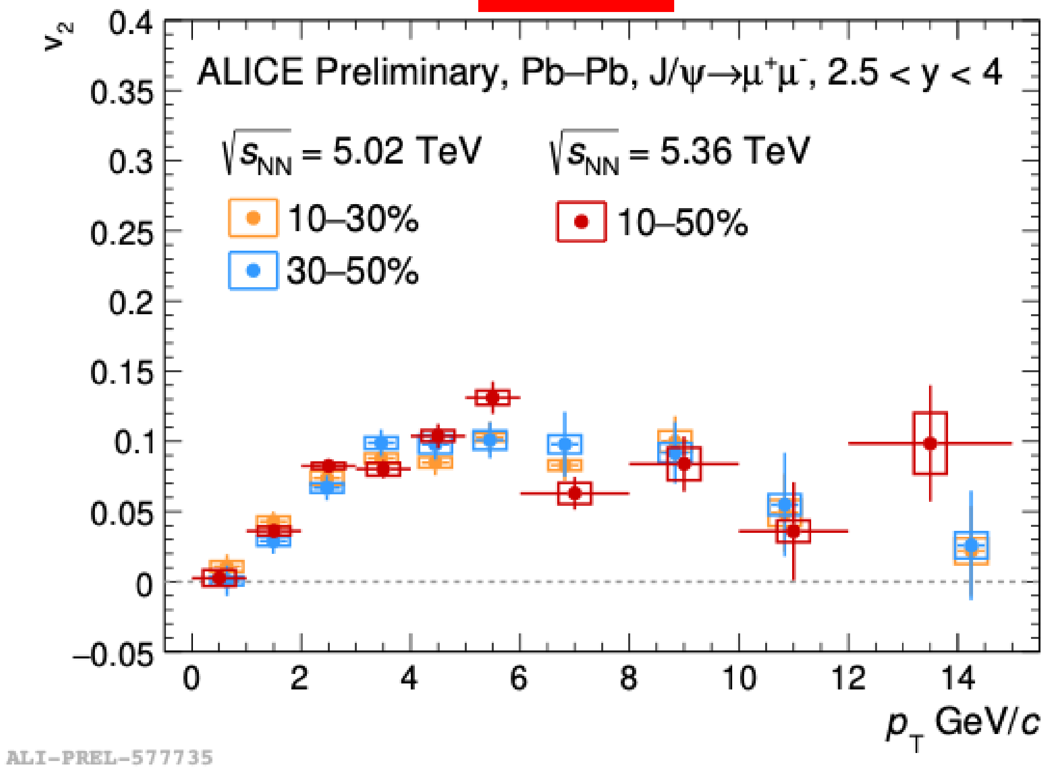

Yiping Wang

- The new result is consistent with Run 2, with statistical precision improved at low p_T at forward rapidity
- A significant J/ψ v_2 is observed at forward rapidity, consistent with the charm quark thermalization

Searching for the quasi-particle in QGP

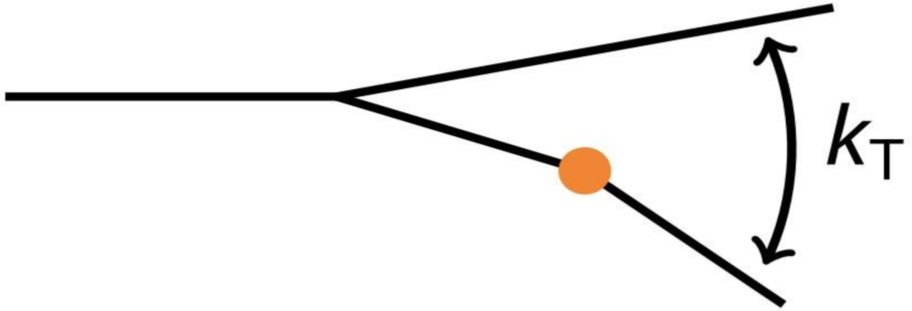

$$k_T = p_{T,\,\mathrm{subleading}} \sin \Delta R$$

$$\Delta R = \sqrt{\Delta y^2 + \Delta \varphi^2}$$

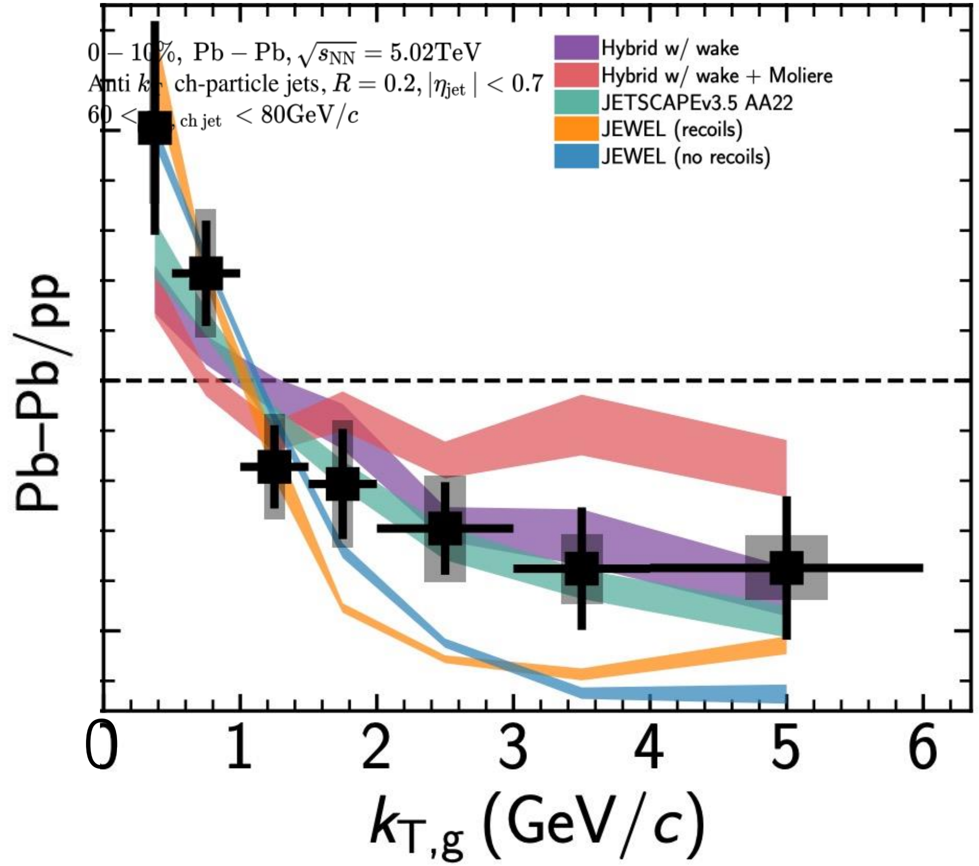

New publication

arXiv:2409.12837

- First measurement of the hardest relative transverse jet splitting
- **Need well-controlled models baseline** from theory to investigate Moliere effects to search quasi-particle in QGP
- Provide new constrain on the microscopic structure and dynamics of the quark–gluon plasma

Quenching with correlated jet substructure

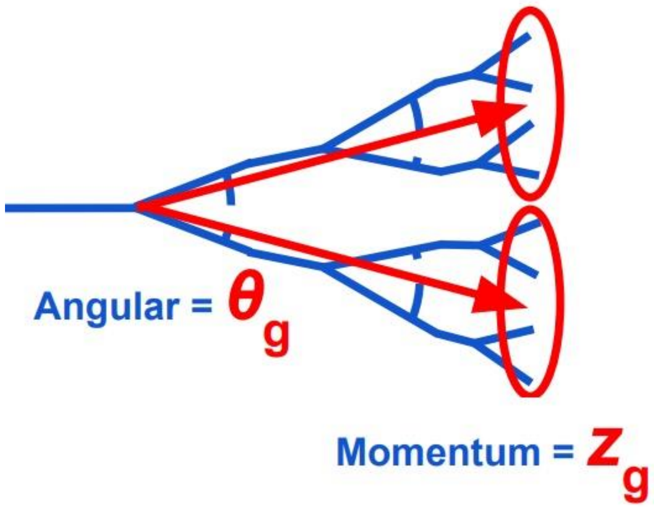

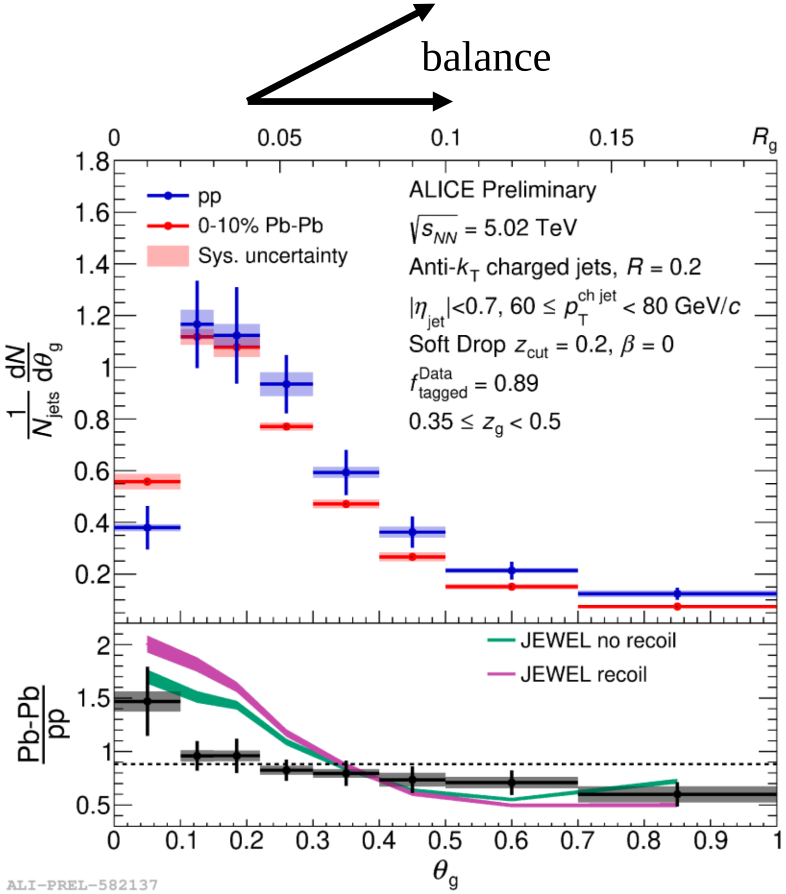

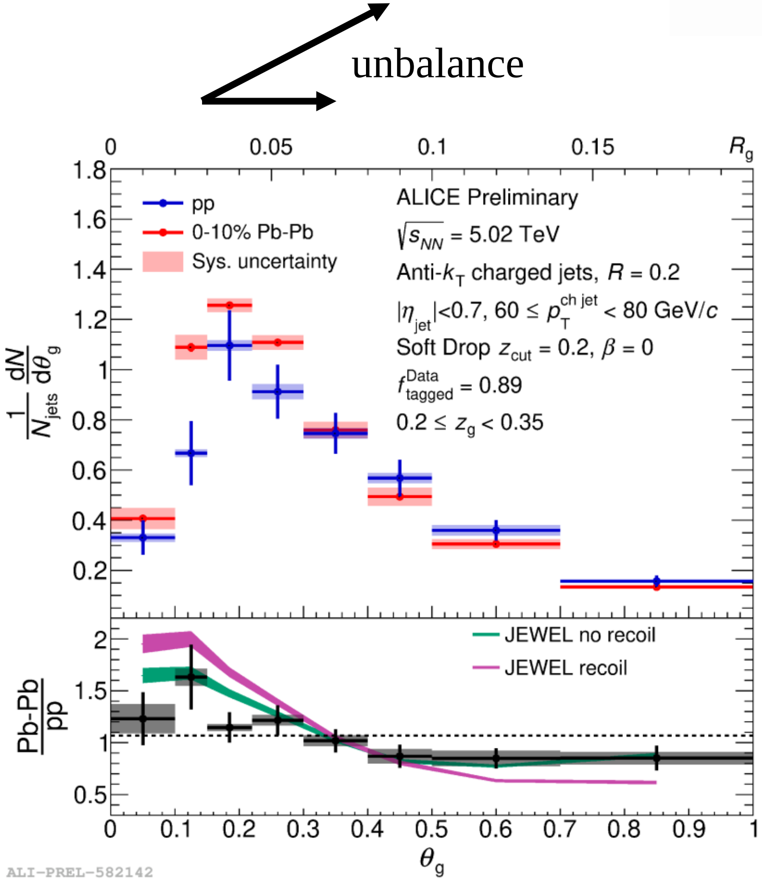

- Multidimensional measurement to disentangle jet survival bias from medium modifications
- Allow disentangling modifications to the substructure of jets from energy loss effects arising from migration of the jet momentum

Dielectron production in Pb–Pb collisions

arXiv:2308.16704

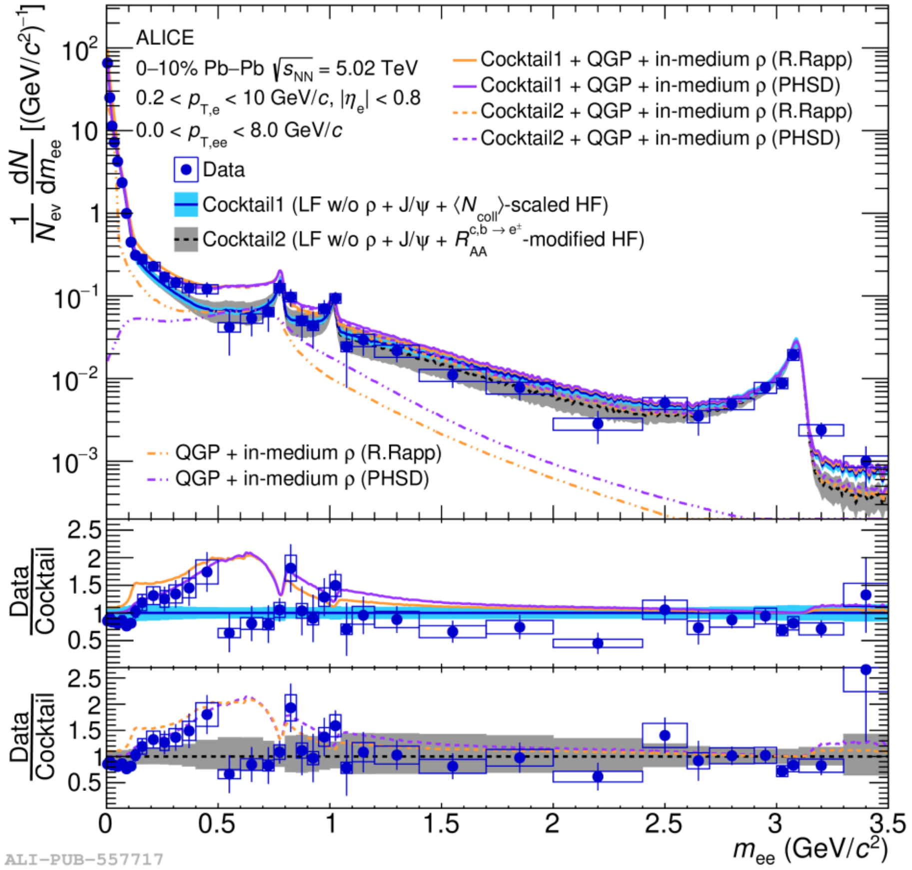

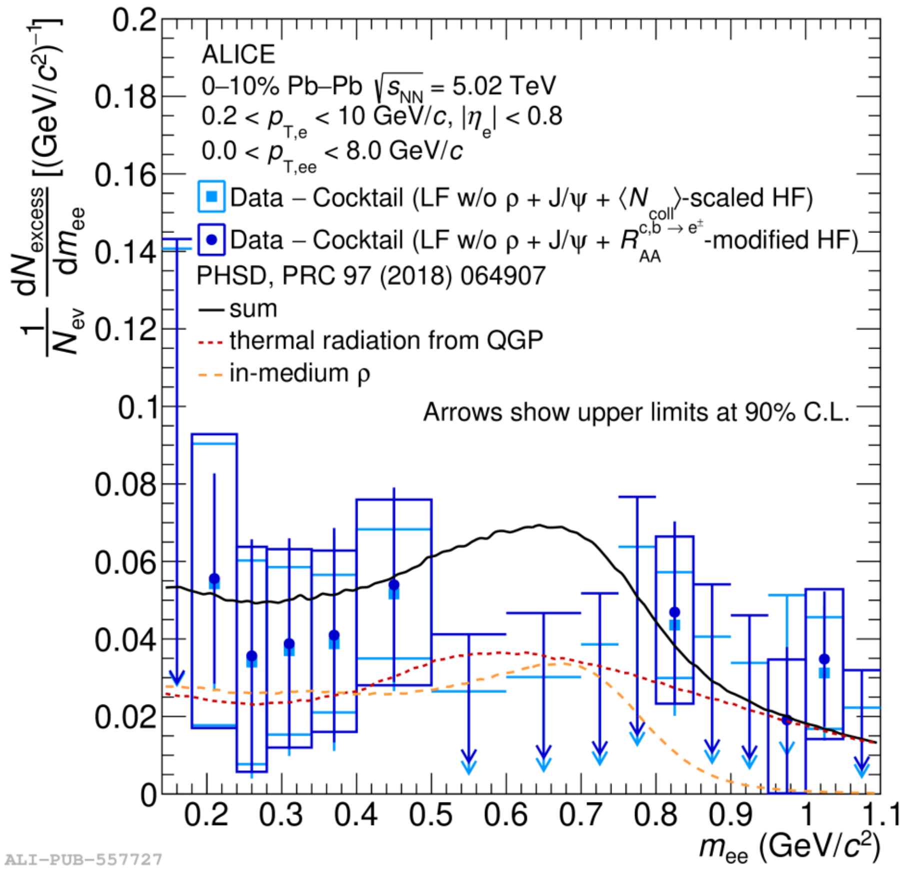

- Dielectron yield is consistent with hadronic cocktail within uncertainty, the excess in the low-mass region is 1.3σ
- More statistics and better control of HF background are needed to quantify the excess: full statistics from Run 3

Di-electron performance in Run 3

Run 3 performance

NEW

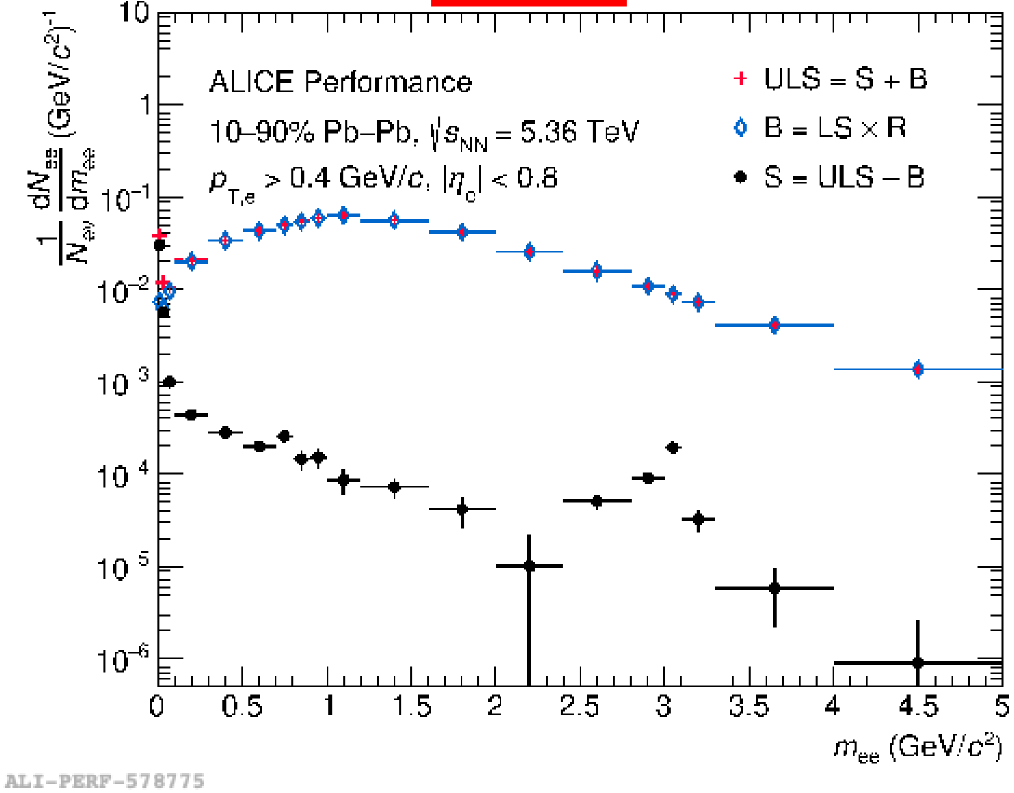

NEW

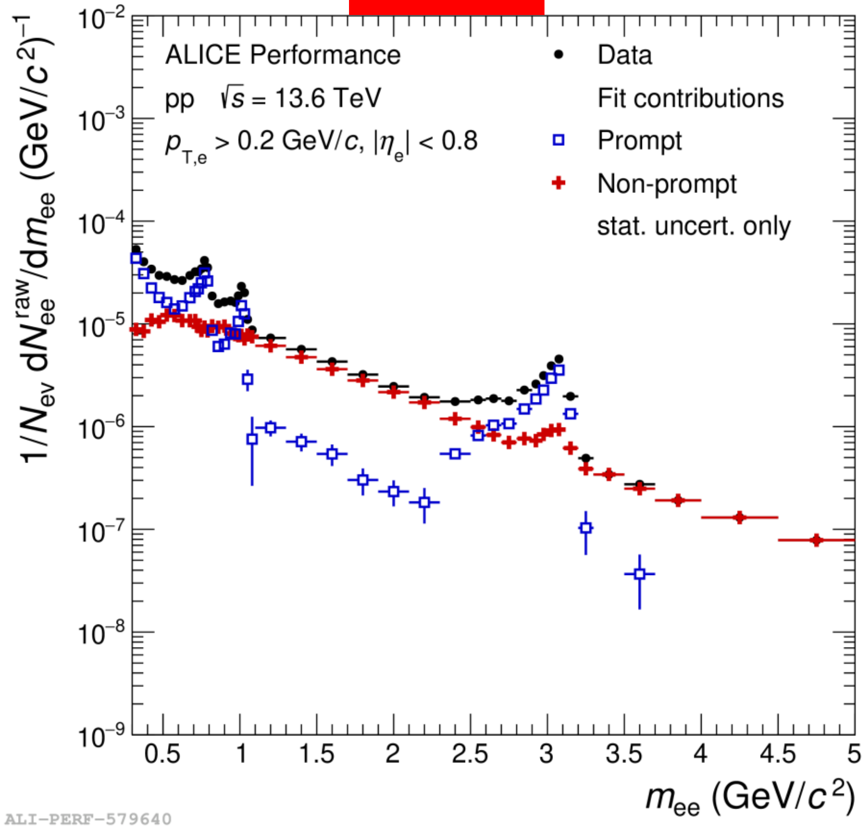

- More statistics and better-pointing resolution thanks to MFT and ITS upgraded in Run 3
- Improved DCA enable the separation of prompt (e.g. thermal) and non-prompt (HF background)

LHC-ALICE中长期计划

Run 3 — Run 6：亮度、精度、读出速率大幅提高

中国组聚焦关键物理：

- 夸克物质性质硬探针的精确测量
- 夸克物质强相互作用动力学
- 手征磁、手征涡旋及手征反常研究
- 冷核效应及末态强子化行为
- 奇特物质结构及新粒子寻找

光子谱仪（PHOS）及前端电子学研制

合作研制ALICE光子谱仪前端电子学系统（1999–2015年）

- 低噪声、大动态范围的电磁量能器读出
- 用以测量直接光子和衰变光子

前置放大器

前端读出板

局域触发主板

前端读出板阵列

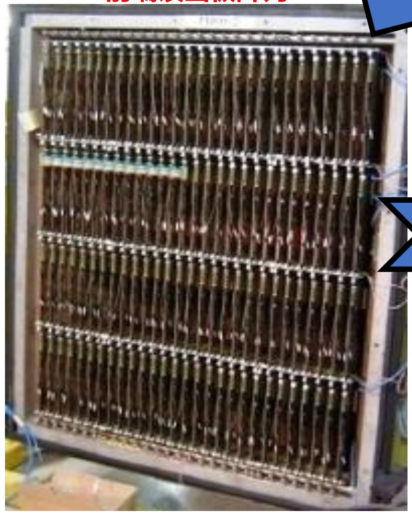

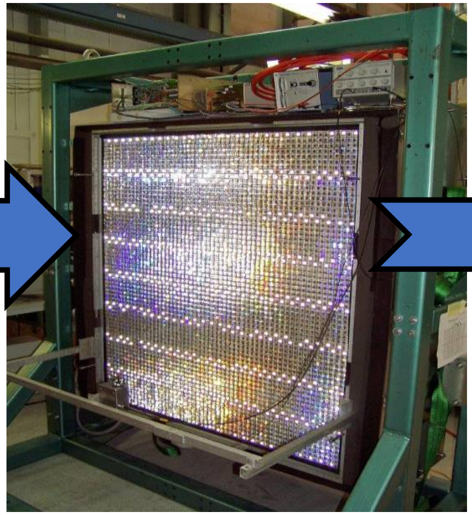

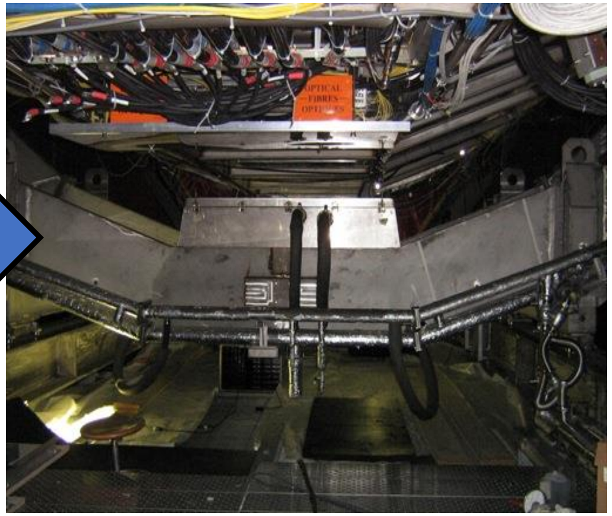

双喷注电磁量能器（DCAL）及其读出电子学

合作研制ALICE取样电磁量能器及其读出系统（2009–2015年）

- 中方建造了一个超级模块及读出系统，掌握了Shashlik取样量能器研制技术
- 测量双喷注、光子-喷注

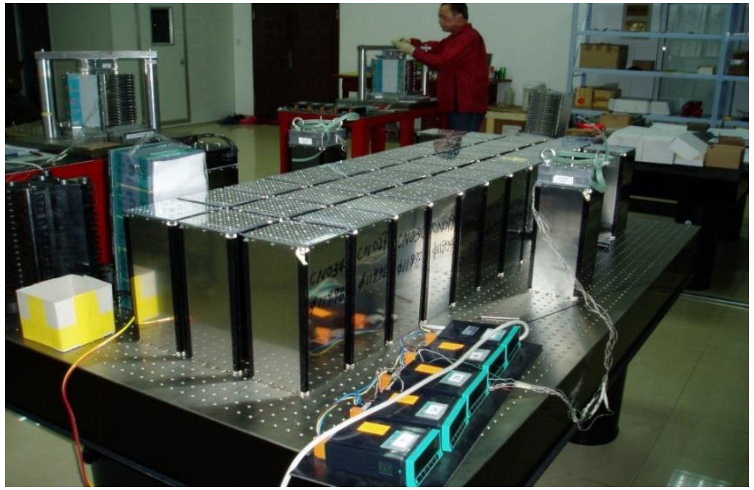
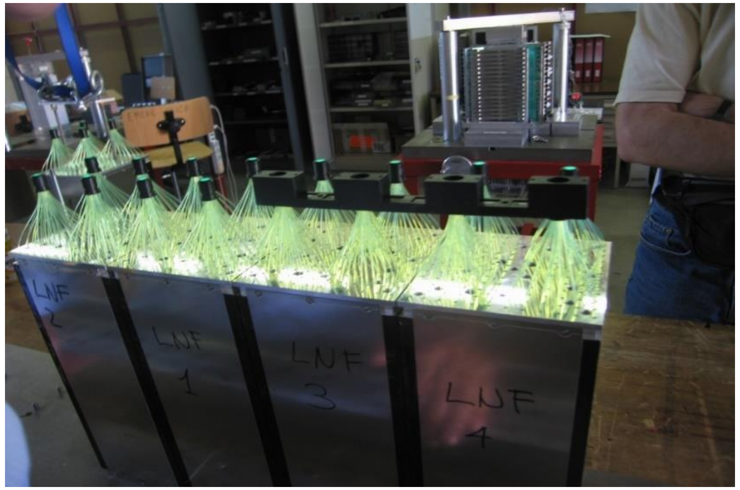
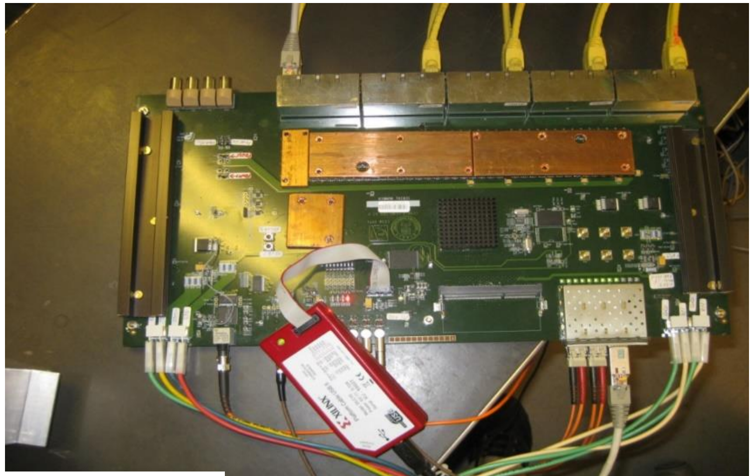
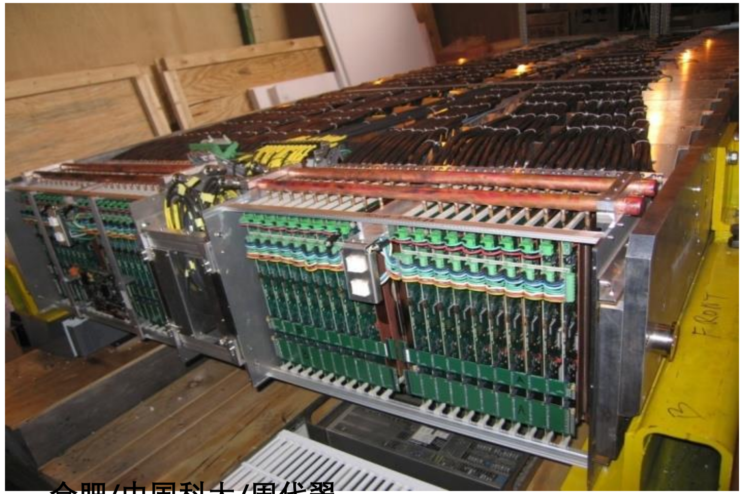

50

硅像素寻迹探测器ITS2芯片设计及硅像素模块研制

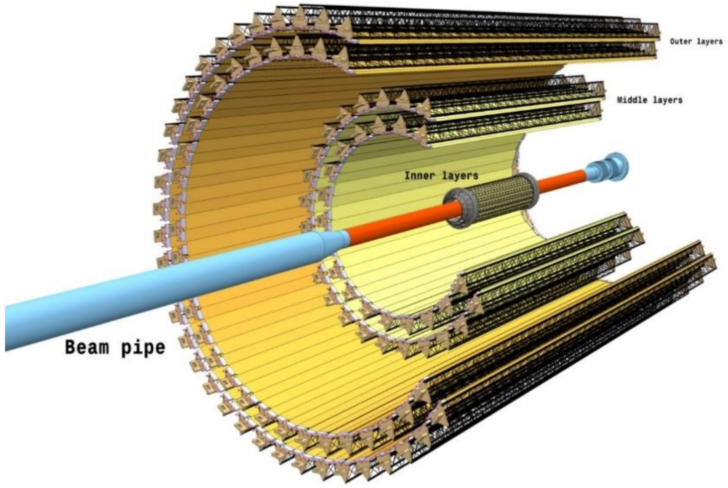

- 基于0.18 μm工艺单片有源硅像素传感器技术
- 用于顶点及带电粒子的高精度测量
  (空间分辨率提高10倍以上，读出速率提高50倍以上)
- 参与硅像素芯片设计；完成了升级探测器1/5芯片模块的建造与安装调试

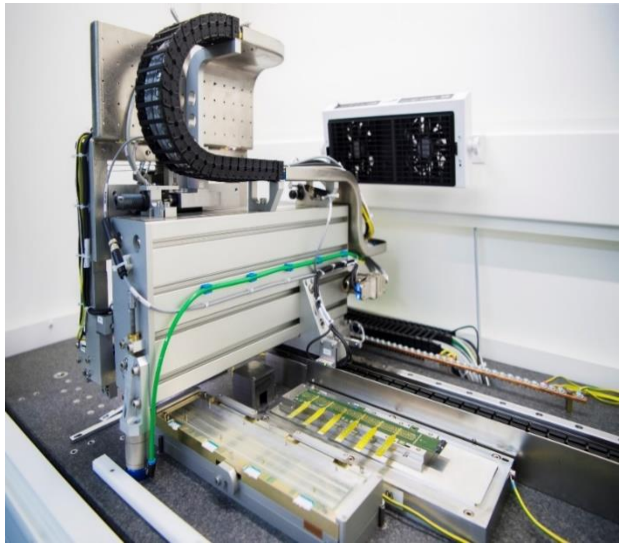

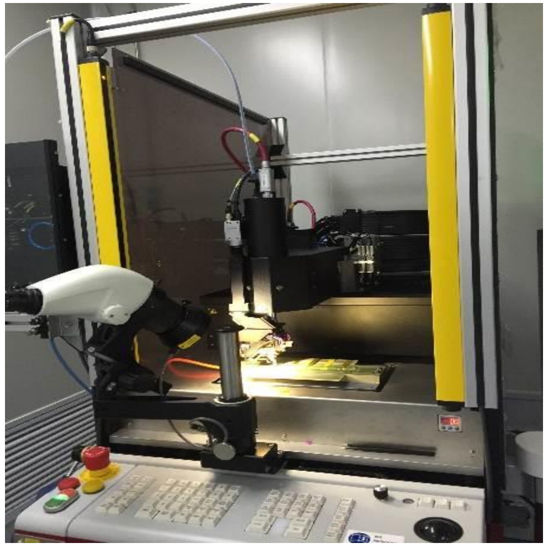

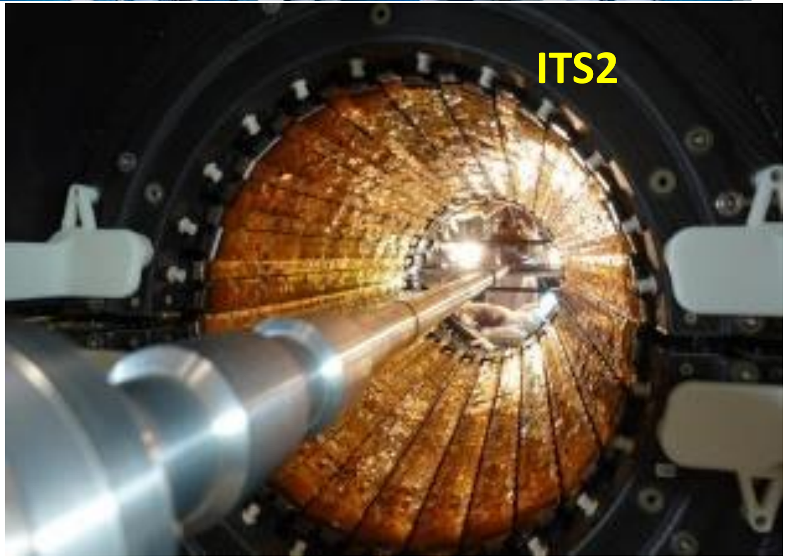

ITS upgrade HIC assembly at CCNU/Wuhan

硬件贡献四：前向缪子径迹探测器—MFT电子学母版研制

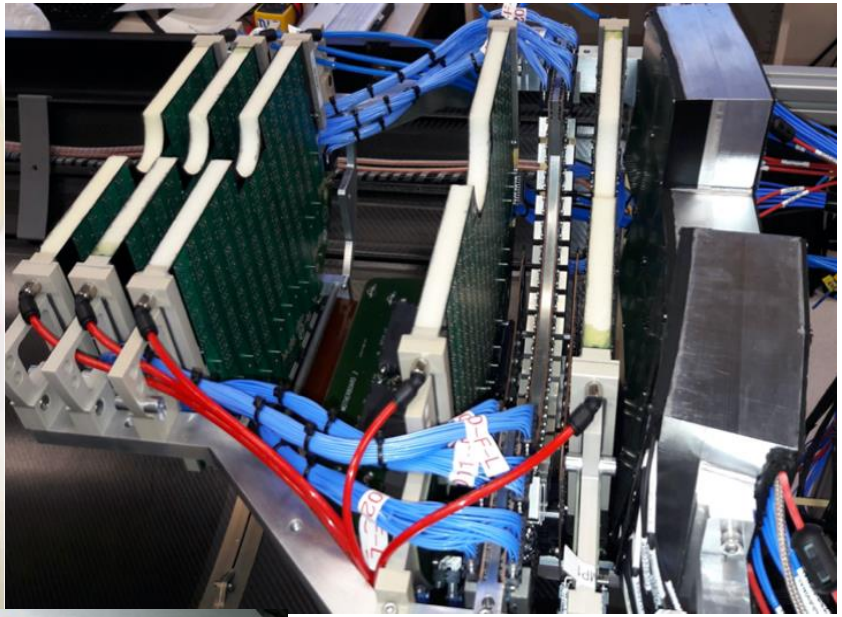

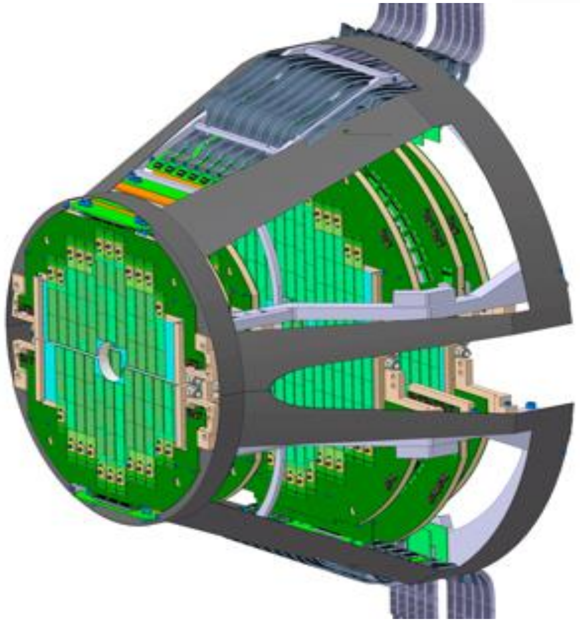

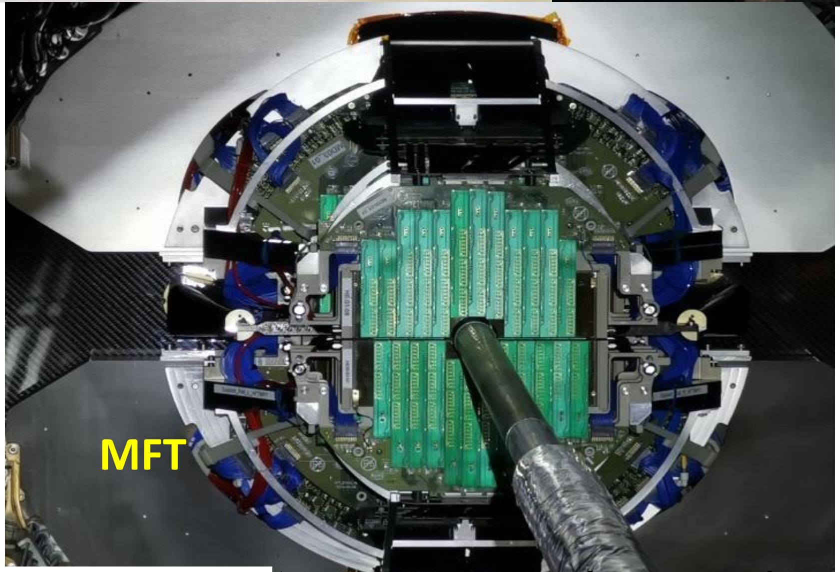

- 参与探测器研发及物理分析可行性研究
- 完成了探测器核心电子学母板设计与建造
- 用于高精度测量重夸克衰变顶点

正在参与的ALICE 探测器升级（2029-2032 运行）

第三代硅像素探测器

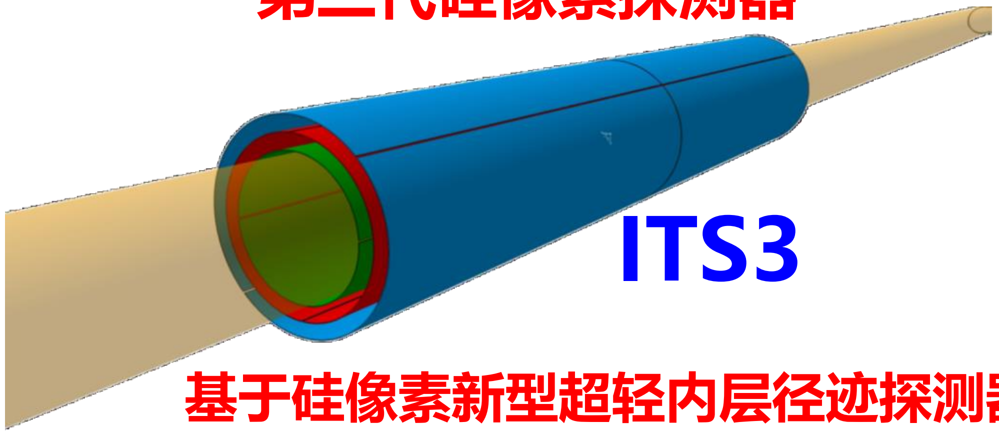

基于硅像素新型超轻内层径迹探测器

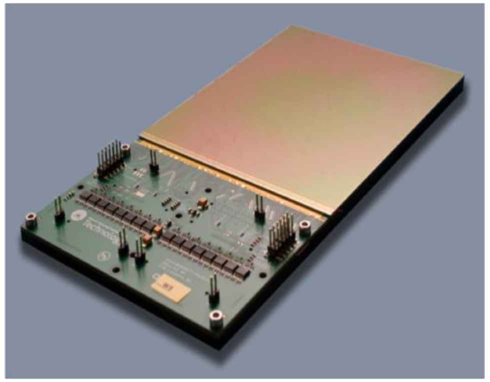

- 提升分辨率和低动量带电粒子重建效率
- 测量强衰变的稀有粒子

Letter of Intent https://cds.cern.ch/record/2703140
On track for TDR in 2022

前向（电磁和强子）量能器

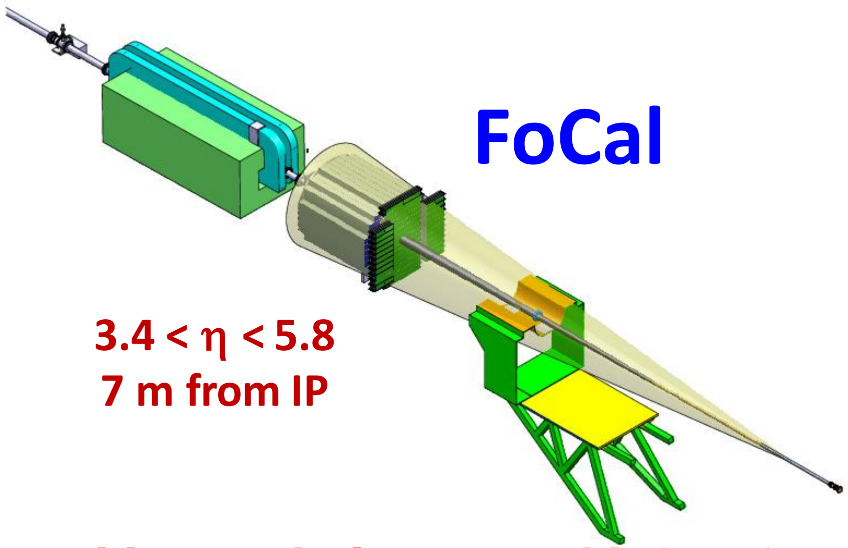

基于硅像素和PAD技术量能器

- 质子和核内胶子分布函数
- 非线性QCD演化方程
- 小系统中类流长程关联的根源
- ……

TDR-https://inspirehep.net/literature/2797164
LoI - CERN-LHCC-2020-009 ; LHCC-I-036

第三代ALICE 探测器（2036-2041运行）

- high-resolution, wide η coverage, high rates for precision QGP physics
- Heavy-ion physics to the fb^{-1} luminosity era* with unique kinematic reach

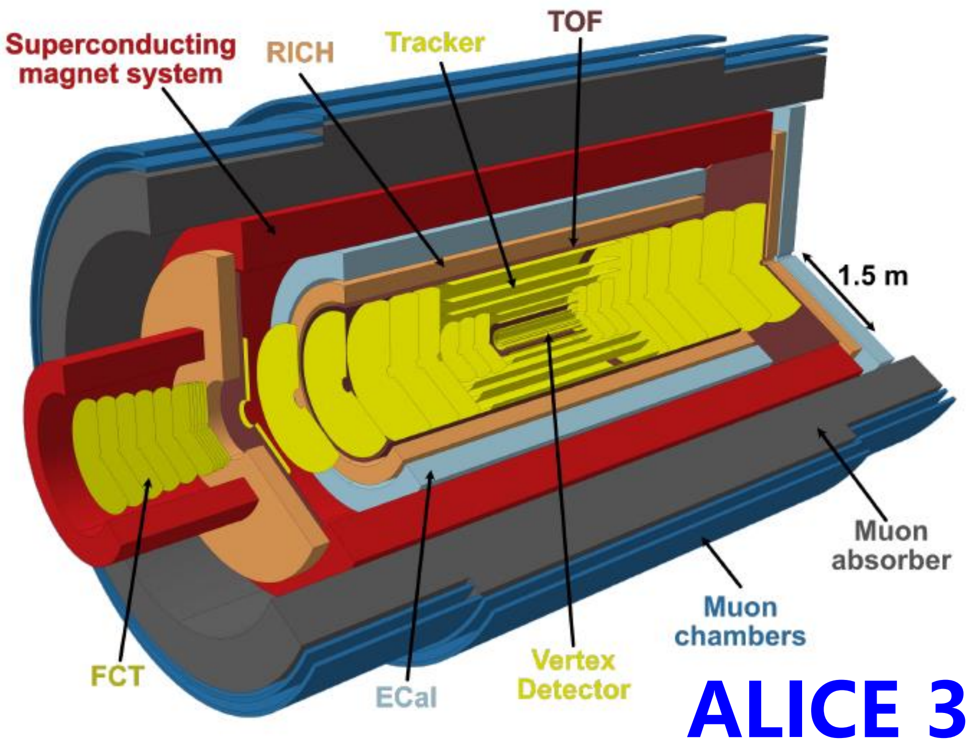

key requirements

- **ultra-low material budget** for low p_T tracking
  - X/X_0 ~ 0.05 % / layer
- **fast** to sample large luminosity
  - 50 - 100x Run 3/4
- **large acceptance**
  - $|\eta| < 4 \Rightarrow \Delta\eta = 8$ (total)
  - $|\eta| < \sim 1.4$ (central barrel)
- **excellent spatial resolution** for tracking and vertexing
  - innermost layers: σ < 3 μm
  - outer layers: σ ~ 5 μm
- **precise time measurement** for particle identification
  - σ ~ 20 ps

科学问题

- 如何从QCD第一性原理出发理解夸克物质性质?
- 能否证明核环境中手征对称性的恢复?
- 核环境中是否存在量子场论基本特性的破坏，以及超出标准模型的新物理现象?

全新的硅像素寻迹与粒子鉴别探测器

高分辨率、大快度、高事例率

arXiv:1902.01211

中国组正在参与全新的ALICE第三代探测器研发和物理分析可行性研究，将重点参与硅像素探测器和基于LGAD 的TOF探测器研发和建造

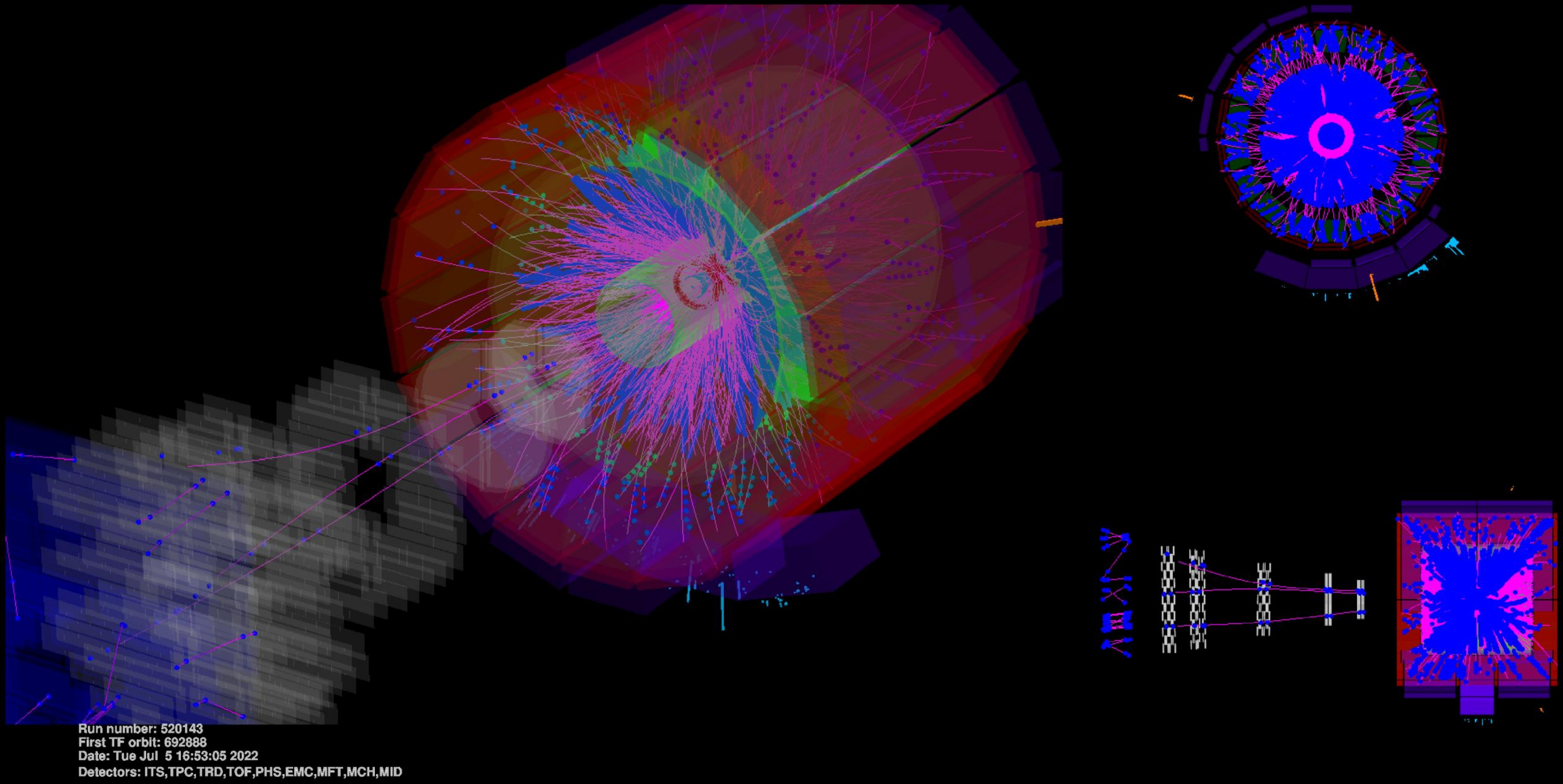
Run number: 520143
First TF orbit: 692888
Date: Tue Jul 5 16:53:05 2022
Detectors: ITS,TPC,TRD,TOF,PHS,EMC,MFT,MCH,MID

感谢各位专家的莅临指导!

ALICE heavy quark programme

Collisions systems (so far) :
Pb-Pb, pp, p-Pb, Pb-p, Xe-Xe

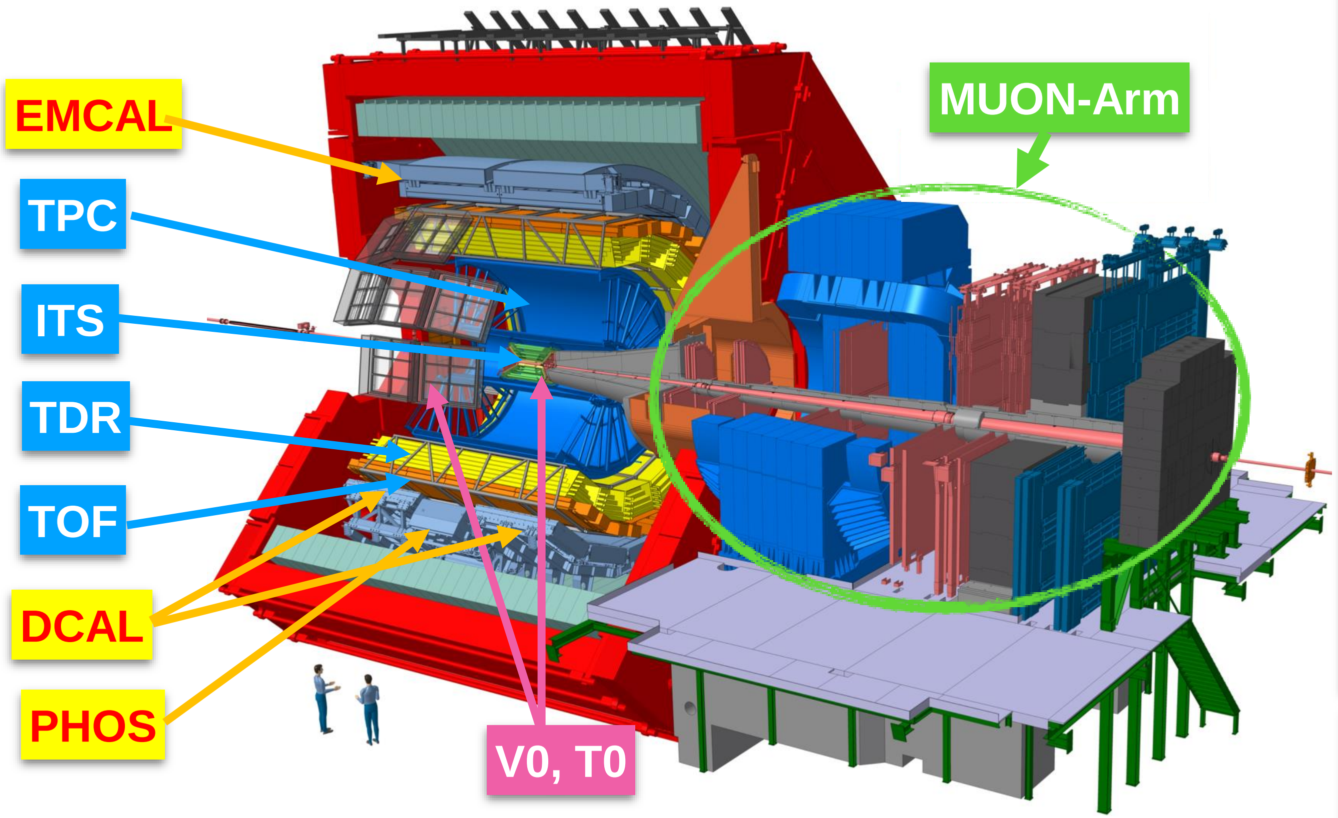

Hadronic decays (|y| < 0.8)

- $D^0 \to K^-\pi^+$
- $D^+ \to K^-\pi^+\pi^+$
- $D^{*+} \to D^0\pi^+ \to K^-\pi^+\pi^+$
- $D_s^+ \to \varphi\pi^+ \to K^-K^+\pi^+$
- $\Lambda_c^+ \to pK^-\pi^+$
- $\Sigma_c^{0,++} \to \Lambda_c^+\pi^{\mp}$
- $\Xi_c^{0(+)} \to \Xi^-\pi^+(\pi^+)$
- $\Omega_c^+ \to \Omega^0\pi^+$

Semi-leptonic decays

- c, b→$e^\pm$ (|y| < 0.7)
- c, b→$\mu^\pm$ (2.5 < y < 4)

中国组在ALICE探测器上已做出的贡献

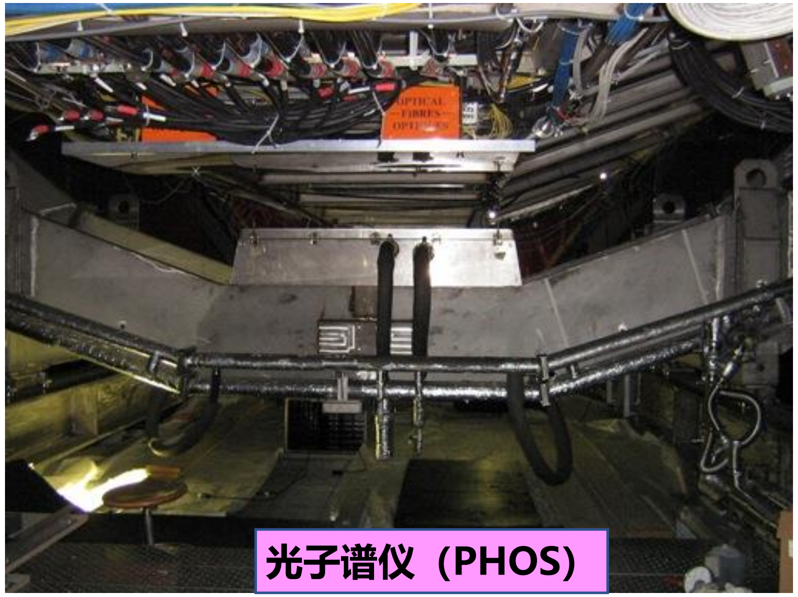
光子谱仪（PHOS）

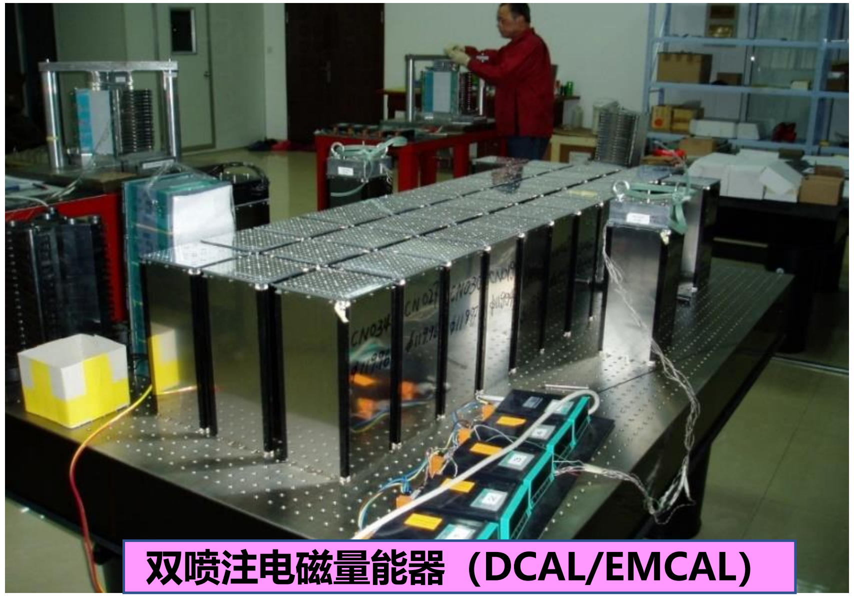
双喷注电磁量能器（DCAL/EMCAL）

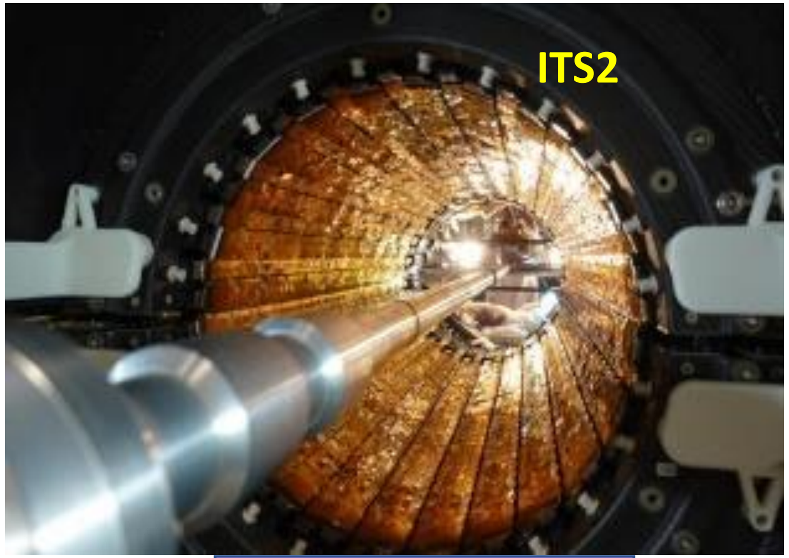

内层径迹探测器（ITS2）

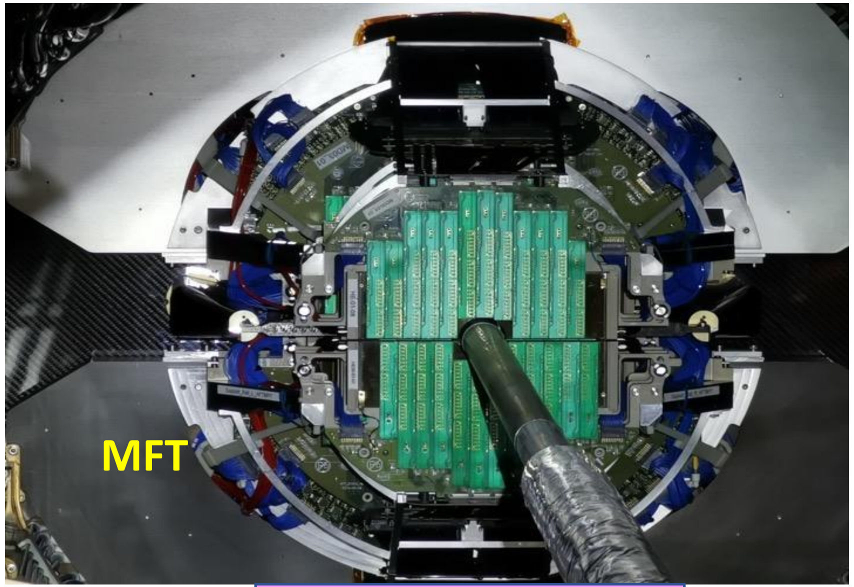

前向缪子径迹器（MFT）

Bjorken's Estimate of the Energy Density

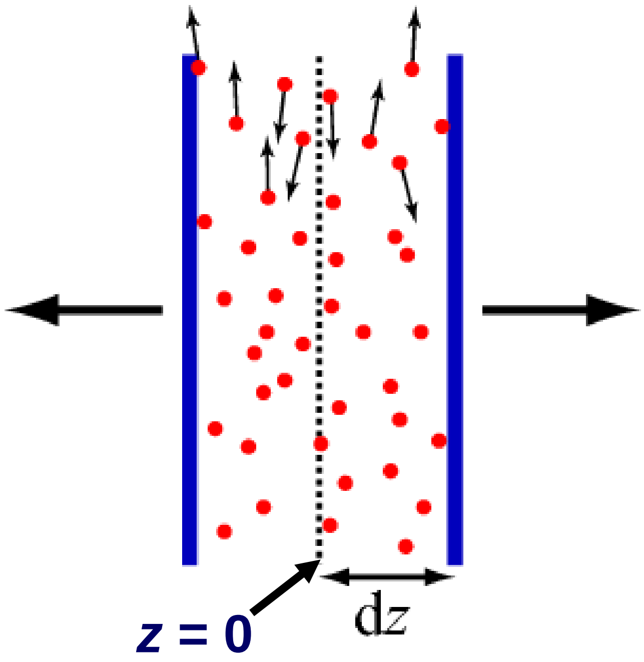

$$\langle \varepsilon \rangle (\tau) = \frac{1}{\tau \pi R^2} \frac{dE_T}{dy} \longleftrightarrow dN/d\eta$$

Related to thermalization time τ_0 (1 fm/*c*)

- Central Pb–Pb collisions at 5.02 TeV d*N*/dη ~ 2000

  → Energy density ε ~18 GeV/fm³

According to LQCD, the QGP is formed when:

$\varepsilon_c = (0.42 \pm 0.06) \quad GeV/fm^3$

$T_c = (156.5 \pm 1.5) \quad MeV$

Bjorken estimate:

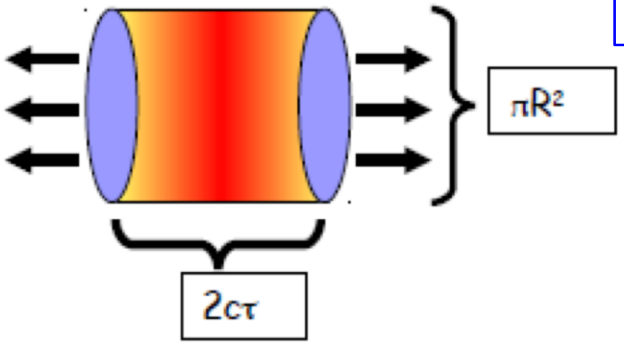

Phys. Rev. D **27**, 140

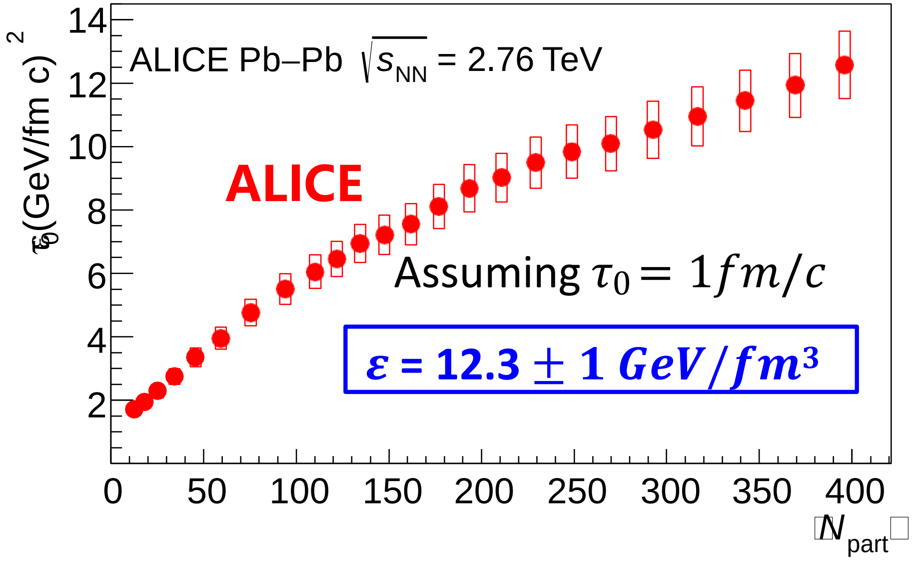

How many particles are created in a collision?

Total Charged particle multiplicity

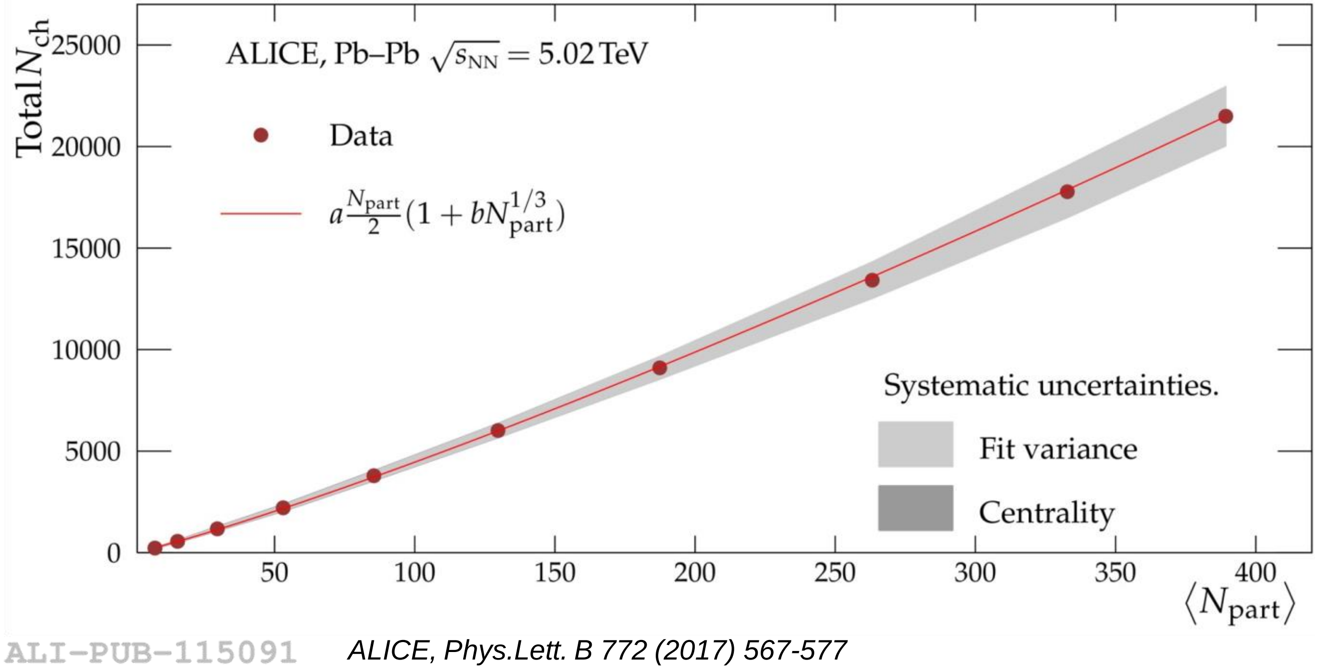

ALICE, Phys.Lett. B 772 (2017) 567-577

In a central Pb-Pb collision at the LHC, more than 20000 charged tracks must be reconstructed.

→ **High granularity tracking systems, primary importance of tracking, vertexing calibration**

Charged particle density in central AA collisions

Average charged particle multiplicity density normalized to the average N_{part} vs $\sqrt{s_{NN}}$

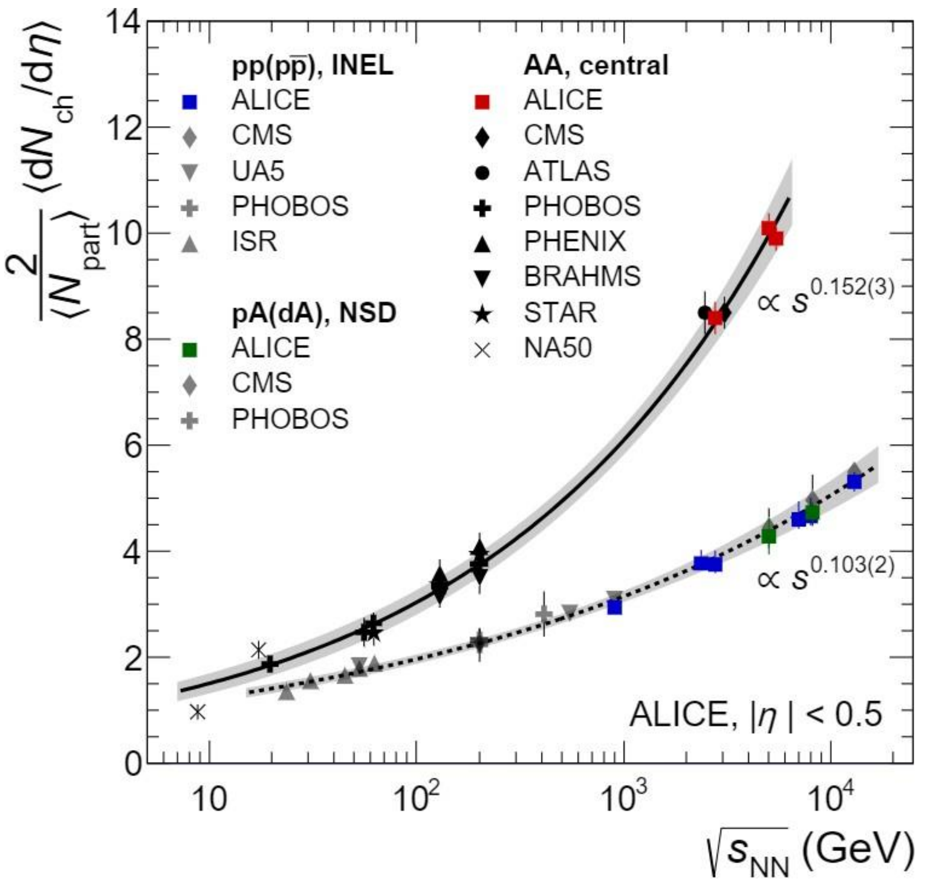

ALICE *Phys. Rev. Lett.* **116** (2016) 222302

ALICE Eur. *Phys. J. C* (2019) 79:307

Particle production per participant in AA collisions follows a steeper power law than in pp, pA and increased by **2-3x** from RHIC to the LHC

AA collisions are more efficient in transferring energy from beam- to mid- rapidity than pp

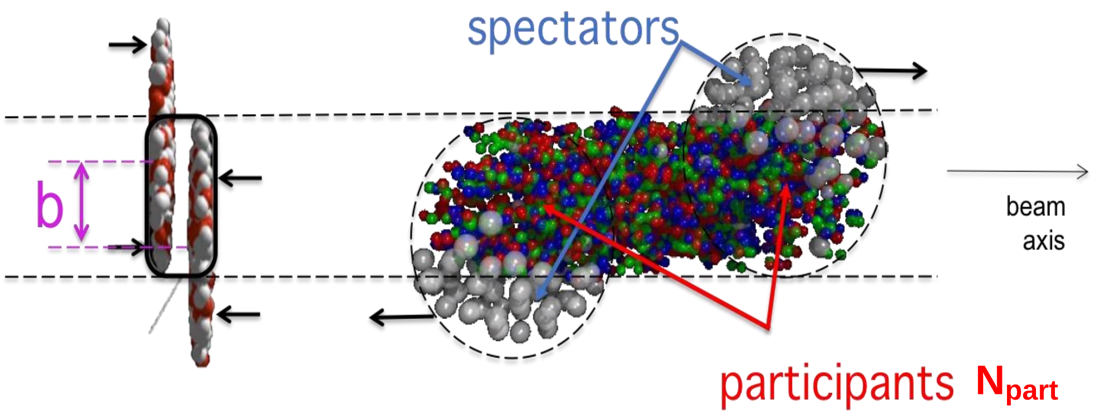

- ALICE: Pb–Pb at 5.02 TeV — highest energy so far
  ➞ For 0–5% most central collisions, confirms trend from lower energies

Temperature of the QGP

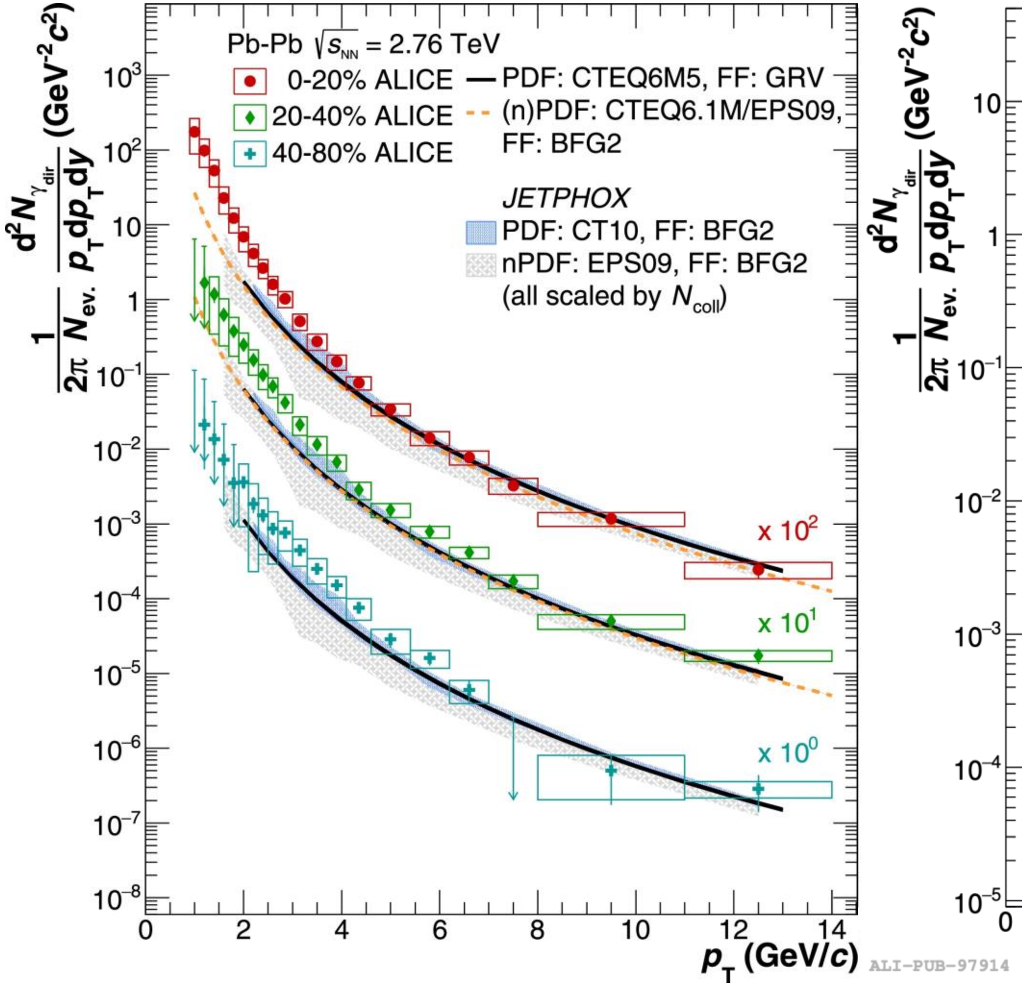

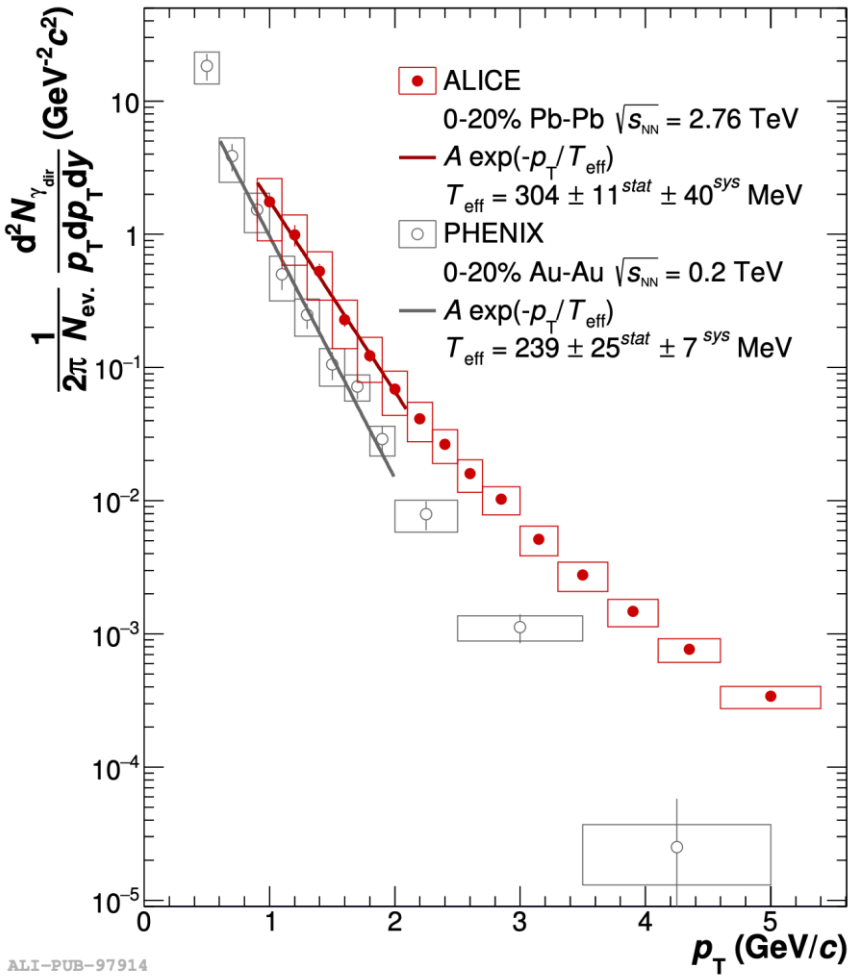

For comparison
T=156 MeV ≙ $1.8\cdot10^{12}$ K
Sun core: $1.5 \cdot 10^{7}$ K
Sun surface: 5778 K

- Low-p_T: 2.6σ excess w. r. t. models in 0–20% central — thermal contribution
- T_{eff} = 304 ± 12(stat.) ± 41 (syst.) MeV in central collisions — above T_c ~ 170 MeV
- 30% higher than at RHIC (Au–Au at $\sqrt{s_{NN}}$=200 GeV)

ALICE *Phys. Lett.* **B754** (2016) 235

Upgrading the ALICE detector (RUN 4)

ITS3: TDR approved

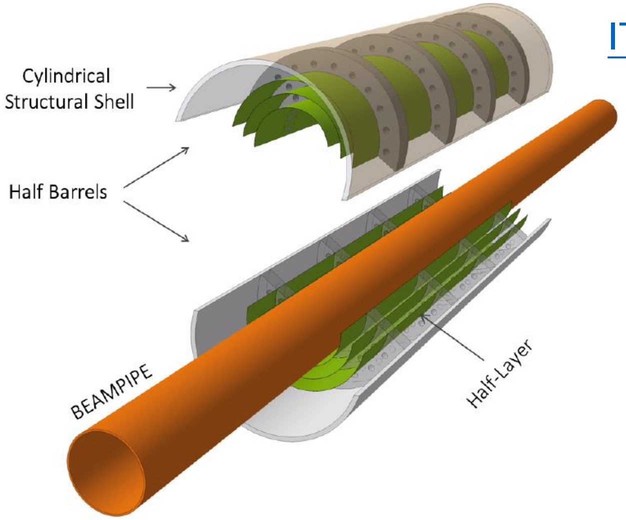

ITS3 CDS LINK

- Replacing the ITS2 inner layers by "silicon-only"
- Inner-most radius 19 mm, x 2 improvement in pointing resolution
- **Improve the measurements of heavy flavor and dielectrons at midrapidity**

FoCal: TDR approved

CERN-LHCC-2020-009

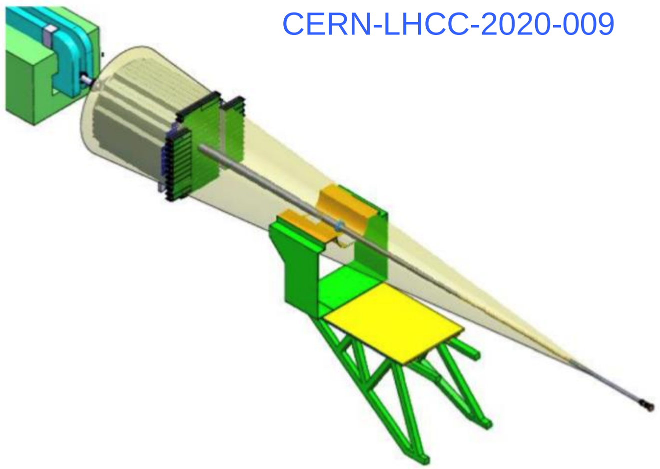

- FoCal-E calorimeter: High-granularity Si-W
- FoCal-H: Cu-scintillator
- Direct photons, π^0, jets at forward rapidity
- **Unexplored regions of small-x and low Q^2 gluons**

LHC LS2	LHC RUN 3	LHC LS3	LHC RUN 4	LHC LS4	LHC RUN 5 and RUN 6
2019-2021					

Upgrading the ALICE detector (RUN 4)

ITS3: Prototype

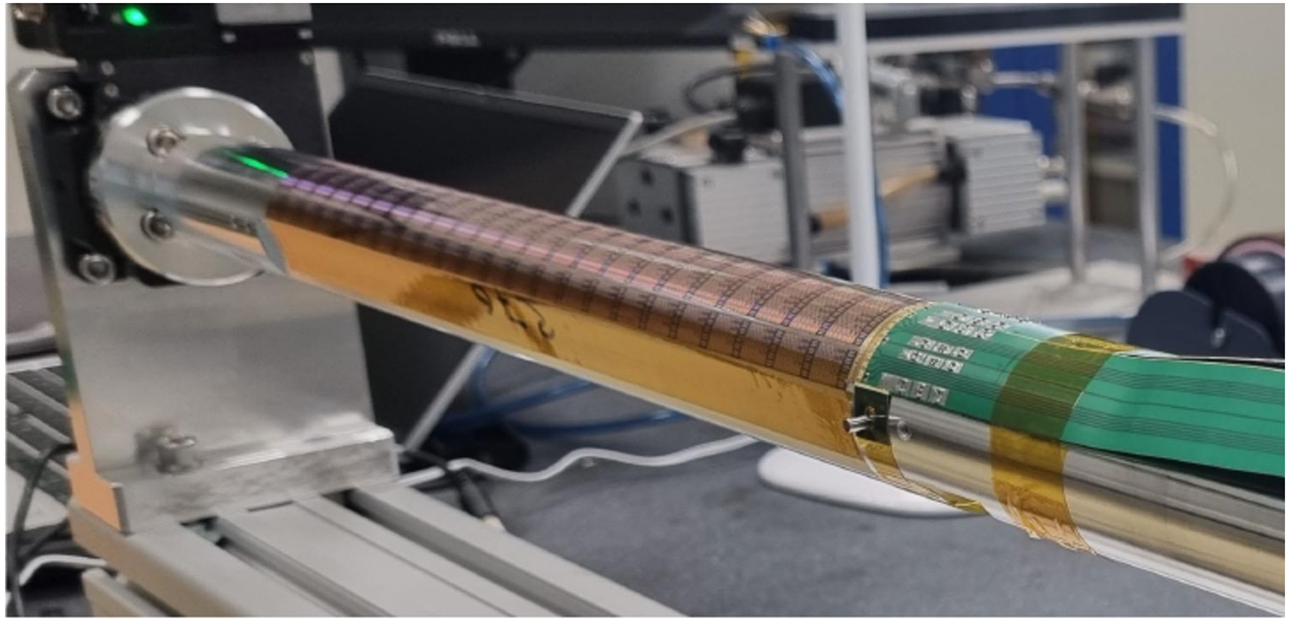

FoCal: Prototype

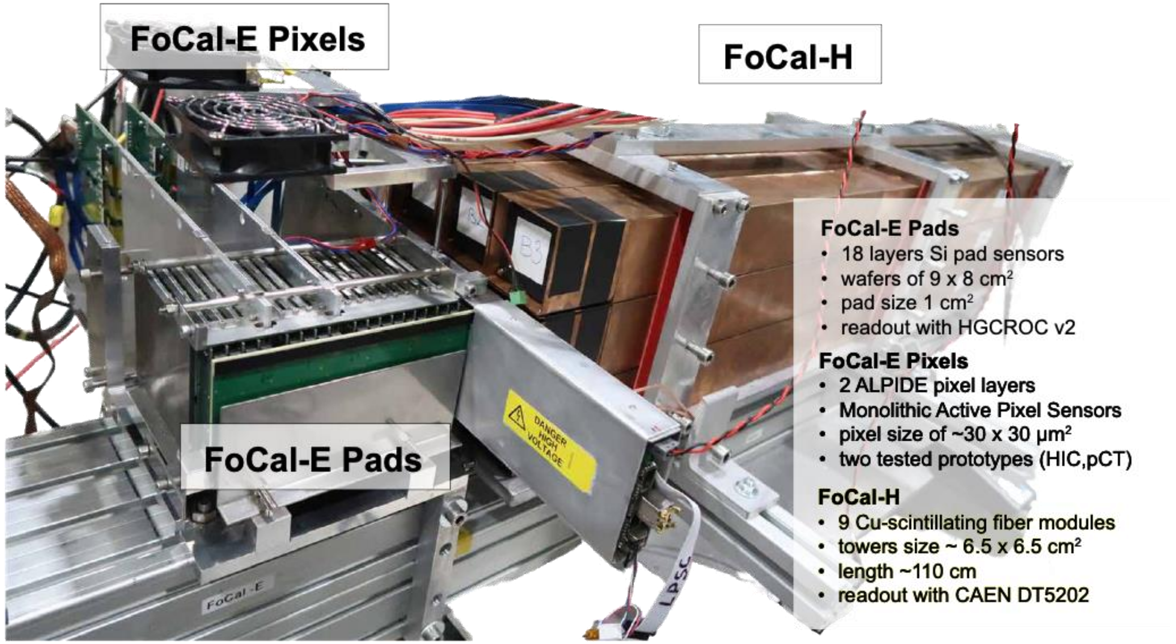

Prototypes constructed to test assembly methods and verify performance

Bong-Hwi Lim 24/09 15:55

Jacek Tomasz Otwinowski 24/09 16:15

LHC LS2	LHC RUN 3	LHC LS3	LHC RUN 4	LHC LS4	LHC RUN 5 and RUN 6
2019-2021					

Upgrading the detector (ALICE 3)

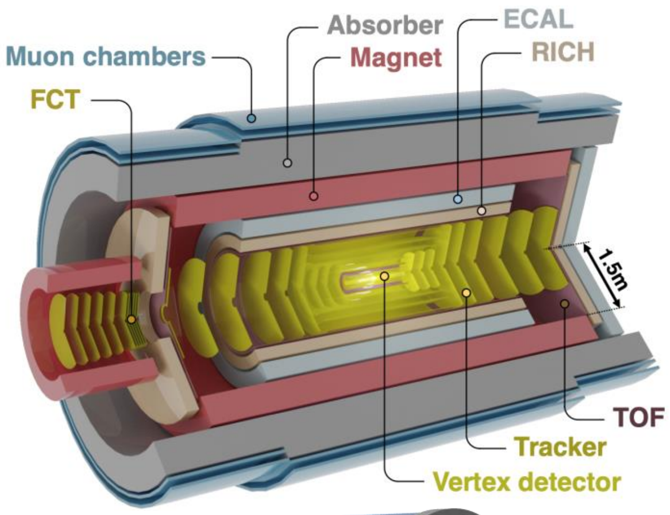

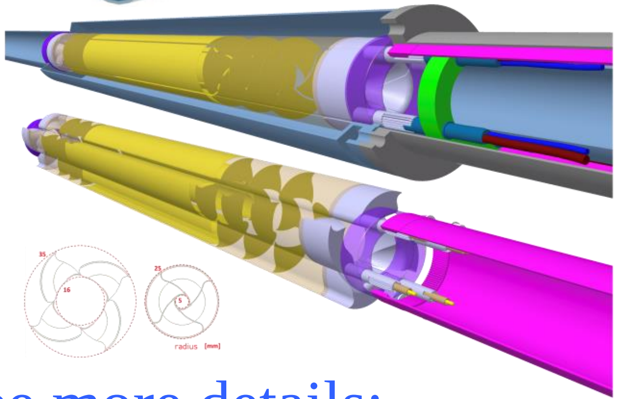

Detector concept:

- Compact **all-silicon tracker** with high-resolution vertex detector
- **Particle Identification** over large acceptance, identification of muons, electrons, hadrons, photons
- Fast read-out and online processing

Physics programs:

- High-precision **beauty** measurements
- **Multi-charm** baryons, **exotic hadrons**, **ultra-soft photons**
- **Time-dependence and flow of thermal radiation**
- D-$\overline{D}$ and D-D* $\Delta\phi$ correlations

Cas Van Veen 24/09 15:35

See more details: arXiv:2211.02491

LHC LS2	LHC RUN 3	LHC LS3	LHC RUN 4	LHC LS4	LHC RUN 5 and RUN 6
2019-2021					

QGP物质基本性质观测：能量密度-温度-寿命

According to LQCD, the QGP is formed when

$$\varepsilon_c = (0.42 \pm 0.06)\ GeV/fm^3$$ critical energy

$$T_c = (156.5 \pm 1.5)\ MeV$$ critical temperature

For comparison
T=156 MeV ≙ $1.8 \cdot 10^{12}$ K
Sun core: $1.5 \cdot 10^7$ K
Sun surface: 5778 K

能量密度

Phys. Rev. D **27**, 140

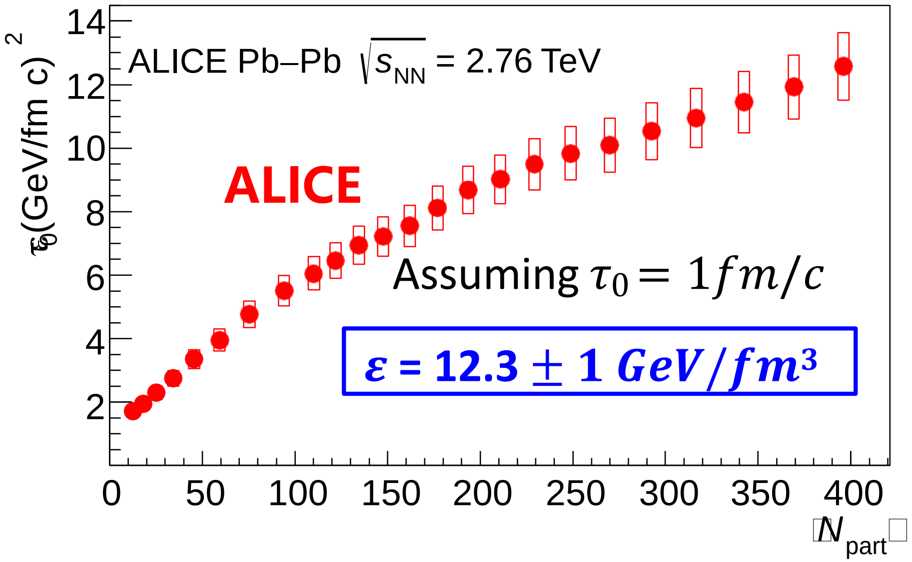

温度

PLB 754 (2016) 235

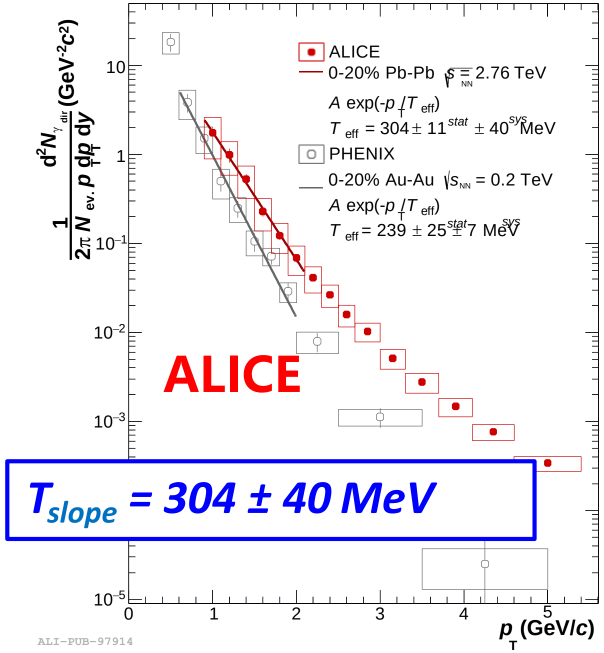

寿命和体积

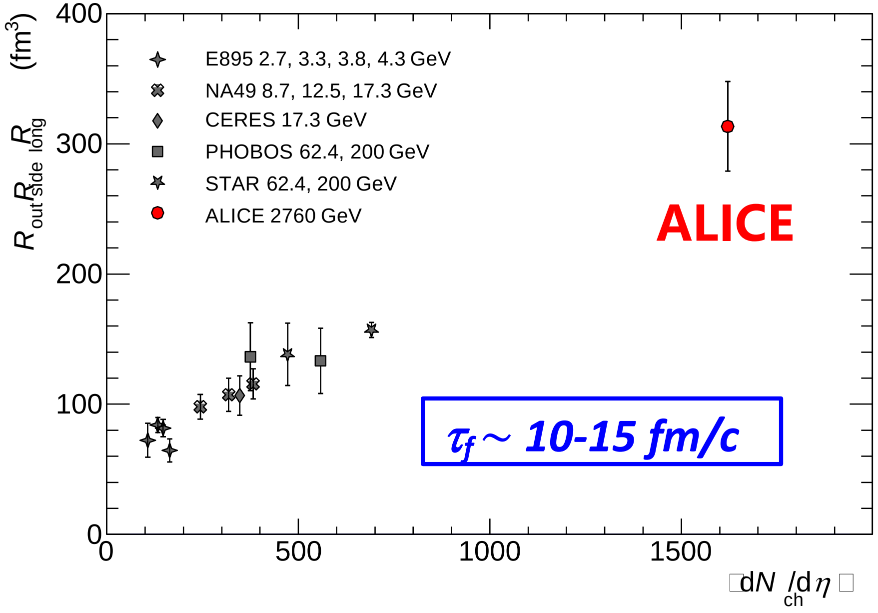

Charm quark transport

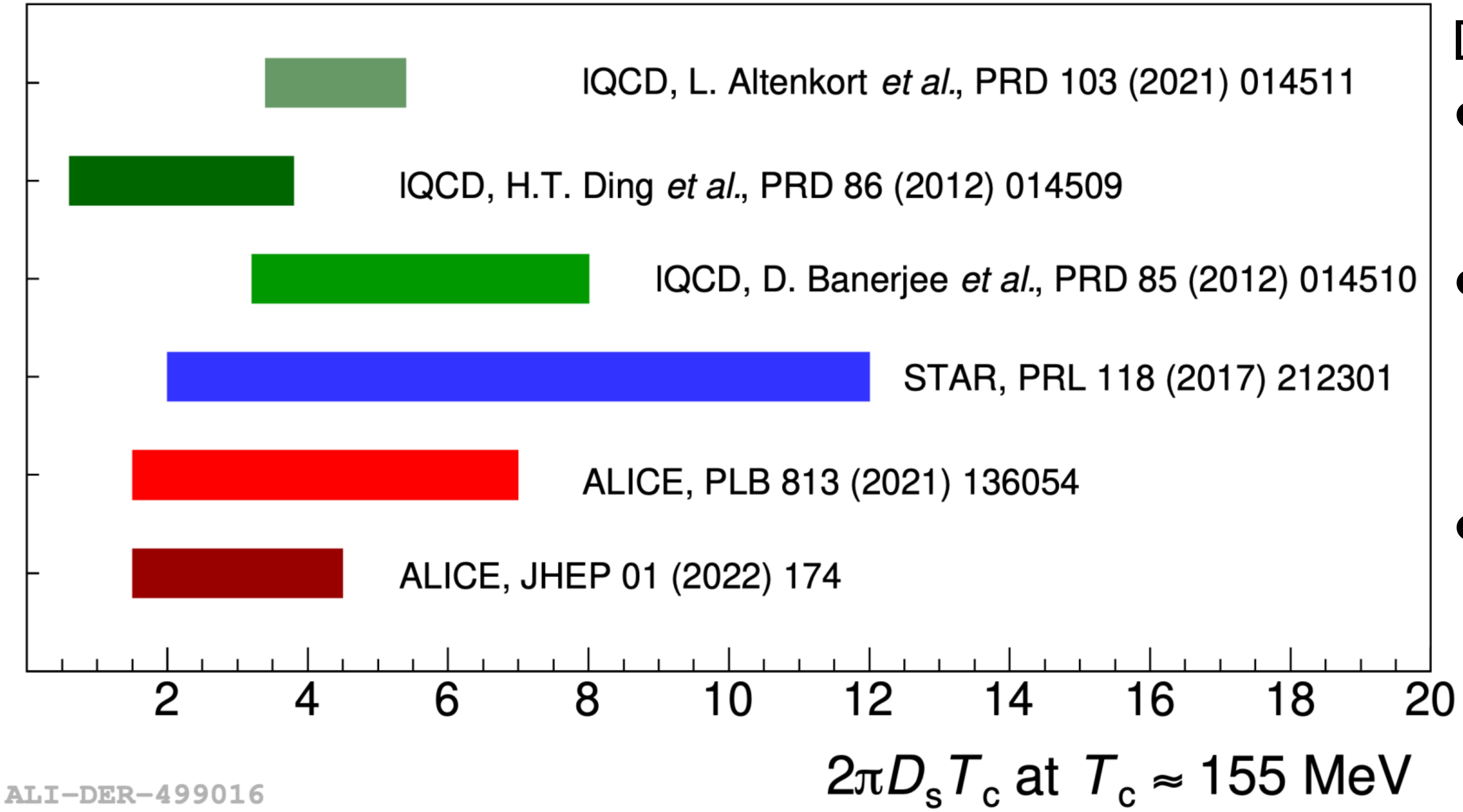

Diffusion coefficient D_s

- Almost independent of quark mass
- Characterization of the transport properties of the medium
- Constrains the specific shear viscosity η/s

The newest constraints from ALICE by combining D meson R_{AA} and v_2

- $1.5 < 2\pi D_s(T) < 4.5$, $\tau_{charm} = (m_{charm}/T)\,D_s(T) = 3–9$ fm/c < $\tau_{medium} \approx 10$ fm/c
- Indicate charm may thermalize in the medium

Gluon emission of a heavy quark

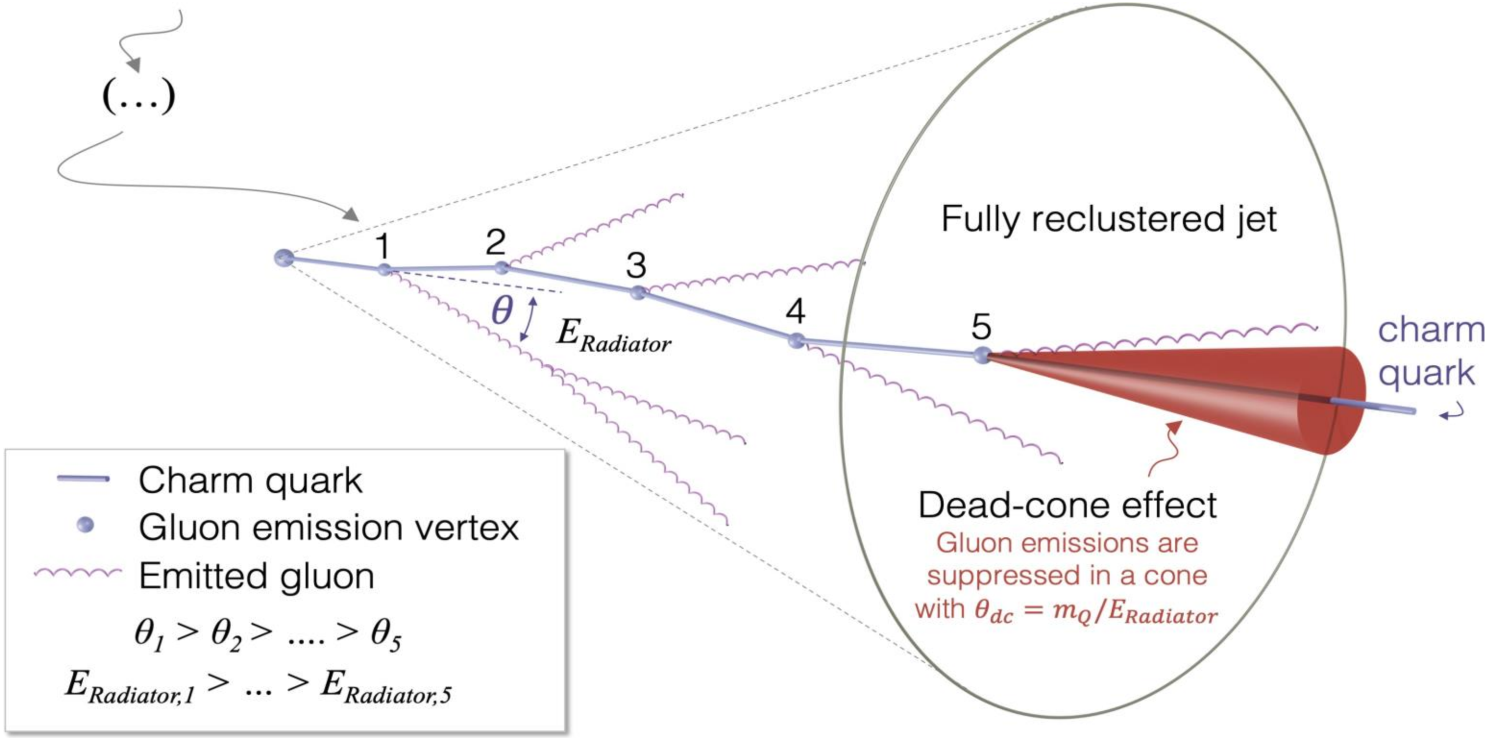

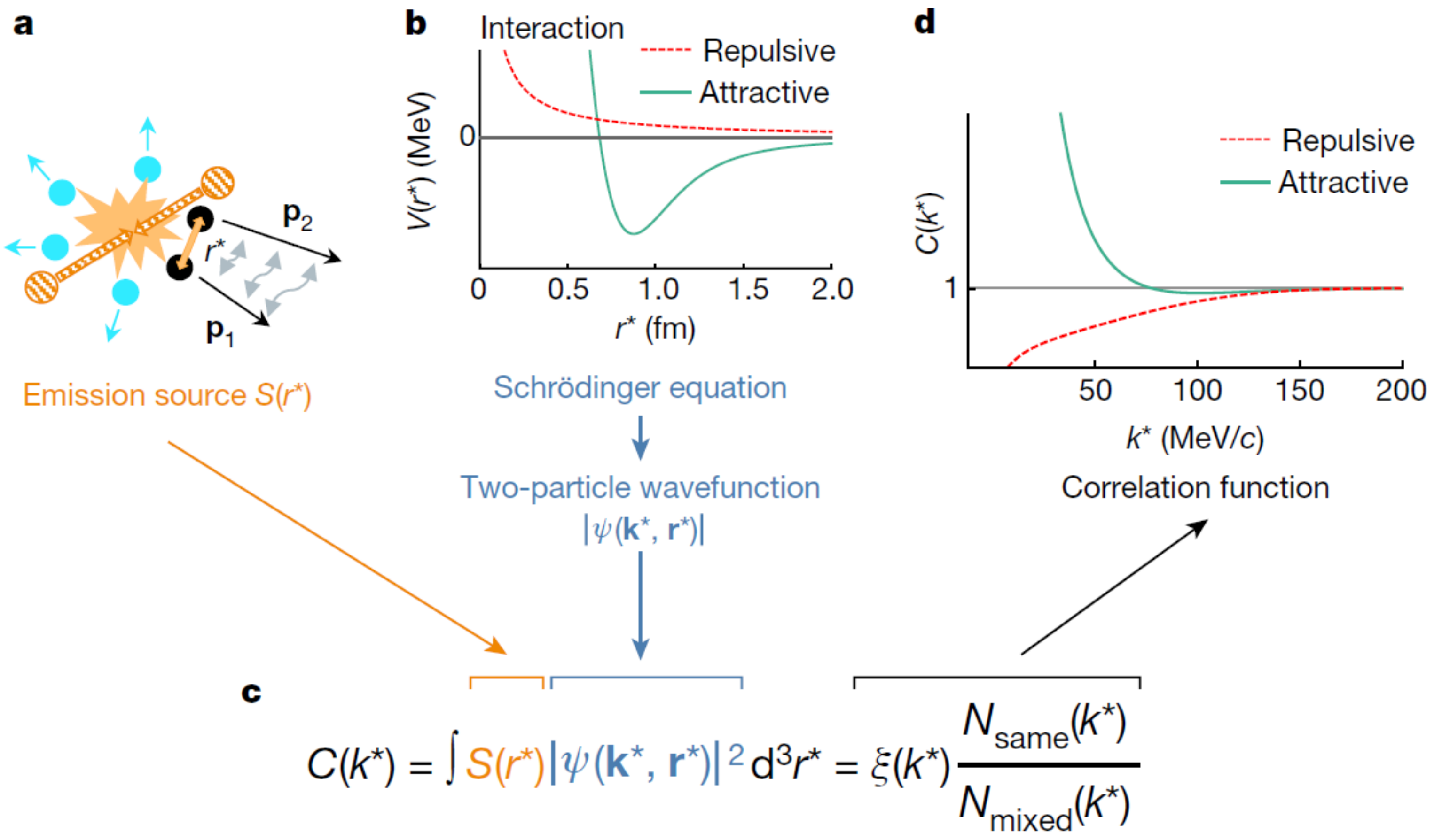
a
p2
r*
p1
Emission source S(r*)
b
Interaction
Repulsive
Attractive
V(r*) (MeV)
0
0.5
1.0
1.5
2.0
r* (fm)
Schrödinger equation
Two-particle wavefunction
|ψ(k*, r*)|
d
Repulsive
Attractive
C(k*)
1
50
100
150
200
k* (MeV/c)
Correlation function
c
$C(k^*) = \int S(r^*) |\psi(\mathbf{k}^*, \mathbf{r}^*)|^2 d^3r^* = \xi(k^*) \frac{N_{same}(k^*)}{N_{mixed}(k^*)}$

揭示质子-超子间强相互作用

ALICE： Nature 558 223-238(2020)

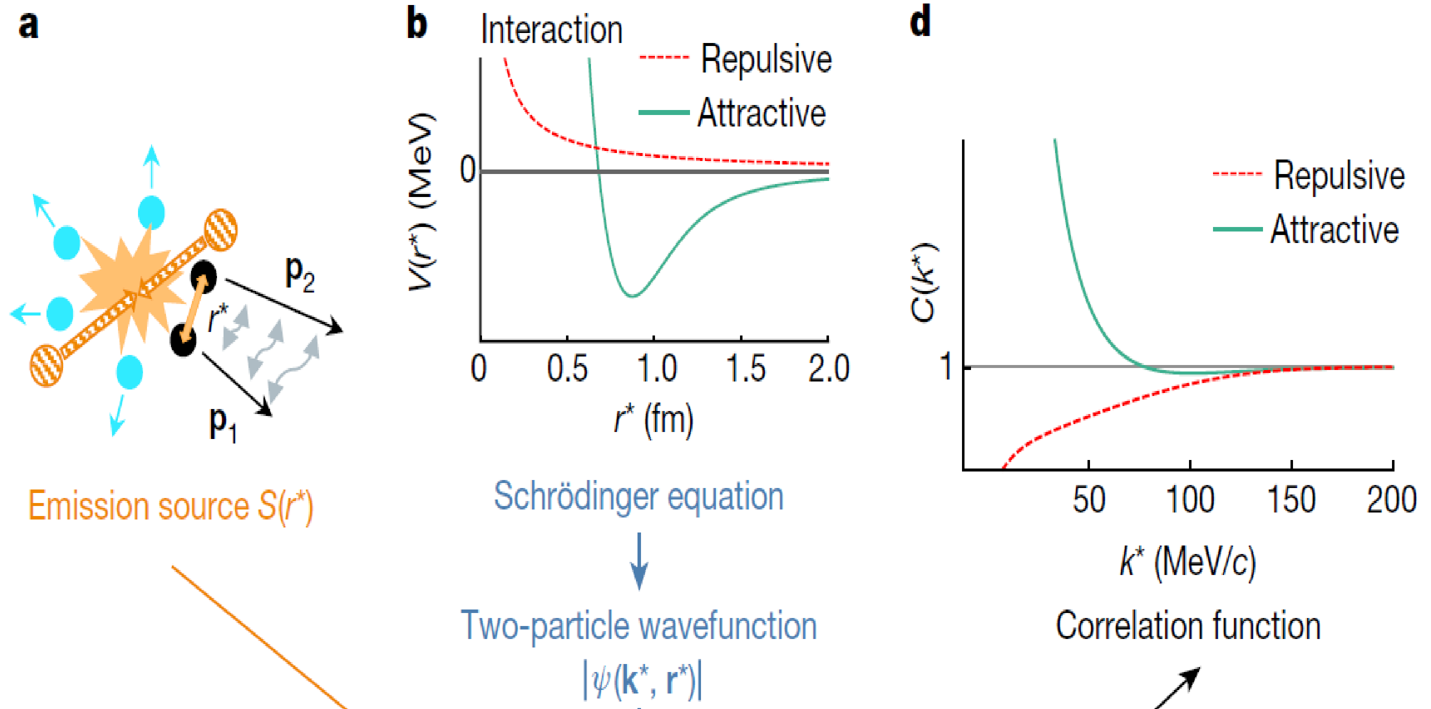

c

$$C(k^*) = \int S(r^*) |\psi(\mathbf{k}^*, \mathbf{r}^*)|^2 d^3r^* = \xi(k^*) \frac{N_{same}(k^*)}{N_{mixed}(k^*)}$$